(2)

EIGENSPACE DESIGN OF HELICOPTER FLIGHT CONTROL SYSTEMS

FINAL REPORT

WILLIAM L. GARRARD
EICHER LOW

NOVEMBER, 1990

U. S. ARMY RESEARCH OFFICE

DAAL03-86-K-0056

DEPARTMENT OF AEROSPACE ENGINEERING
AND MECHANICS
UNIVERSITY OF MINNESOTA
MINNEAPOLIS, MINNESOTA 55455

THE VIEW, OPINIONS, AND/OR FINDINGS CONTAINED IN THIS REPORT ARE THOSE OF THE AUTHOR(S) AND SHOULD NOT BE CONSTRUED AS AN OFFICIAL DEPARTMENT OF THE ARMY POSITION, POLICY, OR DECISION, UNLESS SO DESIGNED BY OTHER DOCUMENTATION.

MASTER COPY KEEP THIS COPY FOR REPRODUCTION PURPOSES

REPORT DOCUMENTATION PAGE

Form Approved
OMB No 0704-0188

1. AGENCY USE ONLY (Leave blank)	2. REPORT DATE	3. REPORT TYPE AND DATES COVERED
	December 1990	

4. TITLE AND SUBTITLE
Eigenspace Design of Helicopter Flight Control Systems, Final Report

5. FUNDING NUMBERS
DAAL03-86-K-0058

6. AUTHOR(S)
William L. Garrard and Eicher Low

7. PERFORMING ORGANIZATION NAME(S) AND ADDRESS(ES)
Department of Aerospace Engineering and Mechanics
University of Minnesota
107 Akerman Hall, 110 Union St. SE
Minneapolis, MN 55455

8. PERFORMING ORGANIZATION REPORT NUMBER

9. SPONSORING/MONITORING AGENCY NAME(S) AND ADDRESS(ES)
U. S. Army Research Office
P. O. Box 12211
Research Triangle Park, NC 27709-2211

10. SPONSORING/MONITORING AGENCY REPORT NUMBER
ARO 23422.9-EL

11. SUPPLEMENTARY NOTES
The view, opinions and/or findings contained in this report are those of the author(s) and should not be construed as an official Department of the Army position, policy, or decision, unless so designated by other documentation.

12a. DISTRIBUTION/AVAILABILITY STATEMENT
Approved for public release; distribution unlimited.

12b. DISTRIBUTION CODE

13. ABSTRACT (Maximum 200 words)

An eigenstructure based design methodology for helicopter flight control systems is developed and evaluated in this report. The report provides a detailed review of the application of multivariable design techniques to helicopter flight control systems, a review of applicable handling quality specifications, a description of the mathematical models used, a presentation of the theory of eigenstructure design, application of the theory to a helicopter design problem, and evaluation of the performance and robustness properties of the resulting control laws.

14. SUBJECT TERMS
Helicopter, Flight Control Handling Qualities, Eigenspace Assignment

15. NUMBER OF PAGES
181

16. PRICE CODE

17. SECURITY CLASSIFICATION OF REPORT	18. SECURITY CLASSIFICATION OF THIS PAGE	19. SECURITY CLASSIFICATION OF ABSTRACT	20. LIMITATION OF ABSTRACT
UNCLASSIFIED	UNCLASSIFIED	UNCLASSIFIED	UL

TABLE OF CONTENTS

LIST OF FIGURES

LIST OF TABLES

EIGENSPACE DESIGN OF HELICOPTER FLIGHT CONTROL SYSTEMS

SUMMARY

An eigenstructure based design methodology for helicopter flight control systems is developed and evaluated in this report. The report provides a detailed review of the application of multivariable design techniques to helicopter flight control systems, a review of applicable handling quality specifications, a description of the mathematical models used, a presentation of the theory of eigenstructure design, application of the theory to a helicopter design problem, and evaluation of the performance and robustness properties of the resulting control laws.

The methodology detailed in this report allows the designer to synthesize control laws which result in desirable response types such as attitude command attitude hold, rate command, and translational rate command position hold. Eigenstructure assignment is used to design inner loop control laws which provide decoupled first order rate command response in each control axis. Outer loop control laws are then designed to achieve desired response types using standard single input single output frequency response design techniques.

Control laws were designed for a typical high performance helicopter operating in the hover flight condition. The performance of these control laws was evaluated with the mathematical models used for design and the control laws were found to yield excellent dynamic response characteristics in both the time and frequency domains. The control laws yielded good tracking of pilot commands and attenuation of atmospheric disturbances. They also provided Level 1 handling qualities when evaluated using the design model.

The stability robustness of the control laws in the presence of modeling uncertainties was evaluated using unstructured singular values. A simple time delay model of the errors due to neglected high frequency dynamics was used in this analysis and the stability robustness of the system was shown to be acceptable. Much more detailed robustness analyses were accomplished using structured singular value techniques and computer simulations. Actuator dynamics, rotor dynamics, time delays due to digital implementation of flight control laws, and errors in aerodynamic stability and control derivatives were included in these robustness analyses. The stability and performance robustness of the feedback control laws were shown to be acceptable and in no case were handling qualities less than Level 2 obtained.

Eigenstructure assignment appears to provide a good method for design of helicopter flight control systems which result improved handling qualities. Eigenstructure assignment provides a straightforward methodology which results in control laws which are relatively simple to implement and which do not require high order dynamic compensators in the feedback loops.. The eigenstructure control laws provide good robustness properties. It is suggested that implementation of these control laws on a piloted simulator be investigated with the goal of eventual flight tests.

PUBLICATIONS AND TECHNICAL REPORTS

Journal Publications

1. W. L. Garrard, Eicher Low, Scott Prouty, "Design of Attitude and Rate Command Systems for Helicopters Using Eigenstructure Assignment," Journal of Guidance Control and Dynamics, Vol. 12, No. 6, pp. 783-792, Nov-Dec, 1989.

2. Ekblad, M., "Reduced Order Modeling and Controller Design for a High Performance Helicopter," Journal of Guidance Control and Dynamics, Vol. 13, No. 3, pp. 439-449, May-June, 1990.

3. W. L. Garrard and B. S. Liebst, "Design of a Multivariable Helicopter Flight Control System for Handling Qualities Enhancement," Journal of the American Helicopter Society, Vol. 35, no 4, pp. 23-30, October 1990.

4. W. L. Garrard and Eicher Low, "Design of Flight Control Systems to Meet Rotorcraft Handling Qualities Specifications," submitted to Journal of Guidance Control and Dynamics, 1990.

5. Eicher Low and W. L. Garrard, "Robustness of a Helicopter Flight Control System Designed Using Eigenstructure Assignment," submitted to Journal of Guidance Control and Dynamics, 1990.

Conference Papers Appearing in Printed Proceedings

1. W. L. Garrard and B. S. Liebst ,"Design of a Multivariable Helicopter Flight Control System for Handling Qualities Enhancement," Proceedings 43rd Annual Forum of the American Helicopter Society, St. Louis, Missouri, May 1987.

2. W. L. Garrard, Eicher Low, and Scott Prouty, "Design of Attitude and Rate Command Systems for Helicopters Using Eigenstructure Assignment," Proceedings AIAA Guidance, Navigation and Control Conference, Minneapolis, MN, August 1988.

3. W. L. Garrard and Eicher Low, "Design of Flight Control Systems to Meet Rotorcraft Handling Qualities Specifications," Proceedings AIAA Atmospheric Flight Mechanics Conference, Portland, OR, August 1990.

4. W. L. Garrard, Eicher Low, and Peter Bidian, "Achievement of Rotorcraft Handling Qualities Specifications via Feedback Control," Proceedings 16 th Annual European Rotorcraft Forum, Glasgow, Scotland, Sept. 1990.

5. Eicher Low and W. L. Garrard, "Robustness of a Helicopter Flight Control System Designed Using Eigenstructure Assignment," submitted to AIAA Guidance, Navigation and Control Conference, New Orleans, LA, August 1991.

There were no inventions developed during this contract.

PARTICIPATING SCIENTIFIC PERSONNEL

FACULTY

Professor William L. Garrard
Professor Bradley S. Liebst

GRADUATE STUDENTS

Peter Bidian - MS
Mark Ekblad - MS
Jerome Farm - MS
Eicher Low - MS, PhD spring 1991
Zoe Mirfakhraie - MS spring 1991
A[illegible]ony Snell - PhD spring 1991
Scott Prouty - MS

UNDERGRADUATE

Joseph Anderson

Chapter 1

Introduction

I. Motivation

The objective of the research described in this thesis is to develop and evaluate a methodology, based on eigenstructure assignment, for the design of advanced flight control laws suitable for modern high performance helicopters.

When operating at hover or low speed (up to approximately 45 knots) helicopters exhibit poor handling qualities and are difficult to fly. Interactions between the longitudinal and lateral axes, coupling of the control inputs, and inherent low frequency instabilities are undesirable characteristics typical of helicopters when flying at low speeds. As a result, helicopters can benefit substantially from the use of automatic flight control systems to enhance handling qualities. Until recently, the development of rotorcraft flight controls has lagged behind more advanced automatic flight controls which are available for fixed wing aircraft [1]-[3].

Recent advances in rotorcraft technology have greatly expanded the role of both military and civilian helicopters. This expanded role has resulted in a requirement for improved handling qualities. Until the niddle 1980's, helicopter handling quality specifications had been poorly defined compared with those for fixed wing aircraft. As part of the U.S. Army LH (Light Helicopter) program, an extensive effort to revise military handling quality specifications was under taken. This program is essentially completed and has resulted in a comprehensive set of rotorcraft handling qualities. These new handling quality specifications are mission oriented and require that advanced rotorcraft exhibit good handling qualities over a diverse spectrum of operational missions.

Precision flight path control and attitude stability are required for single pilot operation in hovering and flight close to the earth, especially in poor weather conditions and/ or at night. For rotorcraft which are intended for air-to-air combat, agility and high maneuverability are required. These new handling qualities specifications are being used for civilian as well as military helicopters.

The revised handling quality specifications are structured in terms of specific Mission-Task-Elements (MTEs) and Operational Flight Envelopes (OFEs). The specifications are expressed in terms of dynamic response to control inputs or response types [4]. These response types are formulated as desired frequency response characteristics between pilot inputs and vehicle outputs. These outputs may include attitude angles, attitude rates, and/or translational velocities. Important characteristics of these frequency response characteristics are their bandwidth, magnitude, and phase. If these desired frequency response characteristics are modeled as either first order or second order transfer functions, it is simple to relate the desired frequency response characteristics to the natural frequencies and damping factors or the time constants of the transfer function models.

The revised military specifications provide a unified framework for design and for evaluation of handling qualities. Requirements and limits are set at levels which if not met, will result in poor flying qualities. Thus the requirements are necessary, but may not be sufficient, to guarantee Level 1 handling qualities. Minimum Level 1 control response bandwidths for rate and attitude response types in the pitch and roll axes have been defined and incorporated into the new military specifications. These bandwidths have been adjusted to reflect the requirements imposed by various mission-task-elements.

Three primary response types [4]-[5] have been proposed. These are Attitude Command/ Attitude Hold (ACAH), Rate Command (RC) or Rate Command/ Attitude

Hold (RCAH), and Translation Rate Command/ Position Hold (TRCPH). The characteristics for a step control input for each of these response types are as follows:

1. The ACAH response type results in a pitch (roll) attitude angle proportional to the longitudinal (lateral) stick input. When the input is removed, the helicopter returns to the trim attitude before the input was applied. This response type typically does not have the agility of the RCAH type but is highly desirable in low visibility conditions, especially in hover, since releasing the control input will return the rotorcraft to its reference trim attitude. A trim control of some type is required in order to change the trim attitude reference.

2. For the RCAH response type, angular velocities about the vehicle roll, pitch, or yaw axis are proportional to the corresponding cockpit controller force and/or deflection. The RCAH response type is characterized as having a high level of agility with capability for extended periods of hands-off operation.

3. For the TRCPH response type, a constant controller force input must result in constant translational rate. The rotorcraft must hold position if the force on the cockpit controller is zero. The TRCPH response type is useful for precision hovering tasks and provides an important tactile cue for low speed maneuvering in poor visual cueing.

Unaugmented helicopters provide control responses which are of the rate command type. Typical open loop rigid body helicopter dynamics include

1. extensive coupling between the lateral and longitudinal responses,

2. low frequency unstable response in forward and side velocities,

3. insufficient bandwidth for Level 1 flying qualities in all four axes.

Most unaugmented rotorcraft will not meet the new handling quality specifications and feedback control systems are necessary to improve handling qualities so that safe operation close to the earth in poor weather conditions and/or at night is possible. Control systems should result in the following characteristics:

1. accurate tracking of pilot commands,

2. high bandwidth and low time delay response characteristics,

3. attenuation of gusts and other disturbances,

4. achievement of specified response types,

5. decreased pilot workload,

6. modal decoupling,

7. acceptable stability and performance robustness.

Typical helicopters have four control inputs. For a single rotor vehicle, these are as follows:

1. Collective pitch which controls the lift produced by the main rotor and is the primary control for vertical velocity.

2. Lateral cyclic pitch which controls the rolling moment produced by the main rotor and is the primary control for roll rate.

3. Longitudinal cyclic pitch which controls the pitching moment produced by the main rotor and is the primary control for pitch rate.

4. Tail rotor collective pitch which controls the lift produced by the tail rotor and consequently the yawing moment on the helicopter. This is the primary control for yaw rate.

Typical flight control sensors measure normal acceleration or velocity, roll, pitch, and yaw rates, and side and forward velocity. Other measurements can include pitch, roll and heading angles and altitude. There is considerable coupling between inputs and outputs. For example, a collective input will create yawing moment as well as lift and a longitudinal cyclic input will produce a rolling moment as well as a pitching moment. Part of the pilot's task is to compensate for these couplings. This results in high pilot work load, particularly during hover. The principal source of coupling is due to the main rotor which is required to produce both lift, forward thrust, and pitching and rolling moments for control. Production of thrust and control moments requires changes in the rotor tip path plane orientation. These changes in tip path plane orientation produce gyroscopic effects which influence all of the forces and moments acting on the helicopter.

Due to the fact that responses to control inputs are highly coupled, helicopter dynamics are characterized by multi-input-multi-output (MIMO) mathematical models and design of flight control systems for such vehicles is a true multivariable synthesis problem. Modern MIMO design techniques are well suited for the design of rotorcraft control laws.

Typical mathematical models used for helicopter control system design are based on rigid body models of the fuselage dynamics with a quasi-static representations of the rotor dynamics [6]-[7]. This representation is appropriate as the state variables representing the

rigid body motions of the helicopter are the quantities which are to be controlled; however effects such as rotor, structural, actuator, sensor, and engine dynamics can have a significant effect on dynamics response [8].

Rotor dynamics can produce non-minimum phase zeros which can result in instabilities if control gains are too large. At present it appears that information on rotor states cannot be used in control laws due to noise and other difficulties associated in the measurement of these states.

Actuators produce phase lags which can result in instabilities and also have both rate and deflection limits. Since saturation of actuators is undesirable, inputs to the actuators should be kept small enough to avoid saturation and this may also limit feedback gains. Also, since the actuators themselves have a limited bandwidth (30 to 60 rad/s), the control laws should not require high frequency actuator responses.

Interaction between the rotor and the airframe generates what are called "n/rev" vibrations (n equals the number of blades). The sensors used to measure the vehicle outputs will pick up these vibrations and the control system will be excited by vibrations at this frequency. For example, a typical helicopter rotor operates at an angular velocity of about 30 rad/s, so for a four-bladed helicopter, the sensors would be subjected to excitation of 120 rad/s. Thus sensor outputs must be filtered before they are fedback into the control system. Typically a Bessel filter is used for this purpose, as this type of filter gives the least phase shift of any type of linear filter in the band pass region. This filter does introduce significant phase shift at frequencies higher than the design filter bandwidth. Thus the bandwidth of the feedback compensator is limited to some fraction of n times the rotor angular velocity. Typically, compensators should be designed with a bandwidth of no more than 10 rad/s.

Structural dynamics of the fuselage may also affect stability and performance and lack of accurate models for these modes makes it difficult to include them directly in the control laws. Gas turbine engines used for propulsion introduce both lags and coupling between yawing motion and collective pitch changes. Also, it is important to avoid large changes in rotor angular velocity (rotor droop) when control inputs are applied.

Rotor, actuator and structural dynamics affect the upper part range of frequencies for flight control and the closed loop response characteristics must be insensitive to these effects as well as to delays due to filtering and digital implementation of the flight control laws. Uncertainties in aerodynamic stability and control coefficients can also be significant and will introduce low frequency errors in the mathematical model used for design.

The key design criteria for the flight control systems are

1. decouple both the internal dynamics and the response to controller inputs,

2. stabilize the helicopter,

3. increase the bandwidth,

4. provide the desired response type or types,

5. reject atmospheric disturbances and sensor noise,

6. provide acceptable response characteristic even if the dynamics of the helicopter differ significantly from those of the mathematical model used for control system design (stability and performance robustness).

II. Previous Work

Methods used for design of helicopter flight control systems [9]-[13] include classical single input single output (SISO) approaches, model following methods [14]-[18], Linear Quadratic Regulator (LQR) and Linear Quadratic Gaussian/ Loop Transfer Recovery (LQG/LTR) procedures [19]-[23], dynamic inversion [24]-[26], H-infinity (H_∞) techniques [27]-[30], and eigenstructure assignment techniques [31]-[34]. An excellent review of research in the area of multivariable design techniques applied to helicopter flight control system design is given in [35].

Classical SISO techniques applied to each control loop individually were used to design control systems for all current production rotorcraft. These systems were designed for stability augmentation and are largely mechanical in nature. Classical SISO design techniques concentrate on achieving a maximal loop gain over a specified frequency range consistent with specified gain and phase margins. Although this has proven to be a very reliable and successful technique, classical SISO techniques treat each control loop separately and do not explicitly include coupling between loops. Since this coupling is very important in rotorcraft, a variety of modern techniques are being studied for use in advanced rotorcraft flight control systems.

The success of digital flight control technology for improving handling qualities of fixed wing aircraft has motivated similar effects for rotorcraft [36] and at least six vehicles have been flight tested using advanced digital control systems. These are the Boeing Advanced Digital Optical Control System (ADOCS) [37], implemented on a Sikorsky UH 60B, the McDonnell Douglas Apache AV05 YAH-64, the German DLR MBB Bo 105, the NASA Ames Research Center CH-47 and UH-1H, and the Aerospatiale Dauphin. The ADOCS and DLR Bo 105 used explicit model following. A variety of techniques were used on the NASA CH-47. The YAH-64 used a MIMO proportional plus

integral (P + I) controller. The NASA UH-1H used a dynamic inversion control and the Dauphin control system was designed using eigenstructure assignment but no details of this design are available. The remainder of this section will review work which had been done so far in the application of multivariable techniques to the design of helicopter flight control systems.

Model Following Concepts

A variety of model following concepts have been proposed for use in flight control systems. The ADOCS design is representative of model following designs and will be described in some detail below. The ADOCS model following concept uses feedforward and inverse plant dynamics to cancel the inherent rotorcraft dynamics and replace them with the desired command responses from a command model. Feedback is used for stability enhancement and reduction of sensitivity to variations in open loop dynamics. Feedforward is used to obtained desired response to commands. Using this approach, the command and stabilization response characteristics can be set independently. A block diagram of the ADOCS system is shown in Fig. 1.1.

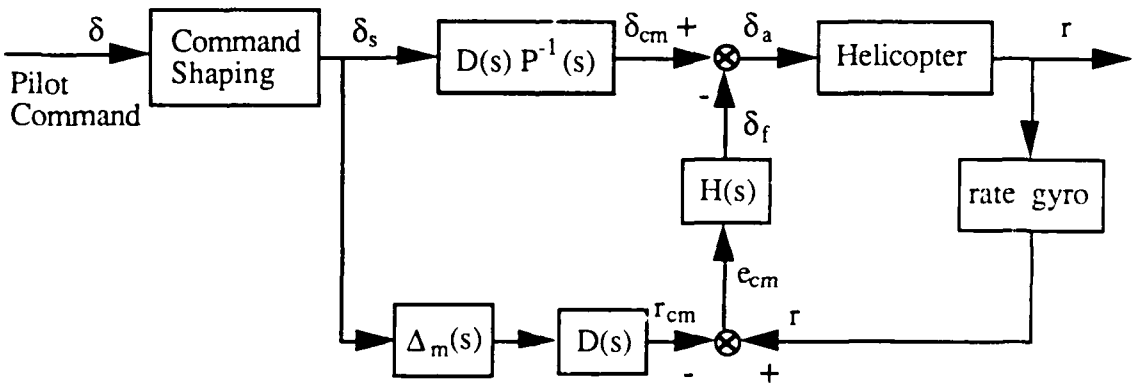

Fig. 1.1 ADOCS Modeling Following Control System.

In Fig. 1.1, the following nomenclature applies:

δ = pilot command (collective pitch, lateral cyclic pitch, longitudinal cyclic pitch, or tail rotor collective pitch),

δ_s = shaped pilot command to achieve desired control sensitivity,

δ_{cm} = command from pre-compensator,

δ_f = command from feedback loop,

δ_a = actuator command,

r_{cm} = output command,

r = output,

e_{cm} = error between output command,

$P(s)$ = transfer function model of stable short period helicopter dynamics,

$D(s)$ = desired transfer function between pilot command and output,

$\Delta_m(s)$ = model of actuator and other stable system dynamics not included in P(s),

$\Delta(s)$ = the actuator and other system dynamics not included in P(s).

Simple block diagram manipulations yield

$$e_{cm} = (1 + P(s) \Delta(s) H(s))^{-1} (\Delta(s) - \Delta_m(s)) D(s) \delta_s(s)$$

and

$$\frac{r}{\delta_s} = (1 + P(s) \Delta(s) H(s))^{-1} D(s) P(s) \Delta(s)$$

If $\Delta_m(s) \rightarrow \Delta(s)$, $e_{cm} \rightarrow 0$ and the output approaches the output command. Furthermore, H(s) can be selected to ensure that $1 + P(s)\,\Delta(s)\,H(s)$ has desirable stability margins. If H(s) is large at low frequencies where command following is desired, then

$$\frac{r}{\delta_s} \cong D(s)$$

and the desired transfer function between input and output will be achieved.

For the ADOCS system, the transfer functions for controlling yaw rate are as follows:

1. The desired response is first order with a bandwidth ω_{cm}

$$D(s) = \frac{K}{s + \omega_{cm}}$$

2. The yaw rate/ tail rotor collective pitch short period transfer function is modeled as

$$P(s) = \frac{N_{\delta_r}}{s + N_R}$$

3. The actuator and other stable dynamics not included in P(s) are modeled by

$$\Delta_m(s) = \left(\frac{a}{s + a}\right) e^{-\tau s}$$

where a is the actuator roll off frequency and τ represents a time delay approximation of rotor dynamics, filters, computational lags etc.

4. The feedback control laws is proportional plus integral

$$H(s) = \left(K_r + \frac{K_\Psi}{s}\right)$$

The ADOCS model following approach is SISO and ignores inter axial coupling. Also since P(s) must be inverted, it must be minimum phase and must not contain unstable poles

(when inverted these will become non-minimum phase zeros), stable poles near the imaginary axis (when inverted these will become near non-minimum phase zeros), non-minimum phase zeros (when inverted these will become unstable poles), or near non-minimum phase zeros (when inverted these will become near unstable poles). Helicopters have intrinsically unstable low frequency poles which must be neglected in the inversion model, thus this model will be inaccurate at low frequencies. Despite these shortcomings, the ADOCS system performed adequately in flight test.

A model following approach similar to ADOCS was used in the successful flight testing of a MBB Bo 105 [38]. It was found that the accurate modeling of the rotor dynamics was critical in the success of this design [39]-[40]. This model following design technique was also used to design control laws for UH-1H and was tested on the NASA Ames flight simulator [15], [18]. The UH-1H and Bo 105 have completely different rotor designs which result in different control characteristics for the two helicopters.

Quadratic Optimal Cooperative - Control Synthesis

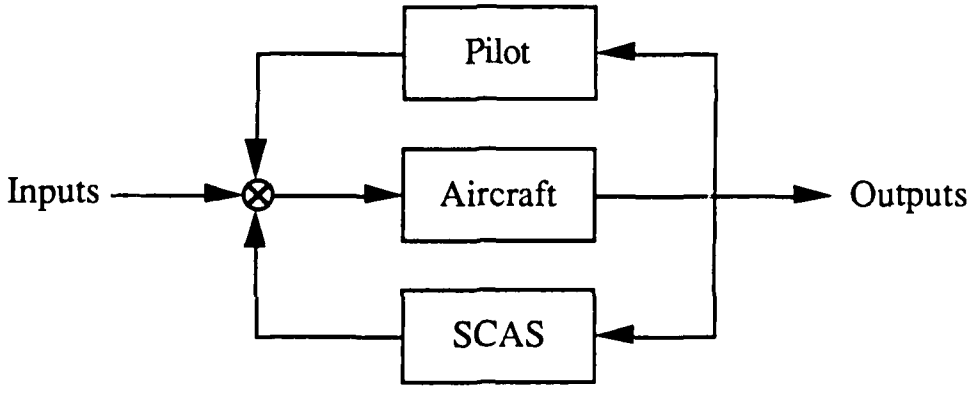

SCAS : Stability and Control Augmentation System

Fig. 1.2 Cooperative Control Synthesis Design Structure.

An extension of LQR/LQG methods, the quadratic optimal control synthesis (CCS) method developed by Innocenti and Schmidt [9], was applied by Townsend to the NASA CH-47 tandem rotor helicopter [11]. The basic structure of the CCS control system is shown in Fig. 1.2. The CCS method incorporates an optimal pilot model as well as an aircraft model and minimizes the weighted sum of the squares of the aircraft states, the control inputs, and the states of the pilot model. Townsend claims the CCS method offers the following two advantages over other methods

1. The CCS method uses output feedback rather than full state feedback, thereby making it simpler for implementation.

2. The CCS method requires, in principle, no detailed a priori design criteria, because an assumed analytic pilot-model structure is an inherent feature of the approach as shown in Fig. 1.2.

The second feature can be an advantage in cases where no design criteria exist . This is not the case with helicopters because of the new handling qualities specifications. Townsend obtained two CCS designs; one using the original approach of Innocenti and Schmidt and a modified approach developed by specifically for helicopters. Results from fixed base piloted simulations indicated that the modified CCS design compared favorably with a classical frequency response design.

MIMO Proportional plus Integral (P + I) Control Laws

An extremely successful approach in classical SISO design is the used of a P+I controller. This type of controller gives high loop gain at low frequencies for good command tracking and provides good high frequency roll off for stability robustness. MIMO generalizations of the P+I technique have been developed and applied to helicopters.

Enns [10] used a multivariable low frequency approximation of the YAH-64 dynamics and designed a MIMO P+ I control law for this helicopter. A pre-compensator was used to approximately cancel the short period dynamics and achieve desired command response characteristics and a P+I feedback control law was used to obtain desirable feedback properties of command tracking, stability and insensitivity to variation in forward loop dynamics. These control laws were successfully flight tested [41]. A similar approach is being studied for use in the Agusta EH 101 helicopter [42].

Linear Quadratic Regulator (LQR) / Linear Quadratic Gaussian (LQG) Methods

LQR theory results in a linear control law which minimizes the integral over an infinite time interval of the weighted sum of the squares of the elements of the system state and control vectors. The LQR control law requires that all system states be fedback (full state feedback) but results in excellent multivariable stability margins [20]-[21], [43]-[45]. In most applications, all of the system states cannot be measured and a state estimator (Kalman Filter) is required in the feedback loop. This estimator can seriously degrade the stability margins of the closed loop systems; however, in the late 1970's Doyle and Stein developed a method for using LQG theory to recover the closed loop feedback properties of the LQR. This procedure, called loop transfer recovery (LTR), can be used in conjunction with LQG theory to shape the frequency response characteristics of the feedback loops. The LQG/LTR methodology has provided an important tool for control law design and is commonly used in design of flight control laws for fixed wing aircraft [46].

Several early papers have described the use of LQR methods for helicopters [47]-[49]. More recent results have used the LQG [50] or LQG/LTR [51] methodologies and at least

one design has been flight tested [50]. Application of LQG loop shaping to helicopter flight control was studied by Holdridge, et al. [50] and Rodriguez [51]. Gribble and Murray-Smith [52] have recently used an LQR version of model following to design a flight control system for the Westland Lynx helicopter operating at a forward speed of 80 knots. Their design was based on a rigid body model with the actuator and blade flapping dynamics were represented as pure delays in order to motivate the choice of the LQR input weighting matrix. Prasad et al. [53] present a design approach based on output feedback with gains selected to minimize a quadratic performance index. This approach uses a lower order state estimator in the feedback loop than is required by the LQG approach, but it does not provide a direct method for achieving desired response types nor does it result in guaranteed stability margins.

Although LQR and LQG/LTR theories guarantee stability robustness, these theories do not provide a direct means to obtain the desired response types. Response types are obtained indirectly through choice of state and control weighting matrices. The LQR method requires full state feedback which is usually not feasible. The LQG/LTR maintains stability margins without full state feedback but requires an estimator in the feedback loop and LQG approach to LTR can result in closed loop poles far into the left half plane, resulting in high compensator bandwidth.

H Infinity (H_∞) Design Techniques

Recently there has been interest in the application of H_∞ design techniques to helicopter flight control systems. The H_∞ approach [54] can be regarded as a MIMO generalization of classical SISO frequency response techniques. Since the desired response types for helicopters are given in terms of frequency response relationships between pilot

inputs and helicopter outputs, the H_∞ approach appears to provide a natural method for design of helicopter flight control laws.

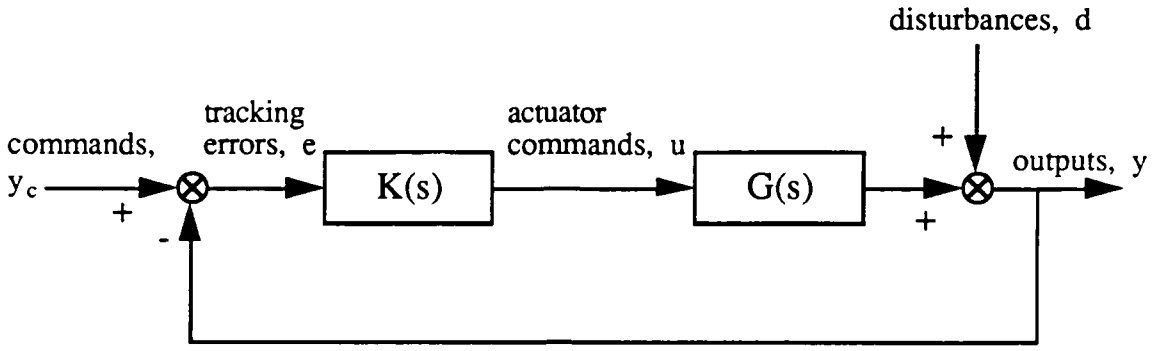

Fig. 1.3 Typical H_∞ Control Structure.

The H_∞ design procedure produces a stabilizing control law, K(s), which fits the feedback structure shown in Fig. 1.3. The H_∞ norm is defined for a transfer matrix as the supremum of the maximum singular value of the matrix taken over all frequencies. The H_∞ design approach is based on the the selection of a control law which minimizes the H_∞ norm of transfer function matrices associated with system performance. Thus the matrices selected for H_∞ optimization should have outputs which are to be small. In the case of helicopters, tracking errors, e, actuator inputs, u, and responses to disturbances, y, are quantities which should be kept as small as possible and consequently are candidates for H_∞ optimization. From Fig. 1.3, the relationship between the command input, y_c, and the error, e, is

$$e = (I + GK)^{-1} y_c$$

also the relationship between the output and disturbances at the output is

$$y = (I + GK)^{-1} d$$

The matrix $(I + GK)^{-1}$ is commonly called the sensitivity matrix. The transfer function matrix between the command input, y_c, and the actuator input, u, is

$$u = K (I + GK)^{-1} y_c$$

The largest singular value of the sensitivity matrix also determines the size of the smallest unstructured output inverse multiplicative perturbation that could destabilize the system and for good stability margins at the plant output, the H_∞ norm of the sensitivity should be less than unity. The H_∞ norm of $(I + KG)^{-1}$ determines the smallest input inverse perturbation which could destabilize the system. The H_∞ norm of the complementary sensitivity $(I + KG)^{-1} KG$ determines the smallest unstructured input multiplicative perturbation which could destabilize the system and the H_∞ norm of $K (I + GK)^{-1}$ determines the largest additive unstructured perturbation which could destabilize the system. Thus minimization of the H_∞ norm of the sensitivity and other related matrices is important for purposes of stability as well as performance. H_∞ design procedures tend to give nearly constant values for the maximum singular values of the matrices which are optimized. Thus in practice it is necessary to weight these matrices with appropriate frequency dependent weighting matrices in order to obtain desired frequency response characteristics. Selection of these weighting matrices is one of the most important tasks for the designer using the H_∞ approach.

Yue and Postlethwaite [55]-[56] have described the application of H_∞ techniques to the determination of feedback control laws for a mathematical model of the Westland Lynx helicopter at hover. They were interested in designing control laws which resulted in ACAH responses in the pitch and roll axes, and first order yaw rate and vertical velocity command responses. They had to include as outputs pitch and roll rates as well as the commanded variables, pitch and roll angles, yaw rate and vertical velocity in order to

achieve acceptable performance. These extra two outputs increased the order of the control laws. Yue and Postlethwaite chose to minimize the H_∞ norm of

$$\begin{bmatrix} W_1 (I + GK)^{-1} W_3 \\ W_2 K (I + GK)^{-1} W_3 \end{bmatrix}$$

Since $(I + GK)^{-1}$ is related to tracking errors and disturbance rejection, W_1 was selected to be large at lower frequencies to improve tracking and disturbance rejection. That is W_1 had integral like characteristics and a bandwidth of about 8 rad/s. Since $(I + GK)^{-1} K$ is related to actuator inputs, W_2 was selected to be small at low frequencies and large at higher frequencies to penalize high frequency inputs to the actuators. W_2 was comprised of first order high pass filters with a cut off frequency of 10 rad/s to limit system bandwidth. W_3 was a constant matrix selected to improve tracking performance.

The flight control laws designed by Yue and Postlethwaite using H_∞ techniques were tested on a piloted moving base simulator at the Royal Aircraft Establishment in Bedford in the U. K. Hover and forward flight at 80 knots were simulated. The flight characteristics at these two conditions are very dissimilar. At the hover design condition, pilot ratings were good. At 80 knots the ratings were less good but still better than the unaugmented helicopter.

Walker and Postlethwaite [57] studied two H_∞ techniques for the design of flight control laws for the Lynx. In order to reduce the order of these compensators, they designed fixed gain, inner loop controllers for stability enhancement. By this method, they were able to use only the four commanded variables as outputs. Their first design used essentially the same H_∞ norm as in Ref [28]. The other method used a loop shaping/ normalized left coprime factor robust design procedure developed by McFarlane and

Glover [58]-[59]. The use of only four outputs gave poorer performance than obtained from the six output design of Yue and Postlethwaite.

H_∞ techniques are relatively new. Until recently, algorithms to calculate H_∞ control laws were primitive, however, new computational reliable algorithms have been developed [54]. The underlying mathematical theory of H_∞ design is sophisticated. Selection of weighting functions is critical to the success of the design and is still an art which may require repeated design iterations. H_∞ techniques can result in high order controllers, and practical implementation often requires reduction of the order of the controller. Since fixed gain controllers probably will not provide adequate handling qualities through out the flight envelope of typical high performance helicopters, some type of control law scheduling will be required regardless of the design technique used. The problem of scheduling H_∞ controllers is not easy as there is no restriction on the control law structure for different flight conditions, i.e. a controller designed for one flight condition may be completely different in structure from that designed for another flight condition. Although more powerful computers for on board flight control may allow different control structures to be used for different flight conditions, the problem of smooth transitions between modes has not yet been studied. On the other hand, H_∞ is a powerful design procedure which when coupled with structured singular value ideas allows the explicit consideration of both nominal performance and stability and performance robustness in the design process. The question of whether this power is required in the design of helicopter flight control systems, has not yet been resolved.

Nonlinear Dynamic Inversion

Nonlinear dynamic inversion or feedback linearization is a simple idea for control of nonlinear systems. It consists of using feedback to cancel the nonlinear terms and then the

design of the linearized system can be accomplished using standard linear controller synthesis procedures. There are several important issues which can affect the use of this method. First, exact linearization of the system depends on exact knowledge of the nonlinear terms. There will always be errors in the mathematical representation of the helicopter and the control system must be robust to the effects of these errors. Second, linearization can not be obtained if any of the control actuators are saturated. Third, if aerodynamic data is available from look up tables as is usually the case, considerable computational time may be required to calculate the terms in the nonlinear inversion control laws. Despite these difficulties, there is considerable interest in this method and a controller using a nonlinear inversion controller has been flown by NASA on UH-1H helicopter [24].

Eigenstructure Assignment

Eigenstructure assignment is a technique for synthesis of feedback control laws which allows the designer to place closed loop eigenvalues in specified configurations and shape closed loop eigenvectors. Eigenstructure assignment can be a very useful technique when performance specifications can be expressed in terms of closed loop eigenvalues and eigenvectors as is the case with aircraft handling quality specifications and many researchers have applied this technique to fixed wing aircraft [60]-[67]. In fact, the flight control system for the Aerospatiale A320 Airbus was designed using eigenstructure assignment [67]. Eigenstructure techniques provide a direct, simple method for achieving desired nominal performance but do not provide any guarantee of either stability or performance robustness.

Eigenstructure assignment is also useful for systems which are not completely controllable. In such systems, the uncontrollable eigenvalues cannot be changed by

feedback but the associated eigenvectors can be altered [68] to adjust the magnitude of the uncontrollable mode in each of the states.

The use of eigenstructure assignment for helicopter control systems has been considered by several authors. Early work in the area was reported by Parry and Murray-Smith [69], Garrard and Liebst [31], and Ekblad [70]. These papers used eigenstructure assignmen: for decoupling and stabilization but not the direct achievement of response types. Apkarian [71] also applied eigenstructure assignment to a helicopter to illustrate his approach to robustness enhancement of control laws designed by eigenstructure assignment. Innocenti and Stanziola [33] have described performance/robustness trade-offs for eigenstructure control laws for rotorcraft. In a recent paper, Hughes, Maness, and Murray-Smith [34] used eigenstructure assignment to design inner loop control laws which stabilize, simplify and decouple the responses to control inputs. Simplification is accomplished by selecting eigenvector/eigenvalue pairs to cancel stable invariant zeros and the associated left zero vectors. This is analogous to pole-zero cancellation for SISO systems. Decoupling and stabilization are accomplished by suitable choices of the remaining eigenvalue/eigenvector pairs. Command following is then achieved by a pre-compensator designed using the Broussard Command Generator Approach. An ACAH system is synthesized. Samablancat, Apkarian, and Patton [72] use a combined eigenstructure and H_∞ approach. Inner loop controllers which decouple the response into longitudinal, lateral, and directional modes are designed using eigenstructure assignment. An ACAH response type is then achieved using the H_∞ technique in a manner similar to that of Yue and Postlelwaite. The objective of the decoupling is to reduce the order of the H_∞ compensators without loss of performance.

Garrard, Low, and Prouty [32] use eigenstructure assignment to design a feedback controller which achieves desired response types directly. This is accomplished by using

the desired response types to generate a state space models which in turn generates desired eigenvalue/eigenvector sets. Eigenstructure assignment is then used to design feedback control laws which give the best least squares approximation of the desired eigenstructure. This control law requires full state feedback. Since only angular body rates and vertical velocity were assumed to be measured, a state estimator was required in the feedback loop. LTR was achieved by an eigenstructure assignment technique due to Kazerooni and Houpt [73]. This control structure gave good decoupling, stability robustness and the desired time and frequency responses but was some what complex.

This study represents a further extension of the work of Garrard, Low, and Prouty. Eigenvalue placement is used to design an inner loop control law which provides decoupled, rate command response in each control loop. Eigenvalue placement is used to stabilize unstable modes and provide appropriate bandwidth, and eigenvector shaping is used for modal decoupling. With the inner loops closed, the helicopter response to pilot commands appears as four decoupled, first order systems. It is then possible to use classical SISO frequency response techniques to design outer loop controllers which give a variety of desired response types. It is believed that the integration of eigenstructure and classical techniques presented in this thesis will encourage wider use of eigenstructure design techniques in helicopter and aircraft flight control law design.

III. Organization of the Thesis

The remainder of this thesis is organized into seven chapters. Chapter II reviews portions of the new specifications on handling qualities which are relevant to control system design for hover and low speed flight. Chapter III describes the theory of eigenstructure assignment. Chapter IV discusses the mathematical models used in control system design and evaluation. Chapter V covers the nominal design for hover and low

speed flight. Chapter VI addresses the topics of stability and performance robustness using a variety of methods. Chapter VII describes the conclusions and recommendations for further research.

References

1. Clark, R. N., and LeTron, X. J. Y., "Oblique Wing Aircraft Flight Control System," *AIAA Journal of Guidance, Control and Dynamics*, Vol. 12, No. 2, March-April 1989, pp. 201-208.

2. Bosworth, J., and Cox T., "A Design Procedure for the Handling Qualities Optimization of the X-29A Aircraft," Proceedings of AIAA Guidance, Navigation and Control Conference, Boston, MA, Aug. 14-16, 1989, pp. 17-34.

3. Porter, B., and Othman, M., "Design of Adaptive Digital Model-Following Flight-Mode Control Systems for High Performance Aircraft," Proceedings of AIAA Guidance, Navigation and Control Conference, Boston, MA, Aug. 14-16, 1989, pp. 593-601.

4. Hoh, R. H., "Dynamics Requirements in the New Handling Qualities Specification for US Military Rotorcraft," Proceedings of Royal Aeronautical Society International Conference on Helicopter Handling Qualities and Control, London, Nov. 1988.

5. Key, David L., "A New Handling Qualities specification for U.S. Military Rotorcraft," Proceedings of Royal Aeronautical Society International Conference on Helicopter Handling Qualities and Control, London, Nov. 1988.

6. Talbot, P. D., Tinling, B. E., Decker, W. A., and Chen, Robert T. N., "A Mathematical Model of a Single Main Rotor Helicopter for Piloted Simulation," NASA TM-84281, Sept. 1982.

7. Chen, Robert T. N., Lebacqz, J. Victor, Aiken, Edwin W., and Tischler, Mark B., "Helicopter Mathematical Models and Control Law Development for Handling Qualities Research," NASA/ Army Rotorcraft Technology, Vol. 2, Feb. 1988, pp. 837-899.

8. Chen, Robert T. N., and Hindson, William S., "Analytical and Flight Investigation of the Influence of Rotor and Other High - Order Dynamics on Helicopter Flight - Control System Bandwidth," Proceedings of the 1st Annual Forum of the Int'l Conf. on Basic Rotorcraft Research, North Carolina, Feb. 19-21, 1985.

9. Innocenti, M., and Schmidt, D. K., "Quadratic Optimal Cooperative Control Synthesis with Flight Control Application," *AIAA Journal of Guidance, Control and Dynamics*, Vol. 7, (2), March 1984.

10. Enns, Dale F., "Multivariable Flight Control for an Attack Helicopter," Proceedings of the 1986 American Control Conference, Seattle, WA, pp. 858-863, June 1986.

11. Townsend, Barbara K., "The Application of Quadratic Optimal Cooperative Control Synthesis to a CH-47 Helicopter," *Journal of the American Helicopter Society*, Jan. 1987, pp. 33-44.

12. Tischler, Mark B., Fletcher, Jay W., Morris, Patrick M., and George, T. Tucker, "Application of Flight Control System Methods to an Advanced Combat Rotorcraft," Proceedings of Royal Aeronautical Society International Conference on Helicopter Handling Qualities and Control, London, Nov. 1988.

13. Hendrick, Russell C., "Flight Controls for Advanced Military Helicopters," *Scientific Honeyweller*, Winter 1989, pp. 144-152.

14. Kriendler, E. and Rothschild, D., "Model-Following in Linear Quadratic Optimization," *AIAA Journal*, Vol. 14, (7), July 1976.

15. Bouwer, G., and Hilbert, K. B., "A Piloted Simulator Investigation of Decoupling Helicopters by Using a Model Following Control System," Paper A-84-40-07-4000, American Helicopter Society 40th Annual Forum Proceedings, Arlington, VA., May 1984.

16. Hilbert, Kathryn B., and Bouwer, Gerhard, "The Design of a Model-Following Control System for Helicopters," Proceedings of the AIAA Guidance, Navigation, and Control Conference, Paper 84-1941, pp. 601-617, Seattle, WA, 1984.

17. Hilbert, Kathryn B., Lebacqz, J. V., and Hindson, W. S., "Flight Investigation of a Multivariable Model-Following Control System for Rotorcraft," AIAA Paper 86-9779, AIAA 3rd Flight Test Conference, Las Vegas, NV, April 1986.

18. Bouwer, G. and Zöllner, M., "Realization and Flight Testing of a Model Following Control System for Helicopters," Twelfth European Rotorcraft Forum, Garmisch-Partenkirchen, West Germany, Sept. 22-25, 1986.

19. Athans, M., "The Role and Use of the Stochastic Linear-Quadratic-Gaussian Problem in Control System Design, " *IEEE Transactions on Automatic Control*, Vol. AC-16, Dec. 1971, pp. 529-551.

20. Safonov, M. G., and Athans, M., "Gain and Phase Margin for Multiloop LQG Regulators," *IEEE Trans. on Auto. Control*, Vol. AC-22, April 1977, pp. 173-178.

21. Lehtomaki, N. A., Sandell, N. R. Jr., and Athans, M., "Robustness Results in Linear-Quadratic Gaussian Based Multivariable Control Designs," *IEEE Trans. on Auto. Control*, Vol. AC-26, Feb. 1981, pp. 75-92.

22. Moore, J. B., Gangsaas, D., and Blight, J. D., "Performance and Robustness Trades in LQG Regulator Design, " Proc. of the 20th Conference on Decision and Control, Vol. 3, Dec. 1981.

23. Stein, Gunter, and Athans, Michael, "The LQG/LTR Procedure for Multivariable Feedback Control Design," *IEEE Trans. on Automatic Control*, Vol. AC-32, No. 2, Feb. 1987, pp.105-114.

24. Meyer, G., Hunt, R. L., and Su, R., "Design of a Helicopter Autopilot by Means of Linearizing Transformations," Guidance and Control Panel 35th Symposium, AGARD CP 321, Paper No. 4, 1983.

25. Smith, G. Allan, and Meyer, George, "Aircraft Automatic flight Control System with Model Inversion," *Journal of Guidance, Control, and Dynamics*, Vol. 10, No. 3, May-June 1987, pp. 269-275.

26. Lane, S. H., and Stengel, R. F., "Flight Control Design Using Non-Linear Inverse Dynamics," *Automatica*, Vol. 24, No. 4, 1988.

27. Francis, B. A., and Doyle, J. C., "Linear Control Theory with an H_∞ Optimality Criterion," *SIAM J. Control Opt.*, Vol. 25, 1987, pp. 815-844.

28. Francis, B. A., *A Course in H_∞ Control Theory*, (Lecture Notes in Control and Information Sciences, Vol. 88), New York: Springer Verlag, 1987.

29. Maciejowski, J. M., *Multivariable Feedback Design*, Addison-Wesley Publishing Company, Reading Massachusetts, 1989.

30. Doyle, J. C., Glover, Keith, Khargonekar, Pramod P., and Francis, Bruce A., "State-Space Solutions to Standard H_2 and H_∞ Control Problems," *IEEE Trans. on Auto. Control*, Vol. 34, No. 8, Aug. 1989, pp. 831-846.

31. Garrard, W. L., and Liebst, B. S., "Design of Multivariable Helicopter Flight Control System for Handling Qualities Enhancement," American Helicopter Society 43rd Annual Forum Proceedings, St. Louis, May 1987, pp. 677-696.

32. Garrard, W. L., Low, E., and Prouty, S. J., "Design of Attitude and Rate Command System for Helicopters Using Eigenstructure Assignment," *AIAA Journal of Guidance, Control and Dynamics*, Vol. 12, No. 6, Nov.-Dec. 1989, pp. 783-791.

33. Innocenti, M., and Stanziola, C., "Performance - Robustness Trade Off of Eigenstructure Assignment Applied to Rotorcraft," *Aeronautical Journal*, Vol. 94, No. 934, 1990, pp. 124-131.

34. Hughes, G., Manness M. A., and Murray-Smith, D. J., "Eigenstructure Assignment for Handling Qualities in Helicopter Flight Control Law Design," Proceedings of 16th Annual Society European Rotorcraft Forum, Glasgow, Scotland, Sept. 1990.

35. Manness, M. A., Gribble, J. J., and Murray-Smith, D. J., "Multivariable Methods for Helicopter Flight Control Law Design: A Review," Proceedings of 16th Annual Society European Rotorcraft Forum, Paper No. III.5.2, Glasgow, Scotland, Sept. 1990.

36. Tischler, Mark B., "Assessment of Digital Flight-Control Technology for Advanced Combat Rotorcraft," *Journal of the American Helicopter Society*, Oct. 1989, pp. 66-76.

37. Glusman, Steven I., Dabundo, Charles, and Landis, Kenneth H., "Evaluation of ADOCS Demonstrator Handling Qualities," Proceedings of the 43rd Annual National Forum of the American Helicopter Society, May 1987, pp. 705-716.

38. Bouwer G., Pausder, H. J., and Grünhagen, W. von., "Experiences with High Authority Helicopter Flight Control," Proceedings of 16th Annual Society European Rotorcraft Forum, Glasgow, Scotland, Sept. 1990.

39. Kaletka, Jürgen, "Identification of Mathematical Derivative Models for the Design of a Model Following Control System," American Helicopter Society 45th Annual Forum Proceedings, Boston, MA, May 22-24, 1989, pp. 655-662.

40. Fu, F. H., and Kaletka, J., "Frequency - Domain Identification of Bo 105 Derivative Models with Rotor Degrees of Freedom," Proceedings of 16th Annual Society European Rotorcraft Forum, Glasgow, Scotland, Sept. 1990.

41. Parlier, Charles A., "An Advanced Digital Flight Control Concept for Single Pilot, Attack Helicopter Operations," American Helicopter Society 43rd Annual Forum Proceedings, St. Louis, Missouri, May 18-20, 1987, pp. 697-716.

42. Fenton, J., Rawnsley, B. W., Potter, K. J., and Andrews, S. J., "An Evaluation of a Simple PID Controller Designed Using Optimal Control Theory when Applied to Helicopter Stabilization," Proceedings of 16th Annual Society European Rotorcraft Forum, Glasgow, Scotland, Sept. 1990.

43. Doyle, John C., "Guaranteed Margins for LQG Regulators," *IEEE Trans. on Auto. Control*, Vol. AC-23, No. 4, Aug. 1978, pp. 756-757.

44. Doyle, John C., and Stein, Gunter, "Robustness with Observers," *IEEE Trans. on Auto. Control*, Vol. AC-24, No. 4, Aug. 1979.

45. Doyle, J. C., and Stein, Gunter, "Multivariable Feedback Design: Concepts for a Classical/ Modern Synthesis," *IEEE Transactions on Automatic Control*, Vol. AC-26, No. 1, Jan. 1981, pp. 4-16.

46. Wendel, T., and Schmidt D., "Flight Control Synthesis for Unstable Fighter Aircraft Using the LQG/LTR Methodology," Proceedings of AIAA Guidance, Navigation and Control Conference, Boston, MA, Aug. 14-16, 1989, pp. 247-254.

47. Murphy, R. D., and Narendra, K. F., "Design of Helicopter Stabilization Systems Using Optimal Control Theory," *Journal of Aircraft*, Vol. 6, No. 2, 1969, pp. 129-136.

48. Hall, W. E., and Bryson, A. E., "Inclusion of Rotor Dynamics in Controller Design for Helicopters," *Journal of Aircraft*, Vol. 10, No. 4, 1973, pp. 200-206.

49. Hofmann, L. G., Riedel S. A., and McRuer, D., "Practical Optimal Flight Control System Design for Helicopter Aircraft, Vol. I - Technical Report," NASA CR-3275, May 1980.

50. Holdridge, R.D., Hindson, W.S., and Bryson, A.E., "LQG - Design and Flight - Test of a Velocity - Command System for a Helicopter," Proceedings of AIAA Guidance, Navigation and Control Conference, Snowmass, CO, August 1985.

51. Rodriguez, A. A., and Athans, M., "Multivariable Control of a Twin Lift Helicopter System Using the LQG/LTR Design Methodology," Proceedings of American Control Conference, Seattle, 1986, pp. 1325-1332.

52. Gribble, J. J., and Murray-Smith, D. J., "Command Following Control Law Design by Linear Quadratic Optimization," Proceedings of 16th Annual Society European Rotorcraft Forum, Glasgow, Scotland, Sept. 1990.

53. Prasad, J. V. R., Schrage, D. P., and Calise, A. J., "Comparison of Helicopter Flight Control System Design Techniques," Helicopter Handling Qualities and Control , International Conference, Royal Aeronautical Society, Paper No. 12, London, England, Nov. 1988.

54. Doyle, John C., Glover, Keith, Khargonekar, Pramod P., and Francis, Bruce A., "State-Space Solutions to Standard H_2 and H_∞ Control Problems," *IEEE Trans. on Automatic Control*, Vol. 34, No. 8, Aug. 1989, pp 831-846.

55. Yue, Andrew, and Postlethwaite, Ian, "Robust Helicopter Control Laws for Handling Qualities Enhancement," Proceedings of Royal Aeronautical Society International Conference on Helicopter Handling Qualities and Control, London, Nov. 1988.

56. Yue, Andrew, and Postlethwaite, Ian, "Improvement of Helicopter Handling Qualities Using H_∞ - Optimization," IEE Proc., Part D, Vol. 137, No. 3, pp. 115-129, May 1990.

57. Walker, D., and Postlethwaite, Ian, "Full Authority Active Control System Design for a High Performance Helicopter," Proceedings of 16th Annual Society European Rotorcraft Forum, Glasgow, Scotland, Sept. 1990.

58. McFarlane, D., "Robust Controller Design Using Normalized Coprime Factor Plant Descriptions," Ph.D. Thesis, University of Cambridge, 1988.

59. McFarlane, D., and Glover, K., "An H_∞ Design Procedure Using Robust Stabilization of Normalized Coprime Factors," Proc. of 27th IEEE Conf. Decision Control, Austin, TX, 1988.

60. D'Azzo, J. J., "Design of Disturbance-Rejection Controllers for Linear Multivariable Discrete-Time Systems Using Entire Eigenstructure Assignment," Proceedings of the 18th Annual Conference on Decision Control, Lauderdale, 1979, pp. 315-321.

61. D'Azzo, J. J., and Kennedy, T. A., "Synthesis of Digital Flight Control Tracking Systems by the Method of Entire Eigenstructure Assignment," Proceedings of IEEE National Aerospace and Electronics Conferences (NAECON), Dayton, Ohio, May 1979, pp. 343-347.

62. Sobel, K. M., and Shapiro, E. Y., "Application of Eigenspace Assignment to Lateral Translation and Yaw Pointing Flight Control," Proceedings of the 23rd IEEE Conference on Decision and Control, Dec. 1984, pp. 1423-1438.

63. Sobel, K. M., and Shapiro, E. Y., "A Design Methodology for Pitch Pointing Flight Control Systems," *AIAA Journal of Guidance, Control and Dynamics*, Vol. 8, March-April 1985, pp. 181-187.

64. Garrard, W. L., and Liebst, B. S., "Application of Eigenspace Techniques to Design of Aircraft Control Systems," Proceedings of the 1985 American Control Conference, Boston, MA, June 19-21, 1985, pp. 475-479.

65. Alag, G. S., Burken, J. J., and Gilyard, G. B., "Eigenspace Synthesis for Flutter Suppression on an Oblique-Wing Aircraft," Proceedings of the 1986 AIAA Guidance and Control Conference, August 1986.

66. Sobel, Kenneth M., and Lallman, Frederick J., "Eigenstructure Assignment for a Thrust - Vectored High Angle - of - Attack Aircraft," Paper 88-4101, AIAA Guidance, Navigation and Control Conference, Minneapolis, MN, Aug. 15-17, 1988.

67. Farineau, J., "Lateral Electric Flight Control Laws of a Civil Aircraft Based on Eigenstructure Assignment Technique," Paper 89-3594, AIAA Guidance, Navigation and Control Conference, Boston, MA, Aug. 14-16, 1989.

68. Moore, B. C., "On the Flexibility Offered by Full State Feedback in Multivariable Systems Beyond Closed Loop Eigenvalue Assignment," *IEEE Trans. on Auto. Control*, Vol. 21, Oct. 1976, pp. 682-691.

69. Parry, David L. K., and Murray-Smith, David J., "The Application of Modal Control Theory to the Single Rotor Helicopter," Proceedings of the Eleventh European Rotorcraft Forum, Paper No. 78, London, England, Sept. 10-13, 1985.

70. Ekblad, M., "Reduced-Order Modeling and Controller Design for a High-Performance Helicopter," *Journal of Guidance, Control, and Dynamics*, Vol. 13, No. 3, May-June 1990, pp. 439-449.

71. Apkarian, P., "Structured Stability Robustness Improvement by Eigenspace Techniques: A Hybrid Methodology," *Journal of Guidance, Control, and Dynamics*, Vol. 12, No. 2, March-April 1989, pp. 162-168.

72. Samblancat, C., Apkarian, P., and Patton, R. J., "Improvement of Helicopter Robustness and Performance Control Law Using Eigenstructure Techniques and H Synthesis," Proceedings of 16th Annual Society European Rotorcraft Forum, Paper No. III.11.3, Glasgow, Scotland, Sept. 1990.

73. Kazerooni, H., and Houpt, P. K., "On the Loop Transfer Recovery," *Int. Journal of Control* Vol. 43, 1986, pp. 981-996.

Chapter 2

Helicopter Handling Qualities

I. Introduction

Recent advances in rotorcraft technology have expanded the role of the modern helicopter. It is desirable that the handling qualities of modern helicopters reflect the demands of particular mission environments. The distinctive characteristics of particular mission environments make handling qualities a challenge for the control designers. The current helicopter handling qualities specification, MIL-H-8501A [1], written in 1952 and mainly unchanged since then, does not address specific handling qualities issues relevant to modern helicopters. The U.S. Army is currently engaged in revising and updating this document to reflect advances in rotorcraft technology since 1952 and link it to the design mission environments of helicopters. The latest version [2] has been adopted by AVSCOM as an Airworthiness Design Standard ADS 33 (May 1988) and used for designing the U.S. Army Light Helicopter Family (LH) in June 1988. This new handling quality specification also appears to be gaining acceptance for civilian use.

Selected features and criteria are proposed for design guidance and the evaluation of handling qualities. The primary feature of the proposed method is the classification of response types required to complete the specified missions in the presence of specified visual environments and displays. In addition, separate criteria are suggested for small, moderate, and large amplitude maneuvering. Frequency domain criteria are suggested for small amplitude, precision, closed loop control, and time domain criteria are provided for low frequency, and/ or large amplitude maneuvering. The new handling quality specifications [2] are very lengthy and only those specifications which directly relate to

flight control system design for hovering and low speed flight are outlined in this Chapter. For higher speed flight, the handling qualities specifications are similar to fixed wing aircraft.

II. Specification Overview

For application in the specification, the requirements have to be translated into specific Mission Task Elements (MTE) and an Operational Flight Envelope (OFE). The MTEs define which requirements need to be satisfied and at what level of performance. The OFE defines the envelope of speed, normal load factor, altitude, rate of climb, sideslip angle and other parameters that are of operational significance, within which the rotorcraft is capable of successfully performing its mission. Within this OFE, the rotorcraft must achieve Level 1 handling qualities.

The Usable Cue Environment (UCE) provided to a pilot is determined by combining information from the operational environment with vision aids and displays. The applicable MTE and UCE are then combined to determine the required response types and the character of these responses.

The requirements which have to be met by a helicopter are dependent on several parameters: Mission Task Element (MTE), Usable Cue Environment (UCE), pilot attention level, and speed range. These are be discussed below.

Mission Task Element (MTE): Rotorcraft performing different tasks may require different handling qualities. Therefore, the rotorcraft specification defines a set of maneuvers which represent the essential ingredients of most missions; these are termed Mission Task Elements. MTEs can further be divided into stationary and translating MTEs for hover and low speed flight.

Usable Cue Environment (UCE): The visual cues available to a pilot are compiled to produce a Usable Cue Environment (UCE). These visual cues include whatever the pilot can see out of the window with or without vision aids. Three levels of UCE are defined, with level 1 being the best and providing cues for aggressive and/or precise maneuvering, and level 3 being the worst and providing cues only for small and/or gentle maneuvers.

Pilot Attention : The two levels of response to controls and disturbances which are defined in the specification are the two levels of pilot attention. Fully attended tasks are performed when pilots apply full attention and are allowed more lenient standards then partially attended tasks, which required the pilot to engage in other activities in addition to flight path management tasks.

Speed Range : There is a major break in the requirements at the speed of 45 knots. For speeds less than 45 knots, (hover and low speed), maneuvers are ground referenced, and these rotorcraft dynamics are assumed to be typical of a hovering helicopter with pitch and roll having similar dynamics, and yaw and vertical velocity ideally having uncoupled first order responses. Above 45 knots, (forward flight), rotorcraft dynamics are assumed to approach those of fixed-wing aircraft.

III. Specification Criteria

Basic stability and control requirements are divided into two categories: hover and low speed, and forward flight. Due to the symmetry of the *xz* plane of a helicopter, pitch and roll have similar requirements. However, yaw and vertical velocity responses have separate requirements.

A. Bandwidth Criterion

Bandwidth describes the ability to follow a range of input frequencies. It is defined as the frequency at which the output magnitude is 3 dB less than the input magnitude (output magnitude is 0.707 of the input magnitude). A good system normally has a high bandwidth relative to the maximum input frequency that it is designed to track. Bandwidth limits are set by system stability considerations.

The bandwidth is referenced to the aircraft as the maximum crossover frequency with all augmentation loops closed. Additional outer loops, (including the pilot) can be closed later. The frequency response data required to measure the bandwidth parameters include all the elements of the analog or digital flight control system, (e.g. anti-aliasing, bending mode and stick filters, zero order hold effects, actuators, sensors and computational delays).

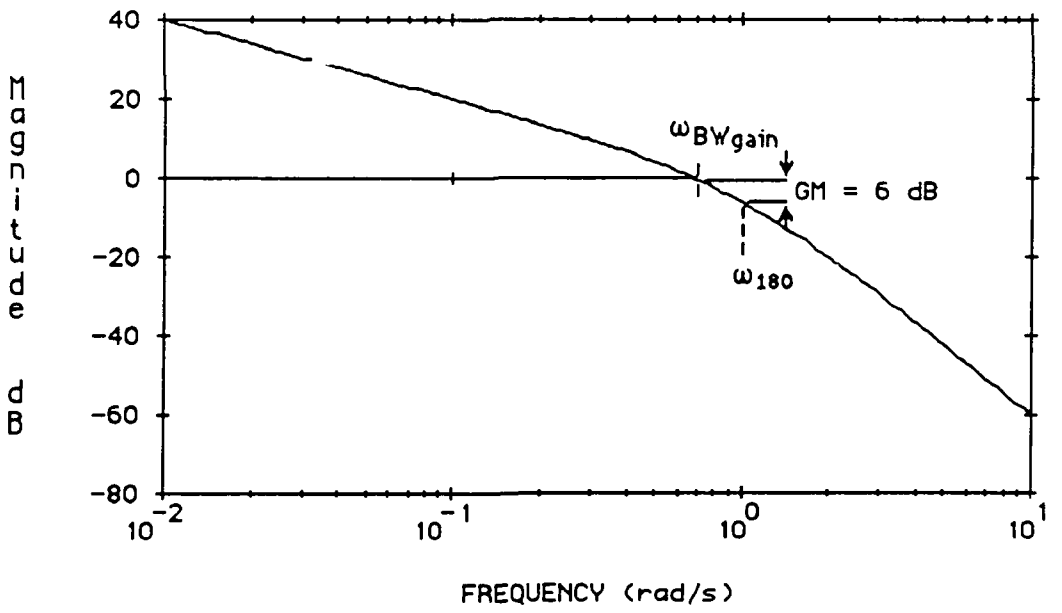

Fig. 2.1 Definition of Gain Margin Limited Bandwidth.

As shown in Figures 2.1 and 2.2, there are two definitions of bandwidth frequency, namely gain margin, ω_{BWgain}, and phase margin, $\omega_{BWphase}$. These two definitions of

bandwidth frequency are defined for a second order system. These figures describe the margin above the augmented vehicle's response in which the pilot can increase the gain or add a time delay or phase lag without causing any instability to the design model.

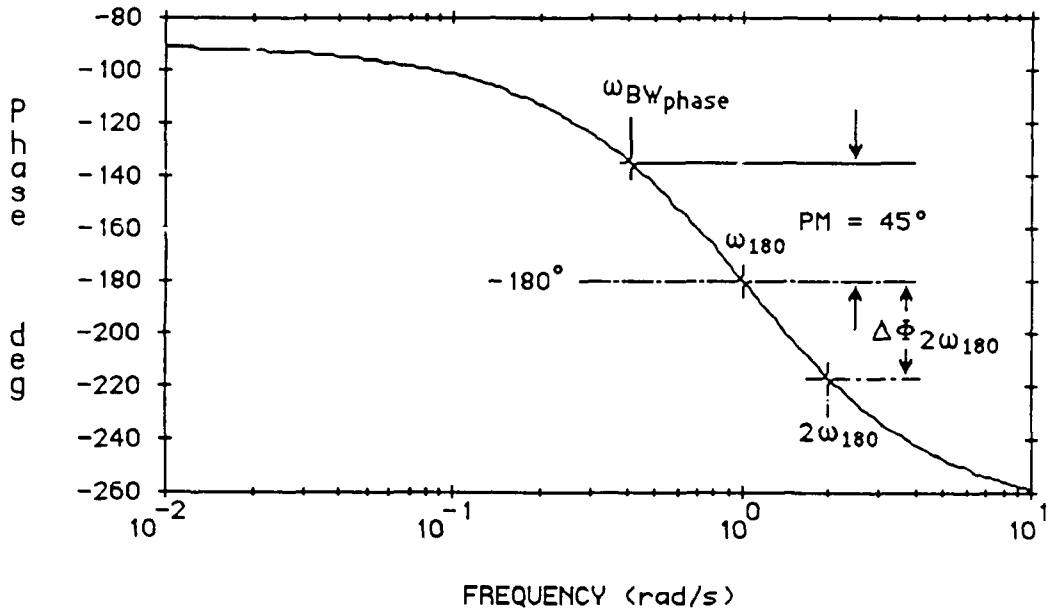

Fig. 2.2 Definition of Phase Margin Limited Bandwidth.

The gain margin bandwidth is defined as the frequency for 6 dB of gain margin. To ascertain the gain margin bandwidth, the gain corresponding to ω_{180} (the frequency at which the phase shift is -180°) must be determined. The frequency at which the magnitude of the gain is 6 dB above the magnitude at ω_{180} equals the gain margin bandwidth. Low gain margin bandwidths tend to result in system configurations which are PIO (pilot induced oscillation, ~1 Hz) prone because small changes in the pilot gain result in a rapid reduction in phase margin. For phase margin bandwidth, the frequency for ω_{180} can be determined from the Bode phase plot (Figure 2.2). The bandwidth for phase margin systems is the frequency at which the phase margin is 45 degrees. The definition of bandwidth for ACAH Response - Types does not include a gain margin limit. Also, gain margin limited ACAH Response - Types lead to PIO for super precision tasks.

Nevertheless, gain bandwidth can be used as a requirement for Rate or RCAH Response - Types, where the pilot attitude loop closure is necessary to maintain stability at hover.

For first order systems, the bandwidth and the eigenvalue λ_n, are identical. The minimum bandwidth [3] that will satisfy Level 1 small amplitude yaw rate or vertical velocity requirements for minimum gain tasks is 2 rad/s.

For a second order system, Eq. 2.1 from Ref. 4 can be used to correlate the bandwidth requ. ments given by the handling quality specification to an appropriate set of time domain parameters which includes the natural frequency, ω_n and damping ratio ζ, of the system

$$\omega_{BW} = \omega_n (\zeta + \sqrt{\zeta^2 + 1}) \qquad (2.1)$$

The typical values for ω_{BW}, ω_n, and ζ that will satisfy Level 1 handling quality requirements for small amplitude pitch (roll) attitude changes are ω_{BW} = 4 rad/s, ω_n = 2.071 rad/s and ζ = 0.707.

Pilots are sensitive to whether the phase curve drops off rapidly or slowly at frequencies beyond the bandwidth frequency. This is characterized by the phase delay parameter. Phase delay is a measure of the steepness at which the phase drops off after -180° and is an indication of the behavior of the rotorcraft as the pilot increases the crossover frequency. Large phase delay means that there is a small margin (range of frequencies) between normal tracking at 45 degrees of phase margin and instability. In addition, rotorcraft with large phase delay are PIO prone. Phase delay is defined as a two-point approximation to the phase curve defined at ω_{180} and $2\omega_{180}$ as in Eq. 2.2.

$$\tau_p = \frac{\Delta\Phi_{2\omega 180}}{57.3\ (2\omega_{180})} \qquad (2.2)$$

where $\Delta\Phi_{2\omega 180}$ is the phase difference between -180° and phase at $2\omega_{180}$ (the frequency that is two times the frequency when the phase angle is -180°). If phase is nonlinear between ω_{180} and $2\omega_{180}$, τ_p is determined from a linear least squares fit to the phase curve between ω_{180} and $2\omega_{180}$. Hoh [5] has shown that for two systems which have essentially the same bandwidth, the system that has a significantly higher phase delay has significantly degraded pilot ratings. This is due to the fact that phase delay is a measure of the shape of the phase curve around the instability frequency. In order to achieve Level 1 handling quality, it is desired to have a value of 0.2 seconds or less for τ_p.

B . Response - Types

As discussed briefly in Chapter I, three Response - Types have been developed to quantify mission oriented rotorcraft handling quality specifications [5]-[6]. These are as follows :

1. Attitude Command with Attitude Hold (ACAH)

2. Rate Command (RC) or Rate Command with Attitude Hold (RCAH)

3. Translational Rate Command With Position Hold (TRCPH)

In ACAH, a constant control input must result in a proportional attitude displacement in the presence of external disturbances. For a pulse control input, the attitude must return to within 10% of its peak value within 20 seconds. This response type is required for hover and low speed operations in conditions of degraded visual cueing and for divided attention tasks.

In RCAH systems, attitude must diverge away from trim for at least 4 seconds following a step command. This response type is preferred for most MTEs for fully

attended operations in conditions of good visual cueing. For TRCPH, a constant controller force input must produce a constant translational rate and the rotorcraft must hold position if the force on the cockpit controller is zero. TRCPH is necessary to achieve Level 1 handling quality in nap of the earth maneuvers in fair to poor visual cue environments.

The desired roll attitude and roll rate transfer functions for ACAH and RCAH respectively are [3], [5], [7]

$$\frac{\phi}{\phi_c} = \frac{\omega^2_\phi}{s^2 + 2\zeta\omega_\phi s + \omega^2_\phi} \tag{2.3}$$

$$\frac{p}{p_c} = \frac{(\tau s + 1)\,\omega^2_\phi}{s^2 + 2\zeta\omega_\phi s + \omega^2_\phi} \tag{2.4}$$

Transfer functions similar to Eqs. 2.3 and 2.4 are required for the pitch axis.

The desired vertical velocity and yaw rate transfer functions for RC are

$$\frac{w}{w_c} = \frac{\lambda_w}{s + \lambda_w} \tag{2.5}$$

$$\frac{r}{r_c} = \frac{\lambda_r}{s + \lambda_r} \tag{2.6}$$

The vertical velocity and yaw rate bandwidths are given by λ_w and λ_r, respectively. In order to satisfy ultra high gain tasks, the values for these eigenvalues are typically 4 rad/s. For ordinary flight path management, λ_w can be much less.

TRCPH can be achieved by second order transfer functions of the form

$$\frac{u}{u_c} = \frac{\omega^2_u}{s^2 + 2\zeta\omega_u s + \omega^2_u} \tag{2.7}$$

$$\frac{v}{v_c} = \frac{\omega^2_v}{s^2 + 2\zeta\omega_v s + \omega^2_v} \qquad (2.8)$$

In general, bandwidths of the order of 1 rad/s are required for TRCPH. This is considerably less than the 4 rad/s required for RC and ACAH.

C. Dynamic Requirements, Hover and Low Speed

Dynamic response to control requirements are divided into small, medium and large amplitude responses. The small amplitude response is characterized by attitude and velocity stability, or low pilot workload in the primary control axis. This mainly involves closed loop tracking tasks and can also be characterized by bandwidth frequency.

1. Small Amplitude Attitude Changes (Pitch and Roll)

The small amplitude response criteria are divided into high frequency and mid-to-low frequency spectra. Small amplitude criteria can be evaluated using linear models. The high frequency criteria are specified in terms of the maximum closed loop bandwidth parameter. The bandwidth is defined as a function of phase or gain margin of the open loop Bode plot as shown in Figures 2.1 and 2.2.

It can be seen from Fig. 2.3 that the required bandwidth increases as the phase delay parameter increases above approximately 0.17 seconds. Fig. 2.3 also shows that the bandwidth is very sensitive to lags and delays in the flight control system. Phase delay is a measure of how quickly the phase lag increases at frequencies beyond that for which phase shift is -180 degrees. A rotorcraft with rapid phase drop off will be more sensitive than one with gradual phase drop off. Therefore a higher bandwidth is required to maintain Level 1 handling qualities.

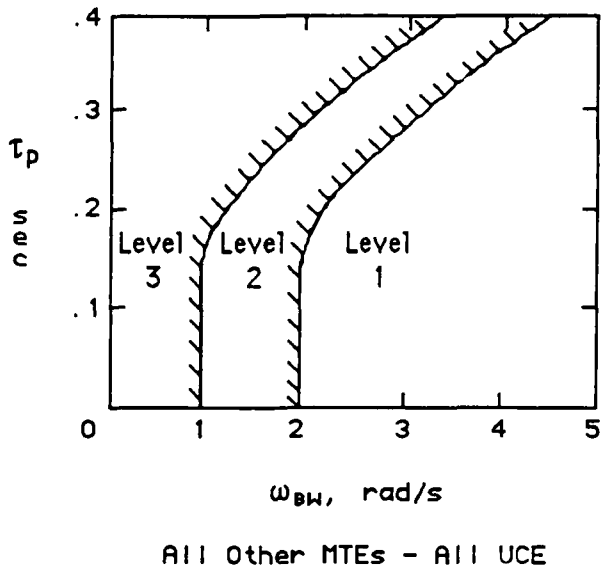

Fig. 2.3 Requirements for Small Amplitude Attitude Changes.

Helicopters exhibit relatively low frequency responses in side and forward velocity which are somewhat analogous to the phugoid response of fixed wing aircraft. These are called the mid-term responses. The handling qualities for these mid-term responses are specified in terms of the frequency and damping ratio. For Level 1 handling qualities, a damping ratio of at least 0.35 is required except when frequencies fall below 0.5 rad/s. For frequencies below 0.5 rad/s, unstable responses are acceptable provided the time to double is not too large.

The mid-term response is specified in terms of frequency and damping of characteristic oscillations as shown in Fig. 2.4. Mid-term is defined as a frequency range below bandwidth but above steady state. Mid-term response characteristics represent the handling qualities most affected by mission requirements for divided attention. Simply stated, the pilot should be able to relinquish control of the helicopter for short periods without encountering significant excursions. Fig. 2.4 represents a more stringent Level 1 boundary and less stringent Level 2 boundary [8] than previously used. Since the old MIL-H-8501A

[1] boundary allowed essentially zero damping at ω_n = 1 rad/s, the revised Level 1 boundary is more consistent with the proposed bandwidth requirement for ω_{BW} > 1 rad/s .

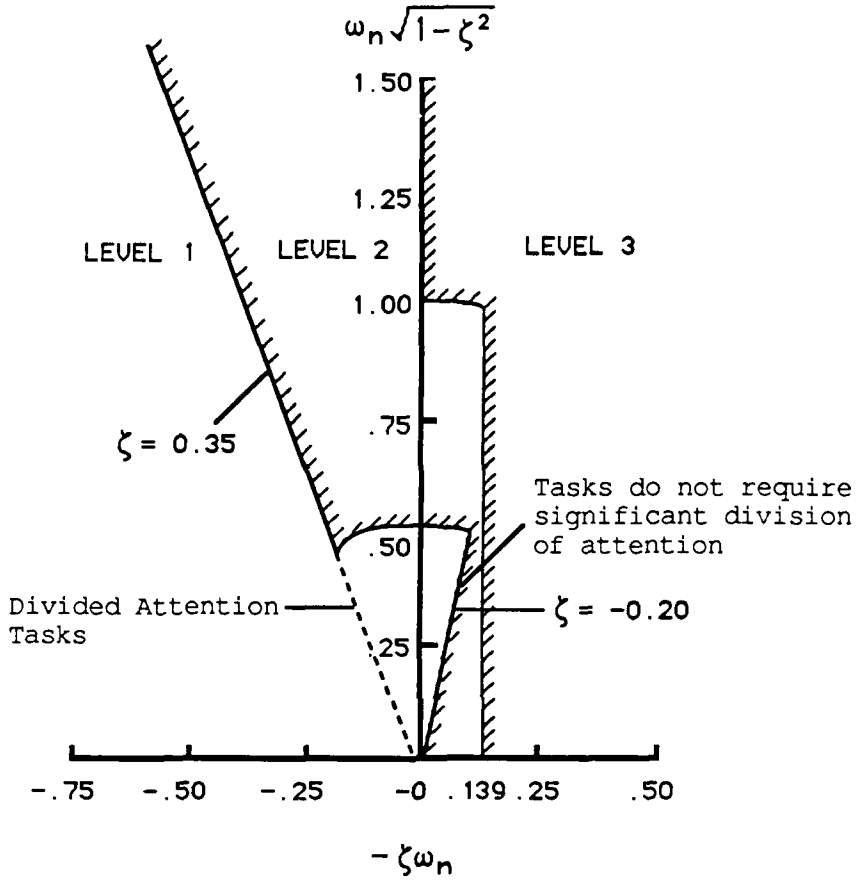

Fig. 2.4 Limits on Mid-Term Eigenvalues.

For Level 1 and divided attention tasks, a damping ratio of at least 0.35 is required for all mid and low frequency oscillations. If full attention is possible, low frequency instabilities at frequencies below 0.5 rad/s are allowed for Level 1. A minimum damping ratio of -0.2 is required for these low frequency unstable eigenvalues. In terms of doubling time, Level 1 requires t_{double} > 6.76 seconds. As can be seen from Fig. 2.4, Level 2 requires low frequency unstable oscillatory modes to have a maximum bandwidth of 0.139 rad/s. This corresponds to a minimum allowable t_{double} of 4.96 seconds.

2. Moderate Amplitude Attitude Changes (Pitch and Roll)

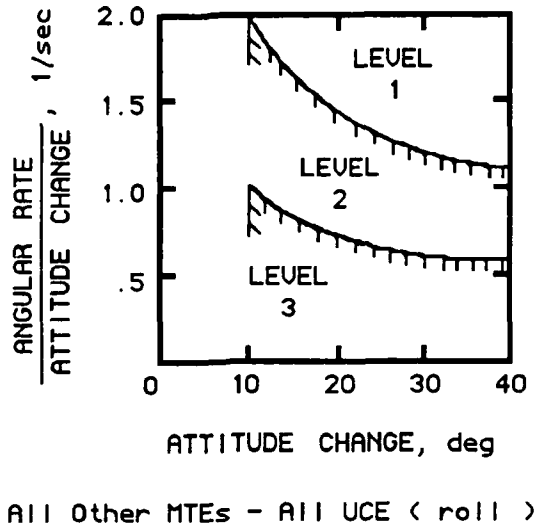

Fig. 2.5 Requirements for Moderate Amplitude Roll Attitude Changes.

Evaluation of moderate amplitude attitude changes require nonlinear analyses and simulations. The requirement for moderate attitude changes are shown in Fig. 2.5. The parameter $p_{pk}/\Delta\phi_{pk}$ is the ratio of the maximum roll rate achieved while changing from one steady roll attitude to another, divided by the roll attitude change. Moderate amplitude specifications given in terms of peak angular rate per attitude change are the same for hover/ low speed and forward flight.

3. Large Amplitude Attitude Changes (Pitch and Roll)

The large amplitude requirements are specified as the minimum achievable angular rate for rate response types and as the minimum achievable angle for attitude response types. As for moderate amplitude changes, evaluation of these criteria require nonlinear analyses and simulations. The criteria are grouped into three levels of aggressiveness corresponding to the needs of the Mission Task Elements, as shown in Table 2.1.

Mission Task Element	Rate Response Types			Attitude Response Types	
	Minimum Achievable Angular Rate, deg/sec			Minimum Achievable Angle, deg	
	Level 1			Level 1	
	p	q	r	ϕ	θ
Limited Maneuvering	± 21	± 6	± 9.5	± 13	± 13
Moderate Maneuvering	± 50	± 13	± 22	± 60	+ 20 - 30
Aggressive Maneuvering	± 50	± 30	± 60	± 60	± 30

Table 2.1 Requirements for Large-Amplitude Attitude Changes.

4. Inter-axis Coupling

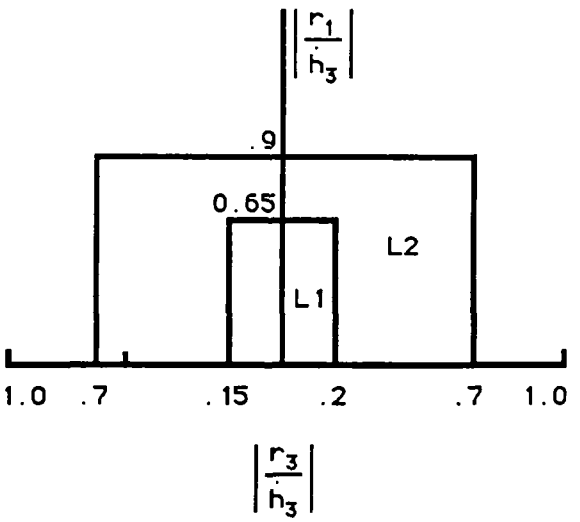

Fig. 2.6 Yaw Cross Coupling Criteria.

Cross-coupling can be a significant problem during aggressive maneuvering. Fig. 2.6 illustrates the requirement that collective control is to achieve vertical velocity response and

shall not cause objectional response in yaw or other axes. Limits on this form of cross-coupling are specified in terms of yaw rate oscillation parameters per rate of climb.

From Fig. 2.6, the vertical axis defines the absolute ratio of yaw rate response at 1 second to vertical velocity response at 3 seconds due to a step collective command. Likewise the horizontal axis defines the absolute ratio of yaw rate response at 3 seconds to vertical velocity response at 3 seconds due to a step collective command. For Level 1 handling qualities, $\left|\frac{r_1}{\dot{h}_3}\right|$ must be smaller than 0.65 and $\left|\frac{r_3}{\dot{h}_3}\right|$ must be between 0.15 and 0.2.

In addition, specific requirements are provided for roll due to pitch, and pitch due to roll. These requirements apply for aggressive maneuvering MTEs. Limits are placed on the ratio of off-axis response to the on-axis response. For at least 5 seconds of time response, the ratio of pitch rate to roll rate for a lateral cyclic step input (or roll rate to pitch rate for a longitudinal cyclic step input) shall be less than 0.25 for Level 1 handling qualities.

5. Response to Disturbances

To ensure adequate disturbance rejection, the specification requires short-term response to wind gusts to have the same bandwidth as the response to control. The specification further requires inputs to be made directly at the control actuator (the swashplate on the helicopter) so that the resulting response can meet the same bandwidth criterion as response to control. The disturbance rejection requirements only apply to Level 1 handling qualities.

References

1. "Military Specification - Helicopter Flying and Ground Handling Qualities; General Requirements for," U.S. Army, MIL-H-8501A, Sept. 1961.

2. Hoh, Roger H., Mitchell, David G., Aponso, Bimal L., Key, David L., Blanken, Chris L., "Proposed Specification for Handling Qualities of Military Rotorcraft, Volume 1 - Requirements," USAAVSCOM Technical Report 87-A-4, May 1985.

3. Tischler, Mark B., Fletcher, Jay W., Morris, Patrick M., and George, T. Tucker, "Application of Flight Control System Methods to an Advanced Combat Rotorcraft," Proceedings of Royal Aeronautical Society International Conference on Helicopter Handling Qualities and Control, London, Nov. 1988.

4. Mitchell, David G., "On Mapping Bandwidth into the Time Domain," Working Paper No. 1194-8, System Technology, Inc., Hawthorne, CA, January 1985.

5. Hoh, Roger H., "Dynamics Requirements in the New Handling Qualities Specification for US Military Rotorcraft," Proceedings of Royal Aeronautical Society International Conference on Helicopter Handling Qualities and Control, London, Nov. 1988.

6. Key, David L., "A New Handling Qualities specification for U.S. Military Rotorcraft," Proceedings of Royal Aeronautical Society International Conference on Helicopter Handling Qualities and Control, London, Nov. 1988.

7. Tischler, Mark B., "Assessment of Digital Flight-Control Technology for Advanced Combat Rotorcraft," *Journal of the American Helicopter Society*, Oct. 1989, pp. 66-76.

8. Aponso, Bimal L., Mitchell, David G., and Hoh, Roger H., "Simulation Investigation of the Effects of Helicopter Hovering Dynamics on Pilot Performance," *Journal of Guidance, Control and Dynamics*, Vol. 13, No. 1, Jan.-Feb. 1990, pp. 8-15.

Chapter 3

Theory of Eigenstructure Assignment

I. Introduction

For a controllable system, eigenstructure assignment techniques use feedback control to place closed loop eigenvalues and shape closed loop eigenvectors to achieve performance specifications. Eigenstructure assignment can be achieved directly by least squares techniques [1]-[7], or asymptotically by linear quadratic regulator (LQR) methods [8]-[9]. Both methods have advantages and disadvantages. For a system with full state LQR controllers, the minimum singular value of the return difference matrix is always greater than or equal to one. This guarantees gain margins of at least ±6 dB with no variations in phase, and phase margins of ±60 degrees with no variations in gain [10]-[11]; however, since a state estimator is almost always required in the feedback loop, the stability margins may be lost in practice (as shown by Doyle in [12]) unless some type of loop transfer recovery (LTR) [13]-[14] procedure is used to partially restore them.

The direct approach does not result in guaranteed stability margins; however in practice, stability margins are often good and Gilbert [15] has shown that sensitivity of eigenvalue locations to parameter variations can be minimized if the closed loop eigenvectors are made as orthogonal as possible. The asymptotic LQR approach requires a controllable system while the direct approach does not. In fact, the direct approach can be used to shape eigenvectors associated with uncontrollable eigenvalues. The direct approach can be used to design a gain matrix which uses sensor outputs for direct output feedback although in this case stability is not guaranteed.

Finally, in the limit, the asymptotic LQR approach drives some of the closed loop eigenvalues to infinity. In practice, this may result in excessively high bandwidth. The direct approach can be used to maintain eigenvalues in their open loop position if the response associated with these eigenvalues is satisfactory and it is not desired to move them. When compared with eigenstructure assignment by LQR theory, the advantages of the direct method outweigh its disadvantages, so the direct method will be used in this study. In addition, an eigenstructure method for the design of state estimators which exhibit LTR has been developed [16].

II. Full State Feedback

Consider a linear time invariant system described by the equations

$$\dot{x} = A x + B u \tag{3.1}$$

$$y = C x \tag{3.2}$$

where $x \in \Re^n$, $u \in \Re^m$, $y \in \Re^r$ are called the state, control input and output respectively. A, B and C are real constant matrices of appropriate dimensions with the assumptions that

$$\text{rank } [B] = m \neq 0$$

and $$\text{rank } [C] = r \neq 0$$

If the system described in Eq. 3.1 and 3.2 is controllable and observable and a linear control law

$$u = - K x \tag{3.3}$$

is assumed, the following results can be proven [2], [4] :

(1) The position of max(m,r) closed loop eigenvalues can be assigned arbitrarily provided that $\{ \lambda_i^d \}$, i = 1, 2, n is a self-conjugate set of scalars.

(2) The shape of max(m,r) eigenvectors can be partially assigned with min(m,r) entries in each vector arbitrarily chosen. $\{ \nu_i^d \}$, i = 1, 2, n is a self-conjugate set of n-eigenvectors (linearly independent) corresponding to the self-conjugate set of eigenvalues $\{ \lambda_i^d \}$.

(3) The eigenvector must reside in the m-dimensional subspace spanned by the columns of $(\lambda_i I - A)^{-1} B$.

The sets $\{ \lambda_i^d \}$ and $\{ \nu_i^d \}$ correspond to the desired closed loop eigenvalues and eigenvectors pair while the matrix K is the constant feedback gain matrix.

The solution of the control problem is a real (mxn) matrix K such that the eigenvalues of A - BK are precisely those of λ_i^d with corresponding eigenvector ν_i^d. Since a fixed eigenstructure uniquely defines (A - BK), it is true that if K exist and rank [B] = m, then K is unique. The number of control variables available determines the dimensions of the subspace which the achievable eigenvectors must reside. The orientation of the subspace is determined by the matrices A, B and the desired closed loop eigenvalues λ_i^d. In general, more than min(m,r) entries in a particular vector have to be assigned in order to shape the transient response characteristics of the system. This may result in a desired eigenvector that does not reside in the subspace spanned by the columns of $(\lambda_i I - A)^{-1} B$. Consequently, the desired closed loop eigenvector that does not lie precisely within the prescribed subspace can not be achieved exactly and can only be achieved in a least squares sense (the orthogonal projection of ν_i^d onto the subspace spanned by the columns of $(\lambda_i I - A)^{-1} B$).

Consider the closed loop system given in Eq. 3.4

$$\dot{x} = (A - BK) x \tag{3.4}$$

If it is desired to move as eigenvalue, the design procedure consists of determining the gain matrix K such that for all desired closed loop eigenvalue/eigenvector pairs (λ_i and v_i),

$$(A - BK) v_i = \lambda_i v_i \tag{3.5.a}$$

or $$v_i = (\lambda_i I - A)^{-1} BK v_i \tag{3.5.b}$$

We define the m-vector m_i as

$$m_i = - K v_i \tag{3.6}$$

This is equivalent to finding m_i such that

$$(\lambda_i I - A) v_i = B m_i \tag{3.7}$$

Once the m_i's have been found, the gain matrix is calculated as

$$K = - MV^{-1} \tag{3.8}$$

where M is a matrix whose columns are m_i and V is a matrix whose columns are v_i. This is the feedback gain when the desired eigenvector resides in the prescribed subspace and can be attained exactly.

In general, the desired eigenvectors are not achievable, therefore, the m_i's are selected to minimize the weighted sum of the squares of the difference between the elements of the desired and attainable eigenvectors. This is expressed as the following performance index

$$J_i = (v_i^a - v_i^d)^* P_i (v_i^a - v_i^d) \tag{3.9}$$

where v_i^a is the achievable closed loop eigenvector, and P_i is a positive definite symmetric matrix whose elements are coefficients that weight certain components of the corresponding desired and achievable eigenvectors more heavily than others. For a fixed λ_i, it is desired to minimize J_i subject to Eq. 3.8. Adjoining Eq. 3.8 to J_i with the Lagrange multipliers μ_i

$$\bar{J}_i = (v_i^a - v_i^d)^* P_i (v_i^a - v_i^d) + \mu_i^* [(\lambda_i I - A) v_i^a - B m_i] \tag{3.10}$$

Now, Eq. 3.10 is minimized when

$$\frac{\partial \bar{J}}{\partial m_i} = - \mu_i^* B = 0 \tag{3.11}$$

$$\frac{\partial \bar{J}}{\partial v_i} = (v_i^a - v_i^d)^* P_i + \mu_i^* (\lambda_i I - A) = 0 \tag{3.12}$$

In matrix form, Equations 3.6, 3.9, and 3.10 become

$$\begin{bmatrix} (\lambda_i I - A) & -B & 0 \\ 0 & 0 & -B^T \\ P_i & 0 & (\lambda_i I - A)^* \end{bmatrix} \begin{bmatrix} v_i^a \\ m_i \\ \mu_i \end{bmatrix} = \begin{bmatrix} 0 \\ 0 \\ P_i v_i^d \end{bmatrix}$$

or

$$N_i \begin{bmatrix} v_i^a \\ m_i \\ \mu_i \end{bmatrix} = \begin{bmatrix} 0 \\ 0 \\ P_i v_i^d \end{bmatrix}$$

Garrard and Liebst [17] have shown that if the system is controllable, N_i is non-singular even if λ_i remains at its open loop position. The achievable v_i and m_i are then given in Eq. 3.13.

$$\begin{bmatrix} v_i \\ m_i \\ \mu_i \end{bmatrix} = N_i^{-1} \begin{bmatrix} 0 \\ 0 \\ P_i v_i^d \end{bmatrix} \tag{3.13}$$

It is obvious that by setting $m_i = 0$ assures that the associated v_i and λ_i remain in their open loop configuration.

III. Full State Estimator for LTR

Once the full state feedback gain matrix, K, has been determined, the problem of constructing a state estimate, $\hat{x}$, from measurements, y, must be addressed. A common regulator/estimator scheme is as follows. Considering the control law given by

$$u = - K \hat{x} \tag{3.14}$$

where $\hat{x}$ is the estimated state vector given by the state estimator's equation

$$\dot{\hat{x}} = A \hat{x} + Bu + L (y - C \hat{x}) \tag{3.15}$$

Using the estimates of the state in the control law results in the compensator transfer function

$$K(s) = K (sI - A + BK + LC)^{-1} L (s) \tag{3.16}$$

The objective is to choose the estimator gain matrix, L, such that (A - LC) is stable and the performance of the regulator/estimator closely resembles that of the full state feedback for some bounded.frequency range.

In the full state feedback case, the return difference matrix is

$$I + K (sI - A)^{-1} B (s) \tag{3.17}$$

which in the combined regulator/ estimator case is

$$I + K(s)\, G(s) \tag{3.18}$$

where K(s)G(s) is the properties when the loop is broken at the input of the plant. It is obvious that in the SISO case if one wishes to recover F(s), then L(s) should be chosen such that

$$K(s) \approx \frac{F(s)}{G(s)} \tag{3.19}$$

inverting the plant from the left by moving the poles of K(s) towards the zeroes of G(s). Hence, it is important that the plant is minimum phase (no right half plane zero) to ensure that the eigenvalues of the estimator, (A - LC), are stable.

A technique for designing the filter gain matrix, L in the MIMO case to recover F(s) by eigenstructure assignment was shown by Kazerooni and Houpt [16]. As shown by Doyle and Stein in [13] and [18], L is chosen such that the filter gain has the following asymptotic behavior as $q \rightarrow \infty$

$$\frac{L(q)}{q} \rightarrow BW \qquad \text{where } WW^T = I \tag{3.20}$$

When this L is used in the loop transfer expression, as q becomes large (assuming G(s) is minimum phase), the filter gain behaves in such a way that

$$\lim_{q\rightarrow\infty} K(s)\, G(s) \rightarrow K\,(\,sI - A\,)^{-1}\, B(s) \tag{3.21}$$

where the convergence is pointwise in s. This design procedure essentially inverts the plant from the left i.e.

$$\lim_{q\rightarrow\infty} K(s) = K\,(\,sI - A\,)^{-1}\, B\,[\,C\,(\,sI - A\,)^{-1}\, B\,]^{-1}(s) \tag{3.22}$$

This inversion is why G(s) is not allowed to have zeros in the right half plane. However, the recovery procedure is effective as long as G(s) has no right half plane zeros with magnitudes in frequency ranges where high loop gain is required.

Thus, by choosing

$$L = qBW \tag{3.23}$$

Eq. 3.20 will be satisfied and the LTR of Eq. 3.21 will be achieved as $q \rightarrow \infty$. Kazerooni [16] shows that, for a minimum phase plant, as $q \rightarrow \infty$ the consequences of choosing L as in Eq. 3.23 are:

1. The $j \leq n - m$ finite closed loop eigenvalues, λ_i, of (A - LC) and (A - BK - LC) approach the finite transmission zeroes, z_i, of the plant.

2. The remaining n - j closed loop eigenvalues approach infinity in the left half plane with the direction of their associated eigenvectors being arbitrary.

3. The left closed loop eigenvectors, ν_i of (A - LC) associated with the finite closed loop estimator eigenvalues, λ_i, approaches the left zero direction, μ_i, of the transmission zero, z_i, which satisfies

$$\begin{bmatrix} \mu_i^T & \zeta_i^T \end{bmatrix} \begin{bmatrix} z_i I - A & B \\ -C & 0 \end{bmatrix} = 0$$

4. As the infinite closed loop poles move away from the imaginary axis, an equal number of closed loop finite eigenvalues of the compensator will cancel out the left finite transmission zeros of the full state model and hence achieving pointwise loop transfer recovery

$$K(s)\,G(s) \rightarrow K\,(\,sI - A\,)^{-1}\,B(s)$$

Therefore, for a minimum phase system, an estimator which combines any stable infinite eigenstructure with the finite eigenstructure of conditions 1 through 3 would result in LTR. Using the procedure for an unstable system results in a loss of accuracy in the approximation of the desired loop shape. If there are no right half plane zeros with magnitudes in frequency ranges where high loop gain is required, then placing the estimator poles at the mirror image of the right half plane zeros achieves reasonable LTR.

IV. Asymptotic Linear Quadratic Regulator Theory

In LQR methods, the designer selects the weighting matrix which includes all the performance requirements and is constrained to be quadratic in states and controls. This section describes a scheme for the selection of quadratic weights asymptotically to achieve a desired closed loop eigenstructure as the weights on the control tend to zero. Eigenvalue and eigenvector properties are developed both for the poles which remain asymptotically finite and for those which go asymptotically to infinity. These properties are used to provide a complete unique characterization of quadratic weights during eigenstructure assignment design.

The detailed derivation of the procedure and the proof of the related theorems and lemmas are provided by Harvey and Stein [8]. This section also includes a summary of asymptotic properties of multivariable regulators. A constructive procedure to define quadratic weights is outlined. This procedure is based on modal design criteria and the asymptotic properties of optimal controllers.

Consider the standard multivariable linear time invariant feedback system

$$\dot{x} = A x + B u \tag{3.24}$$

$$u = - K x \tag{3.25}$$

$$r = H x \tag{3.26}$$

where x is the n-dimensional state vector, u is an m-vector of controls, and H is an m-vector of responses. A, B, K and H are constant matrices of appropriate dimension. It is assumed that the pair (A,B) is controllable, the pair (A,H) is observable, and that the mxm matrix HB has full rank (i.e. rank [HB] = m).

The feedback gains, K are a result of the linear quadratic (LQ) optimization problem [19]. An LQ optimization problem for the system in Eq. 3.24 is one described by linear differential equations with a performance index

$$J = \int_0^\infty (x^T Q x + \rho u^T R u) \, dt \tag{3.27}$$

represented by the integral of a quadratic function of states and control inputs where $Q = Q^T \geq 0$, $R = R^T > 0$, ($A, Q^{1/2}$) observable and scalar $\rho \geq 0$. This criterion is minimized by the control function

$$u = K^* x \tag{3.28}$$

where

$$K^* = R^{-1} B \frac{P}{\rho} \tag{3.29}$$

$P = P^T > 0$ is the unique positive definite solution of the algebraic Riccati equation

$$0 = P A + A^T P + Q - P B R^{-1} B^T \frac{P}{\rho} \tag{3.30}$$

The behavior of both eigenvalues and eigenvectors are used to provide complete, unique specification of the weights Q and R, and in particular, as the scalar ρ tends to zero.

The arbitrary performance index given in Eq. 3.27 is equivalent to

$$J' = \int_0^\infty (r^T r + \rho u^T R u) \, dt \tag{3.31}$$

with r defined by Eq. 3.26 form some mxn matrix H. These two performance indices produce the same gain matrix, K^*, as the solution of their respective LQ optimization problems.

Consider Q matrices of the form $Q = H^T H$ with row dimension of H equal to the dimension of u. If m is unity, then a dyadic Q suffices. If H is full rank, it is always possible to rearrange states and normalize H as follow

$$H = W H_0 \tag{3.32}$$

where

$H_0 = [H_{11} \quad I_m]$ and W is a non-singular mxm matrix.

Consider the linear quadratic regulator from Eq. 3.28 to Eq. 3.30 with performance index given in Eq. 3.31 and normalized H as in Eq. 3.32. Assume further that

(1) rank [HB] = m

(2) the zeros of det (H (sI - A)$^{-1}$ B) lie on the left half plane, are distinct, and do not belong to the σ(A), the spectrum of A.

Then the optimally controlled system has the following properties.

A. Asymptotically Finite Modes

As $\rho \rightarrow 0$, there are (n - m) eigenvalues of the form

$$s_i (\rho) \rightarrow s_i^o$$

$$| s_i^o | < \infty, \qquad i = 1, 2, ..., n - m \tag{3.33}$$

with associated eigenvectors

$$x_i (\rho) \rightarrow (s_i^o - A)^{-1} B v_i^o \tag{3.34}$$

where s_i^o and v_i^o are defined by

$$H (s_i^o - A)^{-1} B v_i^o = 0 \tag{3.35}$$

The finite modes are characterized by (n - m) eigenvalues s_i^o plus (m - 1)x(n - m) parameters for their associated directions v_i^o. These provide a unique definition of $^{\tau}I_0$ via Eq. 3.35.

B. Asymptotically Infinite Modes

As $\rho \rightarrow 0$, there are m eigenvalues of the form

$$s_j (\rho) \rightarrow \frac{s_j^\infty}{\sqrt{\rho}}$$

$$| s_j^\infty | < \infty, \qquad j = 1, 2, ..., m \tag{3.36}$$

with associated eigenvectors

$$x_j(\rho) \rightarrow B v_j^{\infty} \tag{3.37}$$

where s_j^{∞} and v_j^{∞} are defined by

$$R = N^{-T} S^{-2} N^{-1} \tag{3.38}$$

$$W^T W = (H_0 B)^{-T} N^{-T} N^{-1} (H_0 B)^{-1} \tag{3.39}$$

and

$$N \equiv [\, v_1^{\infty} \; v_2^{\infty} \; v_3^{\infty} \; \ldots \; v_m^{\infty} \,] \tag{3.40}$$

$$S \equiv \mathrm{diag}\,(\, s_1^{\infty} \; s_2^{\infty} \; s_3^{\infty} \; \ldots \; s_m^{\infty} \,) \tag{3.41}$$

The asymptotically infinite modes are characterized by (m - 1) parameters for the normalized eigenvalues s_j^{∞} and (m - 1)x(m) parameters for their associated eigenvectors v_j^{∞}. These provide unique definitions of R and W via Eq. 3.38 to Eq. 3.41.

Note that the scalar ρ is the tradeoff parameter for control energy against the degree to which the asymptotic properties are achieved. In addition, the eigenvectors of asymptotically infinite modes are in the range space of B. Hence, if the state model includes actuator dynamics with B non-zero only for actuator rows, the asymptotically infinite modes are actuator modes. The procedures for the construction of H_0 are given below

1. Assume the matrix B has been transformed to the form

$$B = \begin{bmatrix} 0 \\ B_{21} \end{bmatrix} \begin{matrix} n - m \\ m \end{matrix}$$

with mxm matrix B_{21} non-singular.

2. Assume that for each desired asymptotically finite mode, s_i^o, the eigenvectors x_i^* which describe the desired modes can be defined as

$$x(t) = x_i^* e^{(s_i^o)t} \qquad i = 1, 2, ..., n - m \tag{3.42}$$

Note that only a few of the components in x_i^* are actually specified, the rest can be arbitrary.

3. Once the desired eigenvectors are specified, reorder and partition x_i^* as follows :

$$\{ x_i^* \}^{R_i} = \begin{bmatrix} \gamma_i^* \\ \upsilon \end{bmatrix} \tag{3.43}$$

where γ_i^* is the specified subvector, υ's are the unspecified components, and $\{ \cdots \}^{R_i}$ denotes a row reordering operation.

4. The desired mode in Eq. 3.43 may not belong to the set of eigenvectors achievable by LQ design :

$$\begin{bmatrix} \gamma_i^o \\ \upsilon \end{bmatrix} = \{ (s_i^o I - A)^{-1} B \}^{R_i} \nu_i^o$$

$$= \begin{bmatrix} L \\ M \end{bmatrix} \nu_i^o \tag{3.44}$$

5. Using the least square fit method to select ν_i^o so as to best approximate γ_i^* with γ_i^o

$$\nu_i^o = [(\bar{L})^T L]^{-1} (\bar{L})^T \gamma_i^* \tag{3.45}$$

6. Assume that $\{ v_i^o ; i = 1, 2, ..., n - m \}$ have been determined via Eq. 3.34. Then the following matrix of eigenvectors

$$X = [x_1^0 \; x_2^0 \; x_3^0 \; ... \; x_{n-m}^0] \tag{3.46}$$

can be obtained where no linear combination of the x_i^o's fall into the range space of B.

7. Define the projection matrix

$$P = I_n - X [(\bar{X})^T X]^{-1} (\bar{X})^T \tag{3.47}$$

as follows :

$$P = \begin{matrix} \\ \\ \end{matrix} \begin{matrix} n-m & n \\ \end{matrix} \begin{bmatrix} P_{11} & P_{12} \\ P_{12}^T & P_{22} \end{bmatrix} \begin{matrix} n-m \\ m \end{matrix}$$

and note that

$$P B \mu \neq 0 \qquad \text{if} \quad \mu \neq 0 \tag{3.48}$$

8. The non-singularity of B_{21} and the condition given by Eq. 3.48 imply that P_{22} is non-singular. Thus, H_0 is defined as

$$H_0 = [0 \quad P_{22}^{-1}] P = [P_{22}^{-1} P_{12}^T \quad I_m] \tag{3.49}$$

Once the normalized matrix H_0 is obtained from Eq. 3.49, we can then select the eigenvectors and eigenvalue ratios for the asymptotically infinite modes. These were selected to achieve asymptotic decoupling of the modes. Matrices W_0 and R_0 were then computed via Eq. 3.38 and Eq. 3.39. The final step of the performance index selection

procedure is to specify ρ. This can be accomplished by computing LQ solution for a few monotonically decreasing values.

References

1. Cunningham, Thomas B., "Eigenspace Procedures for Closed Loop Response Shaping with Modal Control," Proceedings of the 19th IEEE Conference on Decision and Control, Dec. 1980, pp. 178-186.

2. Andry, A. N., Shapiro, E. Y., and Chung, J.C., "Eigenstructure Assignment for Linear Systems," *IEEE Transactions on Aerospace Electronic Systems*, Sept. 1983, Vol. AES-19, pp. 711-729.

3. Sobel, K. M., and Shapiro, E. Y., "Application of Eigenspace Assignment to Lateral Translation and Yaw Pointing Flight Control," Proceedings of the 23rd IEEE Conference on Decision and Control, Dec. 1984, pp. 1423-1438.

4. Sobel, K. M., and Shapiro, E. Y., "Eigenstructure Assignment: A Tutorial - Part I Theory," Proceedings of the 1985 American Control Conference, Boston, MA, June 1985, pp. 456-460.

5. Sobel, K. M., and Shapiro, E. Y., "A Design Methodology for Pitch Pointing Flight Control Systems," *Journal of Guidance, Control and Dynamics*, Vol. 8, March-April 1985, pp. 181-187.

6. Garrard, W. L., and Liebst, B. S., "Active Flutter Suppression Using Eigenspace and Linear Quadratic Design Techniques," *Journal of Guidance, Control and Dynamics*, Vol. 8, May-June 1985, pp. 304-311.

7. Liebst, B. S., Garrard, W. L., and Adams, W. M., "Design of an Active Flutter Suppression System," *Journal of Guidance, Control and Dynamics*, Vol. 8, Jan-Feb 1986, pp. 64-71.

8. Harvey, Charles. A., and Stein, Gunter., "Quadratic Weights for Asymptotic Regulator Properties," *IEEE Transactions on Automatic Control*, Vol. AC-23, No. 3, June 1978, pp. 378-381.

9. Stein, G., "Generalized Quadratic Weights for Asymptotic Regulator Properties," *IEEE Transactions on Automatic Control*, Vol. 24, Aug. 1979, pp. 559-566.

10. Safanov, M. G., and Athans, M., "Gain and Phase Margins of Multiloop LQR Regulators," *IEEE Transactions on Automatic Control*, Vol. 22, April 1977, pp. 173-179.

11. Lehtomaki, N. A., Sandell, N. R. Jr., and Athans, M., "Robustness Results in Linear Quadratic Gaussian Based Multivariable Control Designs," *IEEE Transactions on Automatic Control*, Vol. AC-26, Feb. 1981, pp. 75-92.

12. Doyle, John C., "Guaranteed Margins for LQG Regulators," *IEEE Transactions on Automatic Control*, AC-23, Aug. 1978, pp.756-757.

13. Doyle, John C., and Stein, Gunter, "Robustness with Observers," *IEEE Transactions on Automatic Control*, AC-24, Aug. 1979, pp.607-611.

14. Stein, G., and Athans M., "The LQG/LTR Procedure for Multivariable Feedback Control Design," *IEEE Transactions on Automatics Control*, AC-32, Feb. 1937, pp. 105-114.

15. Gilbert, E. G., "Conditions for Minimizing Norm Sensitivity of Characteristics Roots," *IEEE Transactions on Automatics Control*, Vol. 29, Aug. 1984, pp. 623-626.

16. Kazerooni, H., and Houpt, P. K., "On the Loop Transfer Recovery," *Int. Journal of Control*, Vol. 43, 1986, pp. 981-996.

17. Liebst, B. S., Garrard, W. L., and Adams W. M., "Design of an Active Flutter Control System," Proceedings of the 1984 AIAA Guidance and Control Conference, Seattle, Washington, Aug. 1984.

18. Doyle, J. C., and Stein, G., "Multivariable Feedback Design: Concepts for a Classical /Modern Synthesis," *IEEE Transactions on Automatics Control*, Vol. AC-26, Feb. 1981, pp.4-16.

19. M. Athans, "The Role and Use of the Stochastic Linear-Quadratic-Gaussian Problem in Control System Design," *IEEE Transactions on Automatic Control*, Vol. AC-16, Dec. 1971, pp. 529-551.

Chapter 4

Mathematical Model

I. Introduction

The dynamic stability and response to control inputs of the rotorcraft rigid body dynamics define its handling qualities. The six rigid body degrees of freedom are the basic motions involved in the analysis of flight dynamics. The rotor is also a major factor in the dynamic response characteristics of helicopters, and therefore it is necessary to consider the rotor degrees of freedom as well, particularly the tip path plane flapping motion. The arrangement of the rotor or rotors on a helicopter is also an important factor in its behavior, notably its stability and control characteristics. Because of the rotation of the rotor, there is considerable coupling between the longitudinal and lateral directional motions.

Since the handling qualities of the helicopter have different characteristics in hover and in forward flight, only the hover regime will be analyzed here. The hovering analysis is simpler than forward flight because of the axisymmetry of the rotor aerodynamics in hover. The equations are developed in this Chapter in the following way. The helicopter is first regarded as a single rigid body, and the equations of motion are derived with respect to a set of axes fixed in it. The derivation will be developed for the single main rotor and tail rotor configuration. This configuration of helicopter uses the tail rotor to provide the anti-torque in order to balance the torque produced by the main rotor and the yaw control.

II. Equations of Motion

A. Rigid Body Dynamics

Consider the rigid body motions of a helicopter with a single main rotor and a tail rotor. It is assumed that the helicopter has complete axisymmetry, although the longitudinal - lateral dynamics are coupled, the vertical and the longitudinal-lateral dynamics are completely separated. Such separation is a basic feature of the rotor in hover, and generally holds for the hover handling qualities even though the entire helicopter is not exactly axisymmetric.

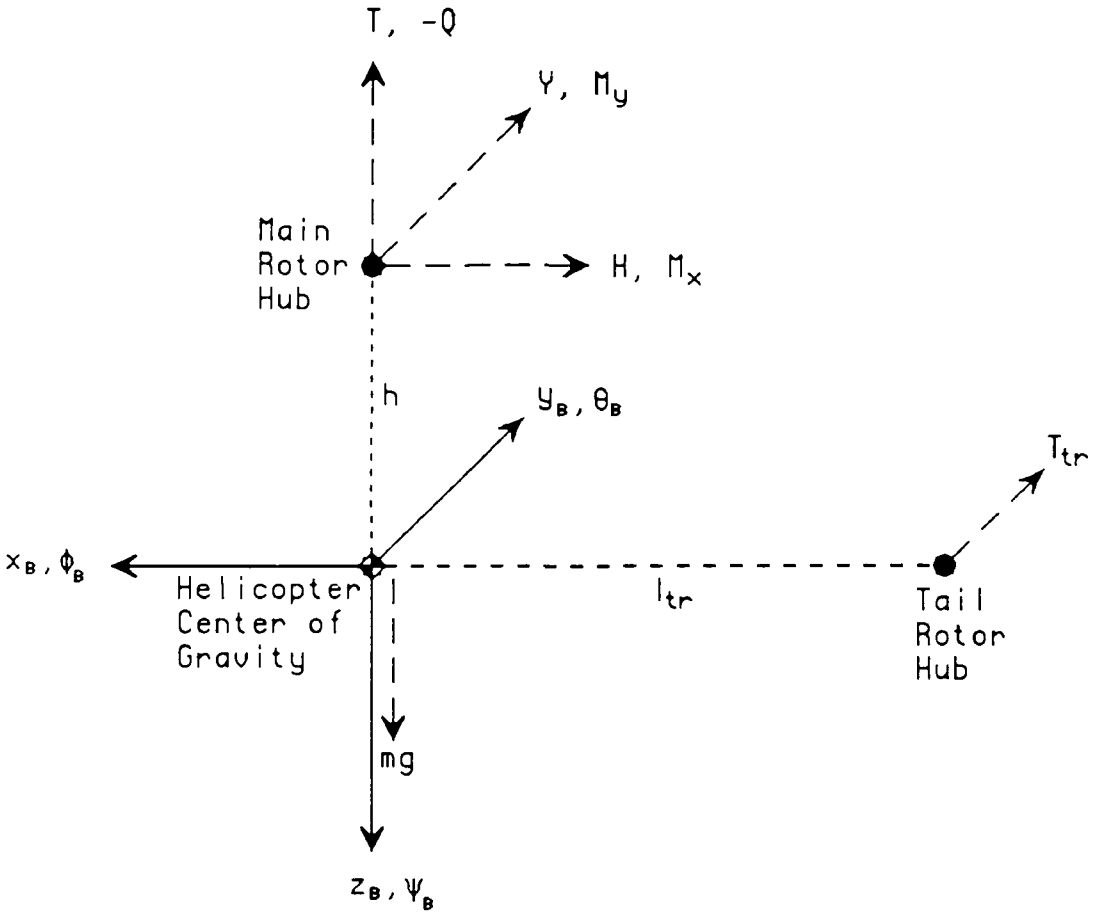

Fig. 4.1 Definition of the Rigid Body Degrees of Freedom of a Helicopter, and the Forces and Moments due to the Main Rotor, Tail Rotor and Gravity.

A body fixed orthogonal coordinate system is used, with the origin at the helicopter center of gravity (mass). The z-axis is vertical with the center of gravity directly under the

rotor hub. The x-axis is positive forward, the y-axis is positive to the right, and the z-axis is positive downward and is lying in the plane of symmetry. It is assumed that these axes are the principal axes of the helicopter, so inertial cross coupling between the yaw and roll axes is neglected. Figure 4.1 shows the free body diagram of the helicopter.

The linear displacement of the center of gravity has the components x_B, y_B, and z_B; the roll, pitch, and yaw angular rotations of the helicopter about the center of gravity are given by the Euler angles ϕ_B, θ_B, and ψ_B. The helicopter angular velocity has components in the body axes

$$p = \dot{\phi}_B - \dot{\psi}_B \sin(\theta_B) \qquad \text{(a)}$$

$$q = \dot{\theta}_B \cos(\phi_B) + \cos(\theta_B) \sin(\phi_B) \qquad \text{(b)} \quad (4.1)$$

$$r = -\dot{\theta}_B \sin(\phi_B) + \dot{\psi}_B \cos(\theta_B) \cos(\phi_B) \qquad \text{(c)}$$

inverting these equations gives the angular rates

$$\dot{\phi}_B = p + q \tan(\theta_B) \sin(\phi_B) + r \tan(\theta_B) \cos(\phi_B) \qquad \text{(d)}$$

$$\dot{\theta}_B = q \cos(\phi_B) - r \sin(\phi_B) \qquad \text{(e)} \quad (4.2)$$

$$\dot{\psi}_B = r \left(\frac{\cos(\phi_B)}{\cos(\theta_B)}\right) \qquad \text{(f)}$$

The components of the linear velocity of the center of gravity V, are

$$u = \dot{x}_B \cos(\theta_B) \cos(\psi_B) + \dot{y}_B [\sin(\phi_B) \sin(\theta_B) \cos(\psi_B) - \cos(\phi_B) \sin(\psi_B)] + \dot{z}_B [\cos(\phi_B) \sin(\theta_B) \cos(\psi_B) + \sin(\phi_B) \sin(\psi_B)] \qquad \text{(a)}$$

$$v = \dot{x}_B \cos(\theta_B) \sin(\psi)_B) + \dot{y}_B [\sin(\phi_B) \sin(\theta_B) \sin(\psi_B) + \cos(\phi_B) \cos(\psi_B)] + \dot{z}_B [\cos(\phi_B) \sin(\theta_B) \sin(\psi_B) - \sin(\phi_B) \cos(\psi_B)] \qquad \text{(b)} \quad (4.3)$$

$$w = -\dot{x}_B \sin(\theta_B) + \dot{y}_B \sin(\phi_B)\cos(\theta_B) + \dot{z}_B \cos(\phi_B)\cos(\theta_B) \qquad (c)$$

The translational acceleration components of $\frac{dV}{dt}$ along the body-fixed axes will contain not only the components $\frac{du}{dt}$, $\frac{dv}{dt}$, and $\frac{dw}{dt}$ but also centripetal acceleration components due to the rotation of the body-fixed axis system relative to inertial space. The set of linear accelerations is given by

$$\frac{du}{dt} = \dot{u} + qw - rv \qquad (a)$$

$$\frac{dv}{dt} = \dot{v} + ru - pw \qquad (b) \quad (4.4)$$

$$\frac{dw}{dt} = \dot{w} + pv - qu \qquad (c)$$

By Newton's 2nd Law for a rigid body, force is equal to the rate of change of linear momentum. The mass of the helicopter, m, remains essentially constant during a maneuver. The force $\boldsymbol{F}$ is resolved into components F_x, F_y, and F_z along the x, y, and z body axes, and the three scalar equations can be written as

$$F_x = m\frac{du}{dt} = m(\dot{u} + qw - rv) \qquad (a)$$

$$F_y = m\frac{dv}{dt} = m(\dot{v} + ru - pw) \qquad (b) \quad (4.5)$$

$$F_z = m\frac{dw}{dt} = m(\dot{w} + pv - qu) \qquad (c)$$

The forces and moments that are generated by the rotor systems and all other aerodynamically generated forces and moments are considered to be the external forces/ moments in the equations of motion. All forces and moments are expressed relative to the body center of gravity for use in the six degrees of freedom rigid body equations of motion. The external aerodynamic and propulsive forces and moments are denoted by X,

Y, Z, and L, M, N respectively. Since the center of gravity coincides with the center of mass, the gravity force produces no external moments about that point. Gravity can contribute components only to the summation of the external forces. The components of the weight in the directions of the axes are

$$X_g = - mg \sin(\theta_B) \quad \text{(a)}$$

$$Y_g = mg \cos(\theta_B) \sin(\phi_B) \quad \text{(b)} \quad (4.6)$$

$$Z_g = mg \cos(\theta_B) \cos(\phi_B) \quad \text{(c)}$$

with the aerodynamic forces (including propulsive forces), the resultant external forces are

$$F_x = X - mg \sin(\theta_B) \quad \text{(a)}$$

$$F_y = Y + mg \cos(\theta_B) \sin(\phi_B) \quad \text{(b)} \quad (4.7)$$

$$F_z = Z + mg \cos(\theta_B) \cos(\phi_B) \quad \text{(c)}$$

The resulting equations of motion for the translational degrees of freedom are

$$\frac{d}{dt}\begin{pmatrix} u \\ v \\ w \end{pmatrix} = \begin{bmatrix} 0 & -r & q \\ r & 0 & -p \\ -q & p & 0 \end{bmatrix}\begin{pmatrix} u \\ v \\ w \end{pmatrix} + g\begin{pmatrix} -\sin\theta_B \\ \cos\theta_B \sin\phi_B \\ \cos\theta_B \cos\phi_B \end{pmatrix} + \frac{1}{m}\begin{pmatrix} X \\ Y \\ Z \end{pmatrix} \quad (4.8)$$

Since gravity does not contribute to the moments about the mass center, then the external couples, L, M, and N, acting on the helicopter are entirely aerodynamic. For all practical purposes, the inertia tensor is time invariant. The body fixed xz plane of the helicopter is further assumed to be the plane of symmetry, so the products of inertia I_{xy} and I_{yz} are zero. Given these assumptions, the equations for the external moments are

$$L = \dot{p}\, I_{xx} - \dot{r}\, I_{xz} + qr\,(I_{zz} - I_{yy}) - pq\, I_{xz} \qquad (a)$$

$$M = \dot{q}\, I_{yy} + pr\,(I_{xx} - I_{zz}) - r^2\, I_{xz} + p^2\, I_{xz} \qquad (b) \quad (4.9)$$

$$N = \dot{r} I_{zz} - \dot{p}\, I_{xz} + pq\,(I_{yy} - I_{xx}) + qr\, I_{xz} \qquad (c)$$

The equations of motion for the rotational degrees of freedom can be derived from Eq. 4.9 by rearranging the moment inertial terms

$$\frac{d}{dt}\begin{pmatrix} p \\ q \\ r \end{pmatrix} = \begin{pmatrix} I_1\, pq + I_2\, rq \\ I_3\,(p^2 - r^2) + I_4\, pr \\ I_5\, pq + I_6\, qr \end{pmatrix} + \begin{bmatrix} I_7 & 0 & I_8 \\ 0 & I_9 & 0 \\ I_8 & 0 & I_{10} \end{bmatrix} \begin{pmatrix} L \\ M \\ N \end{pmatrix} \qquad (4.10)$$

where

$$I_1 = \frac{-(I_{yy} - I_{xx} - I_{zz})I_{xz}}{I_{xx}I_{zz} - I_{xz}^2} \qquad I_2 = \frac{(I_{yy} I_{zz} - I_{xz}^2 - I_{zz}^2)}{I_{xx}I_{zz} - I_{xz}^2}$$

$$I_3 = \frac{-I_{xz}}{I_{yy}} \qquad I_4 = \frac{(I_{zz} - I_{xx})}{I_{yy}}$$

$$I_5 = \frac{(I_{xx}^2 + I_{xz}^2 - I_{xx} I_{yy})}{I_{xx}I_{zz} - I_{xz}^2} \qquad I_6 = \frac{-(I_{xx} - I_{yy} + I_{zz})I_{xz}}{I_{xx}I_{zz} - I_{xz}^2}$$

$$I_7 = \frac{I_{zz}}{I_{xx}I_{zz} - I_{xz}^2} \qquad I_8 = \frac{I_{xz}}{I_{xx}I_{zz} - I_{xz}^2}$$

$$I_9 = \frac{1}{I_{yy}} \qquad I_{10} = \frac{I_{xx}}{I_{xx}I_{zz} - I_{xz}^2}$$

Equations 4.8 and 4.10 are the six degree of freedom, rigid body equations of motion. If equations 4.8 and 4.10 are combined with the kinematical equations governing the evolution of the Euler angles (Eqs. 4.1 or 4.2), then the dynamics of the helicopter can be described by

$$\dot{x} = f(x,u) \tag{4.11}$$

where x is the state vector and u is the input vector. Equations 4.1, 4.8, and 4.10 contain products of the dependent variables, some of which appear as transcendental function and are in general nonlinear.

The equation of motion are frequently linearized for the use in stability and control analyses. It is assumed that the motion of the helicopter consists of small perturbations from a trim condition of steady flight. Equation 4.11 can then be linearized about a trim flight condition to yield the coefficients of a linear, first order set of differential equations that represents the rigid body dynamics of the helicopter for small perturbations. The operating point equations are obtained by recognizing that zero translational and rotational accelerations are implicit in the concept of a trim condition. Then denoting the trim condition with zero subscript, the perturbed angular velocity has components

$$\begin{aligned} p &= \dot{\phi}_B - \dot{\psi}_B \sin(\theta_0) \\ q &= \dot{\theta}_B \\ r &= \dot{\psi}_B \cos(\theta_0) \end{aligned} \tag{4.12}$$

The components of the linear velocity perturbation are

$$\begin{aligned} u &= (\dot{x}_0 + \dot{x}_B)\cos(\theta_0) - \dot{x}_0 \theta_B \sin(\theta_0) + \dot{z}_B \sin(\theta_0) \\ v &= \dot{x}_0 \psi_B \cos(\theta_0) + \dot{y}_B \\ w &= -(\dot{x}_0 + \dot{x}_B)\sin(\theta_0) - \dot{x}_0 \theta_B \cos(\theta_0) + \dot{z}_B \cos(\theta_0) \end{aligned} \tag{4.13}$$

The differential equations are in the standard state space representation

$$\dot{\delta x} = A\,\delta x + B\,\delta u$$

where δx represents the perturbation from the trim condition of the state variables and δu represents the deviations of the control displacements from trim. Although the components of A and B matrices are function of forward velocity, they are often approximated by an average value so that the resulting linear model is velocity and time invariant. The linearized six-degree-of freedom representation of the helicopter dynamics is valid only if the initial body angular rates are zero.

B. Rotor Dynamics

The rotor of a helicopter is used for generating lift, forward thrust and control moments. Consequently, modeling the dynamics of the rotor is very important in accurately representing the overall dynamic response of a helicopter. The rotor model used in this study is the tip path plane representation of blade flapping [3]. This model is commonly used in helicopter dynamics and control studies.

The blade loads and motions of a helicopter blade are periodic in the azimuth angle ψ, and the blade flapping angle β can be represented as a Fourier series in ψ

$$\beta(t,\psi) = \beta_0(t) + \sum_{n=1}^{\infty} [\,\beta_{nc}(t)\cos(n\psi) + \beta_{ns}(t)\sin(n\psi)\,] \qquad (4.14)$$

The azimuth angle is

$$\psi = \Omega t \qquad (4.15)$$

where Ω is the rotor angular speed. Since the frequency of the rotor, approximately 30 rad/s, is so much greater than that of the rigid body motions, less than 4 rad/s, only the lowest harmonics in the Fourier expansion for the blade flapping angle are required to

describe the motions of the rotor adequately for purposes of dynamic stability analysis and control law synthesis. In fact the tip path plane model uses only the first harmonics of blade motion.

$$\beta(t,\psi) \cong \beta_0(t) + \beta_{1c}(t) \cos (\psi) + \beta_{1s}(t) \sin (\psi) \qquad (4.16)$$

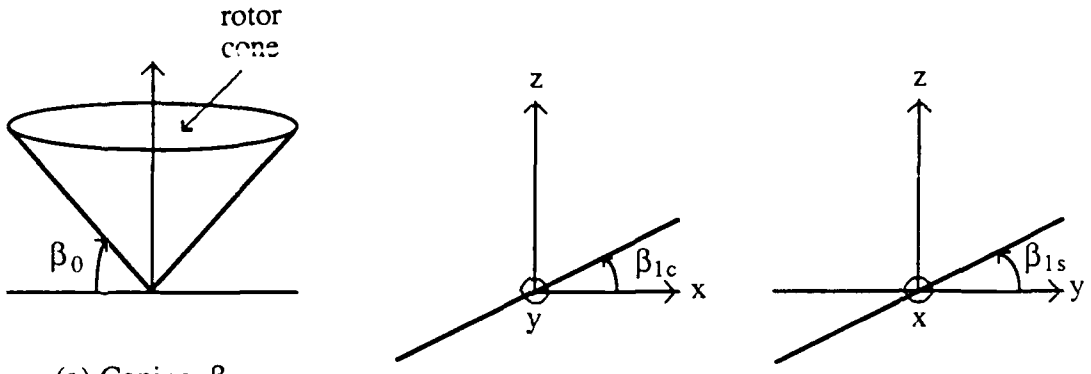

(a) Coning, β_0

(b) longitudinal tip path plane, β_{1c} viewed from the left

(c) lateral tip path plane, β_{1s} viewed from aft

Fig. 4.2 Blade Flapping Harmonics.

A graphical interpretation of the blade cone angle $\beta_0(t)$ and first two flapping harmonics $\beta_{1s}(t)$ and $\beta_{1c}(t)$ are shown in Fig. 4.2. The two flapping harmonics define a plane known as the tip path plane. The higher harmonics distort this plane but are not needed if only rigid body motions are to be modeled.

A diagram of the forces acting on the rotor is shown in Fig. 4.3. The lift on the blade is denoted as L and the components of the moment created by the lift about the c.g. of the helicopter are

$$M_{CGX} = - h L \sin (\beta_1) \sin (\psi) \cong - h L \beta_1 \sin (\psi) \qquad (4.17)$$

$$M_{CGY} = - h L \sin (\beta_1) \cos (\psi) \cong - h L \beta_1 \cos (\psi) \qquad (4.18)$$

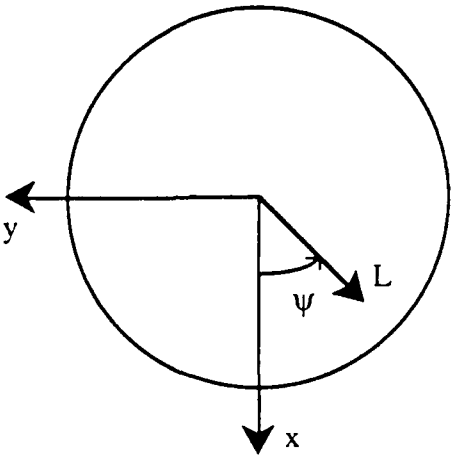

Top View

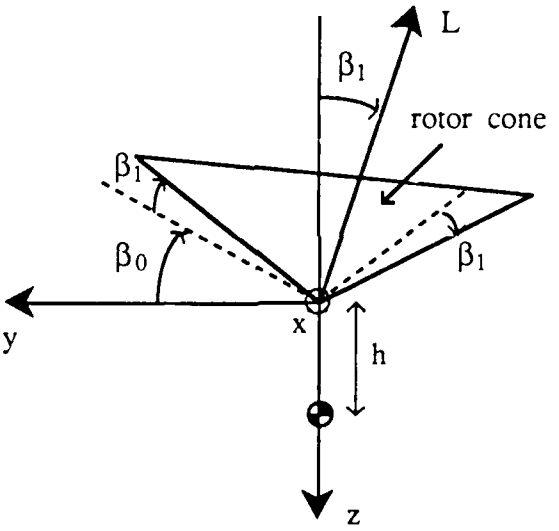

Plane view, view from forward

Fig. 4.3 Rotor Force Diagram.

The angle β_1 is represented by the first two elements in its Fourier series expansion,

$$\beta_1(t) \cong \beta_{1c}(t)\cos(\psi) + \beta_{1s}(t)\sin(\psi) \qquad (4.19)$$

Since $\psi = \Omega\ t$, these components are periodic functions of time. If the moment expressions given in Eqs. 4.17 and 4.18 were inserted directly into the rigid body equations, a set of ordinary differential equations with time variable coefficients would result. Few theories exist for the design of control laws for systems described even by linear time variable ordinary differential equations. Furthermore, those theories which are available lead to time variable gains which are not desirable because of difficulty of implementation. Fortunately, the frequency of the rotor is so much greater than that of the rigid body motions that the averaged values of the rotor moments can be used in the rigid body equations. These averaged equations are obtained by integrating Equations 4.17 and 4.18 with respect to ψ over the interval 2π, and result in

$$M_{CGX_{AVG}} = -\frac{hL}{2}\beta_{1s} \tag{4.20}$$

$$M_{CGY_{AVG}} = \frac{hL}{2}\beta_{1c} \tag{4.21}$$

These expressions can be substituted into the rigid body equations to give a set of ordinary differential equations which give a good representation of the rigid body motions of the helicopter fuselage.

Since the blades themselves have inertia, their motions must be described by differential equations. The dynamics of the coning angle have little effect on rigid body dynamics and can be ignored; however, accurate modeling of the rigid body motions requires that the dynamics of the harmonic coefficients be included. The harmonics are described by a set of coupled second order linear differential equations

$$\begin{bmatrix} 1 & 0 \\ 0 & 1 \end{bmatrix}\begin{bmatrix} \ddot{\beta}_{1s} \\ \ddot{\beta}_{1c} \end{bmatrix} + c\begin{bmatrix} 1 & -\varepsilon \\ \varepsilon & 1 \end{bmatrix}\begin{bmatrix} \dot{\beta}_{1s} \\ \dot{\beta}_{1c} \end{bmatrix} + k\begin{bmatrix} 1 & -\alpha \\ \alpha & 1 \end{bmatrix}\begin{bmatrix} \beta_{1s} \\ \beta_{1c} \end{bmatrix}$$

$$= \begin{bmatrix} -f & \sigma & -g & \nu \\ \sigma & f & \nu & g \end{bmatrix} \begin{bmatrix} u \\ v \\ p \\ q \end{bmatrix} + b \begin{bmatrix} 1 & -\gamma \\ \gamma & 1 \end{bmatrix} \begin{bmatrix} \theta_{\text{lateral cyclic}} \\ \theta_{\text{longitudinal cyclic}} \end{bmatrix} \qquad (4.22)$$

The "damping" and "stiffness" matrices are determined by aerodynamic damping, centrifugal and structural stiffness of the blade, and gyroscopic forces. The inputs are the latera' and longitudinal cyclic pitch. The above flapping equations are coupled with the rigid body equations result in a 12th order set of differential equations (an 8th order rigid body model and two coupled 2nd order models representing the rotor dynamics). There is also coupling with the rigid body linear and angular velocities. More complex rotor models which include lag and torsional dynamics can be formulated but 12th order models of the type described above appear to be adequate for control law synthesis for most articulated rotor helicopters.

III. Design Model

The mathematical model used for design represents a modern attack helicopter in the hover condition. The state space representation is a linear, coupled, eight degree of freedom helicopter model which includes eight rigid body states (u,v,w,p,q,r,ϕ,θ), and two second order modes of the advancing and regressing rotor tip path plane (a_1,b_1). Main rotor collective pitch, lateral cyclic pitch, longitudinal cyclic pitch, and tail rotor collective pitch are the control inputs. These equations are written in the standard form

$$\dot{x}_{12} = A_{12}\, x_{12} + B_{12}\, u \qquad (4.23)$$

where A_{12}, B_{12}, are dimensional matrices containing the analytical data for the linearized dynamics of a helicopter and are given in Appendix A.

The sensors measure vertical velocity, and roll, pitch and yaw rates, and the output equation can be written as

$$y = C x_{12} \tag{4.24}$$

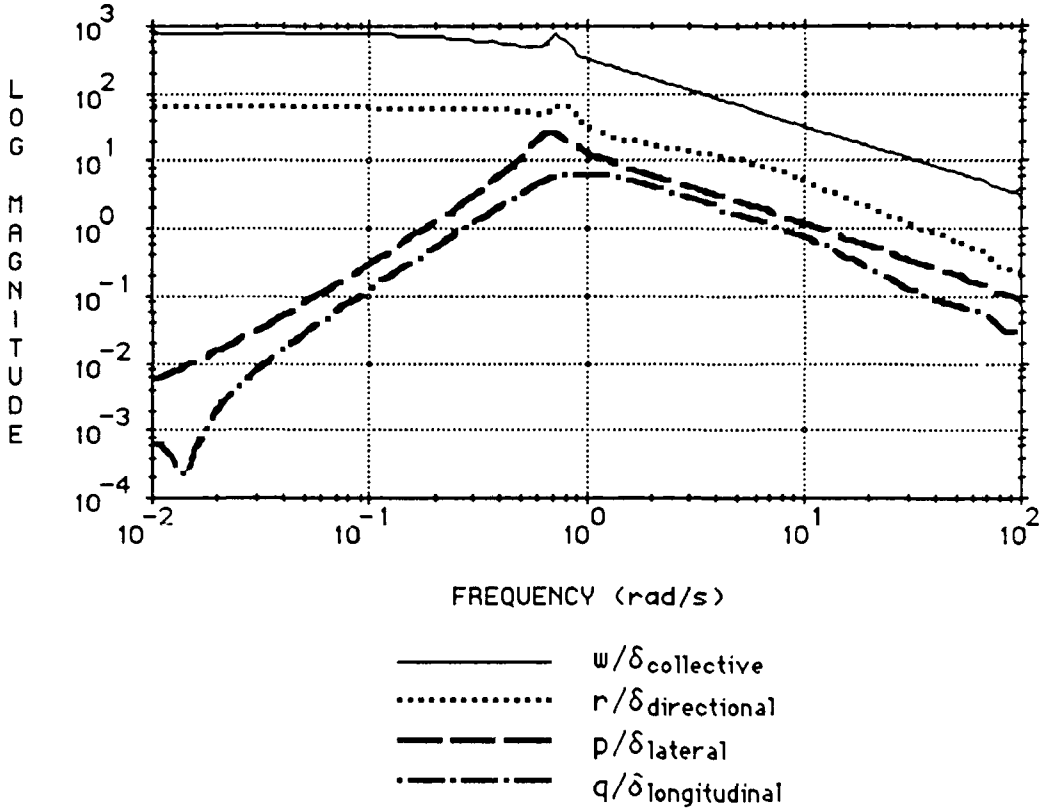

Fig. 4.4 Singular Value Plot of 12th Order Open Loop Helicopter at Hover.

The singular values for the state space equations 4.23 and 4.24 that represent the 12th order helicopter at hover are plotted in Fig. 4.4. The twelve eigenvalues and their respective modal identifications are given in Table 4.1.

As can be seen from Table 4.1, the rotor dynamics result in a set of high and a set of relatively low frequency eigenvalues. The high frequency set of rotor eigenvalues have a natural frequency of 73.4 rad/s and a damping factor of 0.189. This is sometimes called

the rotor advancing flapping mode. Examination of the residues of this mode indicate that it does not have much affect on the rigid body modes. On the other hand, the lower frequency set of rotor eigenvalues has a natural frequency of 12.3 rad/s and a damping factor of 0.96. The mode associated with this set of eigenvalues is known as the regressing flapping mode. Since the rigid body roll mode has an eigenvalue of -4.3434 rad/s, the regressing flapping mode will affect the rigid body dynamics. Examination of the residues of this eigenvalues verifies that it does have a significant impact on pitch and roll rate responses.

Twelfth Order Model		
-4.3434 +	.0000i	roll rate
.2130 ±	.5270i	forward velocity
.0328 ±	.7499i	side slip
-.9421 +	.0000i	pitch rate
-.5654 +	.0000i	yaw rate
-.3234 +	.0000i	heave velocity
-13.6446 ±	72.1554i	advancing rotor mode
-11.7698 ±	3.6620i	regressing rotor mode

Table 4.1 Open Loop Eigenvalues and Corresponding Modes of 12th Order Model.

Thus the design model should contain the effects of rotor dynamics. In practice, the measurement of the rotor states appears impossible with current technology. It was decided to develop a reduced eighth order design model which explicitly contained only the rigid body modes. The use of a lower order model for control law design simplifies the design and implementation of the feedback compensator. Two methods of order reduction: truncation and residualization, were applied to the twelfth order model.

Truncation involved eliminating or truncating the fast modes from the original model. In this case, the tip path plane modes (rotor flapping modes) were truncated from the

twelfth order model. In Eq. 4.25, x_8 represents the eight rigid body states and x_4 represents the 4 rotor states. Truncation involves crossing out the rows and the columns of the A matrix correspond to $\dot{x}_4$, and the rows of the B matrix correspond to $\dot{x}_4$, leaving just the eight rigid body equations as the nominal model.

$$\begin{bmatrix} \dot{x}_8 \\ \dot{x}_4 \end{bmatrix} = \begin{bmatrix} A_{(8,8)} & A_{(8,4)} \\ A_{(4,8)} & A_{(4,4)} \end{bmatrix} \begin{bmatrix} x_8 \\ x_4 \end{bmatrix} + \begin{bmatrix} B_8 \\ B_4 \end{bmatrix} u \qquad (4.25)$$

For residualization, the higher frequency motions are assumed to reach steady state conditions so rapidly that the time rate of change of these states ($\dot{x}_4$) may be set to zero. Following the procedure shown in Eq. 4.26, this assumption allowed unique algebraic solution for the four tip path plane states in terms of the eight rigid body states. These four state equations were then substituted into the rigid body equations and placed in standard state space form in order to obtain the residualized nominal model.

$$\begin{bmatrix} \dot{x}_8 \\ 0 \end{bmatrix} = \begin{bmatrix} A_{(8,8)} & A_{(8,4)} \\ A_{(4,8)} & A_{(4,4)} \end{bmatrix} \begin{bmatrix} x_8 \\ x_4 \end{bmatrix} + \begin{bmatrix} B_8 \\ B_4 \end{bmatrix} u \qquad (4.26)$$

$$\therefore \; x_4 = - A_{4,4}^{-1} A_{4,8} x_8 - A_{4,4}^{-1} B_4 u$$

$$\Rightarrow \dot{x}_8 = (A_{8,8} - A_{8,4} A_{4,4}^{-1} A_{4,8}) x_8 + (B_8 - A_{8,4} A_{4,4}^{-1} B_4) u$$

The nominal models resulting from truncation and residualization were evaluated by comparing their open loop eigenvalues with the eight rigid body eigenvalues obtained from the original twelfth order model. As can be seen from Table 4.2, the eigenvalues of the residualized model matched the eigenvalues of the twelfth order model much more closely than did those of the truncated model. Thus the residualized model was used as the design model.

Full State	Truncated	Residualized	
-4.3434 + .0000i	-1.4032 + .0000i	-3.2377 + .0000i	roll rate
.2130 ± .5270i	.2705 ± .8338i	.2110 ± .5296i	forward velocity
.0328 ± .7499i	.2076 ± .4825i	.0353 ± .7431i	side slip
-.9421 + .0000i	-.6249 + .0000i	-.9021 + .0000i	pitch rate
-.5654 + .0000i	-.4476 + .0000i	-.5695 + .0000i	yaw rate
-.3234 + .0000i	-.1939 + .0000i	-.3221 + .0000i	heave velocity
-13.6446 ± 72.1554i			advancing rotor mode
-11.7698 ± 3.6620i			regressing rotor mode

Table 4.2 Comparison of Open Loop Eigenvalues of 12th Order Model with 8th Order Truncated and Residualized Models.

The design model is written in standard state space form as given in Eq. 4.27 where A_8 and B_8 are obtained from Eq. 4.26. The measured outputs are heave velocity, roll, pitch and yaw rates. The dimensional A_8, B_8 and C_8 matrices are given in Appendix A.

$$\dot{x}_8 = A_8 x_8 + B_8 u \tag{4.27}$$

$$y = C_8 x_8 \tag{4.28}$$

The singular value plot of the 8th order residualized model given by Eqs. 4.27 and 4.28 is shown in Fig. 4.5. As compared to the 12th order model shown in Fig. 4.4, the singular values for $\frac{w}{\delta_{collective}}$, $\frac{p}{\delta_{lateral}}$, $\frac{q}{\delta_{longitudianl}}$, and $\frac{r}{\delta_{directional}}$ are essentially the same for both models for frequencies less than 10 rad/s. This similarity is also verified by the comparison of the open loop eigenvalues in Table 4.2.

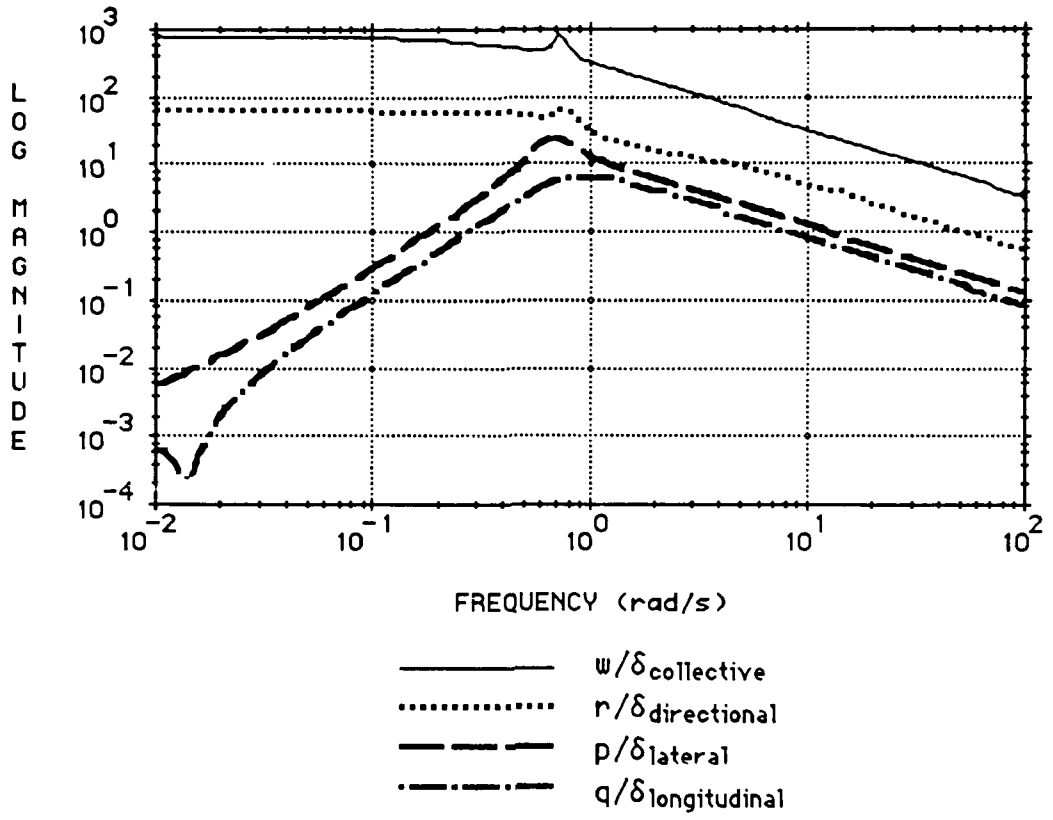

Fig. 4.5 Singular Value Plot of 8th Order Residualized Helicopter Model.

Due to the fact that the elements of a given dimensional eigenvector have different units, (linear and angular units), it is difficult to identify the dominant modes and couplings associated with a particular dimensional eigenvector. Hence it is desirable to non-dimensionalized the state and control vectors so that modal coupling can be more easily identified. The maximum expected value of each state variable applicable to the model was used for non-dimensionalization. All linear velocities were divided by 16.877 ft./s (10 knots), angular velocities by 0.349 rad/s (20 deg./s), and angular displacement by 0.349 rad (20 degrees). The control inputs were non-dimensionalized by dividing by their maximum values. The collective pitch was divided by 0.157 rad (9 degrees), the lateral cyclic pitch by 0.153 rad (8.75 degrees), the longitudinal cyclic pitch by 0.262 rad (15 degrees), and the tail rotor collective pitch by 0.323 rad (18.5 degrees). The open

loop eigenvalues and non-dimensional eigenvectors for the residualized hover model are tabulated in Table 4.3.

	roll rate	side slip	forward velocity
	λ = -3.2377 + .0000i	λ = .0353 ± .7431i	λ = .2110 ± .5296i
u	.0071 + .0000i	.1239 ± .0691i	.1078 ∓ .4243i
v	.0692 + .0000i	-.1740 ± .5073i	-.1781 ∓ .1191i
w	.0063 + .0000i	-.0429 ∓ .0285i	-.0023 ± .0273i
p	.9407 + .0000i	.0898 ∓ .4337i	.1138 ∓ .0301i
q	-.0308 + .0000i	.0936 ± .0437i	-.0952 ∓ .1698i
r	-.1557 + .0000i	.3095 ± .1069i	-.4358 ∓ .5712i
ϕ	-.2913 + .0000i	-.5791 ∓ .1419i	.0433 ∓ .2102i
θ	.0112 + .0000i	.0703 ∓ .1368i	-.3800 ± .0565i

	pitch rate	yaw rate	heave velocity
	λ = -.9021 + .0000i	λ = -.5695 + .0000i	λ = -.3221 + .0000i
u	.3738 + .0000i	-.1589 + .0000i	-.0858 + .0000i
v	.0364 + .0000i	.0710 + .0000i	-.1097 + .0000i
w	.1027 + .0000i	-.2290 + .0000i	-.3863 + .0000i
p	.0031 + .0000i	.0633 + .0000i	-.0317 + .0000i
q	-.4160 + .0000i	.0413 + .0000i	.0419 + .0000i
r	-.6597 + .0000i	.9421 + .0000i	-.9080 + .0000i
ϕ	-.0145 + .0000i	-.0857 + .0000i	.0550 + .0000i
θ	.4860 + .0000i	-.1291 + .0000i	-.0332 + .0000i

Table 4.3 Open Loop Eigenvalues and Associated Non-Dimensional Eigenvectors.

The values in Table 4.3 show that cross coupling exists between all modes. Roll rate is coupled to yaw rate. Side slip is coupled to yaw rate and forward velocity. Forward velocity is coupled to side slip, roll and yaw rate. Pitch rate is coupled to yaw rate and heave velocity. Yaw rate and heave are also coupled to each other. It is also evident that there are two pairs of unstable complex conjugate roots for side slip and forward velocity with a time to double amplitude of 19.5 seconds and 3.27 seconds respectively. Also the

bandwidths for pitch rate, yaw rate and heave modes are far lower than desired. These factors greatly degrade the handling qualities of the helicopter.

Besides the modal coupling described above, examination of the control distribution matrix B reveals strong coupling of yaw angular acceleration in all inputs. Collective cyclic pitch has primary effect on yaw acceleration, and about equal effect on heave velocity and roll angular acceleration. Lateral cyclic has strong effect on roll acceleration, and pitch angular acceleration is significantly influenced by the longitudinal cyclic pitch only. Lateral and longitudinal cyclic pitch have about equal effect on yaw. Roll and yaw acceleration are coupled considerably in tail rotor collective pitch.

IV. Error Model

An error model which gives an approximation of the modeling uncertainties is developed so that the maximum attainable bandwidth for the flight control system that ensures stability robustness can be estimated and the performance robustness determined.

Flying quality problems of modern flight control systems are most often related to the introduction of time delays in the rotorcraft flight control system. These time delays can produce a significant degradation in the flying qualities of the rotorcraft during demanding tasks. Therefore the error model used in this study approximates the unmodeled high frequency dynamics of rotor dynamics, structural modes, actuators, filters, sensors, sampling delays, and computational delays associated with digital implementation of the flight control system with effective time delays. The total effective time delay for each of the four input channels is assumed to be the same. Additional assumptions are: (1) there is no cross-coupling of the uncertainties between channels, and (2) the nominal design model has a 10% error at low frequencies.

The multiplicative (relative) error model [9], given by Eq. 4.29 is utilized in the calculation of the unmodeled dynamics error bound for the stability robustness test. The multiplicative error matrix is defined as

$$G_{true}(s) = G(s)(I + E(s)) \tag{4.29}$$

and is related to the effective time delay, $\Delta\tau$ by the following equation [10],

$$I + E(s) = \text{diag}\{ e^{-s\Delta\tau} \} \tag{4.30}$$

Using a first order Pade approximation for the total effective time delay, the error can then be evaluated as

$$E(s) = \left(\frac{- 2\Delta\tau s}{\Delta\tau s + 2} \right) I \tag{4.31}$$

V. Simulation Model

This section formulates a helicopter mathematical model suitable for evaluation of control laws. The basic simulation model will consist of 12th order dynamics model, i.e. 8th order rigid body dynamics plus two second order rotor flapping dynamics, first order actuators with bandwidths of 50 rad/s, and a first order Pade approximation of the computational and filter delays as shown in the block diagram below.

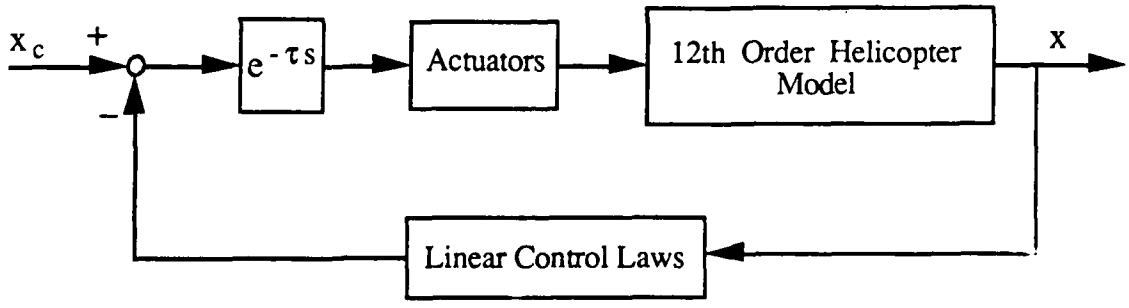

Fig. 4.6 Block Diagram of the Simulation Model.

A more realistic model will include nonlinear dynamics and kinematics model, computational and filter delays, and rate and position limits in the actuator dynamics as given in Fig. 4.7.

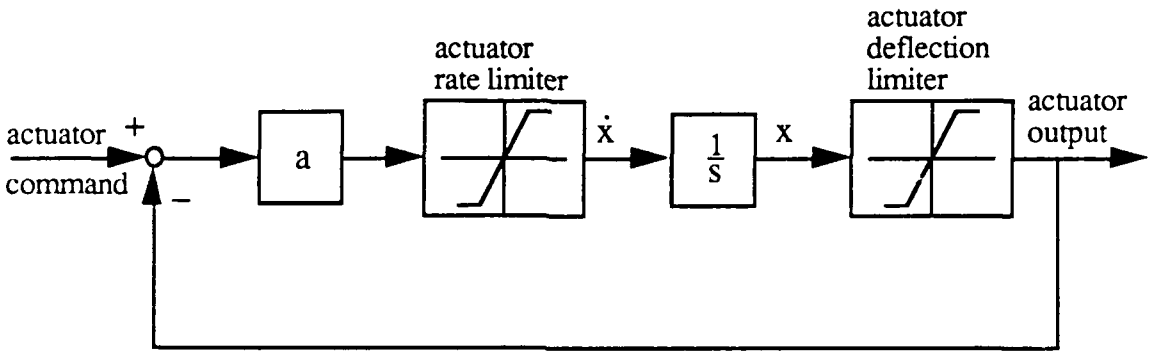

Fig. 4.7 Actuator Dynamics.

References

1. Etkin, Bernard, *Dynamics of Flight - Stability and Control*, 2nd Edition, John Wiley & Sons, Inc., New York, 1982.

2. McRuer, Duane, Ashkenas, Irving, and Graham, Dunstan, *Aircraft Dynamics and Automatic Control*, Princeton University Press, Princeton, New Jersey, 1973.

3. Johnson, Wayne, *Helicopter Theory*, Princeton University Press, Princeton, New Jersey, 1980.

4. Prouty, Raymond W., *Helicopter Aerodynamics*, PJS Publications Inc., Peoria, Illinois, 1985.

5. Stepniewski, Mieslaw Z., *Rotary - Wing Aerodynamics*, Vol. I, Dover Publications Inc., New York, 1984.

6. Talbot, Peter D., Tinling, Bruce E., Decker, William A., and Chen, Robert T. N., "A Mathematical Model of a Single Main Rotor Helicopter for Piloted Simulation," NASA TM-84281, Ames Research Center, Moffett Field, CA.

7. Chen, Robert T. N., "Effects of Primary Rotor Parameters on Flapping Dynamics, NASA TP-1431, Ames Research Center, Moffett Field, CA, Jan. 1980.

8. Chen, Robert T. N., "A Simplified Rotor System Mathematical Model of a Single for Piloted Dynamics Simulation," NASA TM-78575, Ames Research Center, Moffett Field, CA, May 1979.

9. Lehtomaki, N. A., Castanon, D., Levy, B., Stein, G., Sandell. Jr., N. A., and Athans, M., "Robustness Test Utilizing the Structure of Modelling Error," Proceedings of the 20th IEEE Conference on Decision & Control, San Diego, CA, Dec. 16, 1981, pp. 1173- 1190.

10. McRuer, D. T., Myers, T. T., Thompson, P. M., "Literal Singular-Value-Based Flight Control System Design Techniques," *Journal of Guidance, Control and Dynamics*, Vol. 12, No. 6, Nov.- Dec., 1989, pp 913-919.

Chapter 5

Nominal Design

I. Introduction

The purpose of this chapter is to develop a simple control law structure for low speed and hovering control of an advanced combat helicopter. In the first section of this chapter, the philosophy for the feedback system design is presented and in the second section, a methodology using eigenstructure assignment to design the inner loop control law is discussed. In the third section, the use of a simple feedback or feedforward outer loop that wraps around the inner loops to achieve selectable command response types is discussed.

II. Design Philosophy

A modern four-bladed attack helicopter operating at low speed or hover flight regimes is used to illustrate the design of the flight control system. The dynamic response characteristics for the helicopter modeled in this study are typical of most high performance helicopters. Simulations and flight tests have shown that with such helicopter dynamics, even experienced helicopter pilots are unable to accomplish divided attention operations or relatively simple tasks in degraded visual environments. Handling qualities that minimize the involvement of the pilot in basic stabilization tasks are required to accomplish such operations. This requires a high bandwidth (high gain), multiply-redundant flight control system.

As discussed by Tischler [1], high gain flight control systems require high bandwidth actuators. Hence the rate and deflection limit characteristics of the actuators will impose significant limitations on the feedback gains. Additional factors that limit the maximum

feedback gains are : (1) sensor noise amplification, (2) in-plane (lead-lag) rotor coupling and inflow dynamics [2], (3) phase-margin requirements and high frequency modeling uncertainty (rotor and structural flexure modes) and (4) total effective time delays [3]-[4] due in part to digital implementation of the flight control laws.

This chapter presents a control law structure that will provide good command tracking (decoupling), gust attenuation, stability robustness, and meet the proposed handling qualities specifications in the face of errors in the mathematical model used for design. In this Chapter, the performance of the system is evaluated using the design model. In Chapter 6, the performance of the control law will be demonstrated by: (1) time response simulations with more realistic models, (2) unstructured singular value analysis, (3) structured singular values (μ analysis [5]-[8]). The control law structure consists of "inner" and "outer" feedback loops. This chapter also describes an eigenstructure methodology used to design inner loop control laws which decouple the vertical velocity, yaw, longitudinal, and lateral modes. The resulting closed inner loop system has an integral or $\frac{\omega_c}{s}$ [9]-[13] (ω_c is the desired crossover frequency) characteristic in the lateral and longitudinal attitude loops and first order type responses in the vertical velocity and yaw rate loops. If altitude and directional hold response is desired, the inner loop control exhibits integral response in these loops as well. The inner loop control laws require all states be fed back. Thus measurements of linear velocities, body angular rates, and roll and pitch attitudes are all required. In practice, only the body angular rates and the vertical velocity relative to body axes are measured, therefore an estimator is required in the inner loop. Various command response types can then be achieved by simple feedforward and feedback outer loops wrapped around the inner loops. Since the inner loop feedbacks are flight critical, redundancy [14] will be required in these loops. The outer loops are flight critical only under severely degraded flight conditions.

A. Inner Loops

The inner loop flight control system involves four loops. Vertical velocity, roll, pitch and yaw rates are the four sensor outputs (measurements) and collective pitch, cyclic lateral, cyclic longitudinal, and tail rotor collective pitch are the four actuator inputs for these loops. At hover, the mathematical model of the open loop helicopter exhibits two undamped unstable modes (forward velocity and side slip) with frequencies of approximately 0.57 rad/s and 0.74 rad/s, and damping ratios ζ of -0.37 and -0.048 respectively. The doubling times for forward velocity and side slip are 3.27 seconds and 19.5 seconds respectively. Level 1 handling qualities specify a minimum of 6.8 seconds for allowable time to double amplitude for low frequency second order modes [15]-[16].

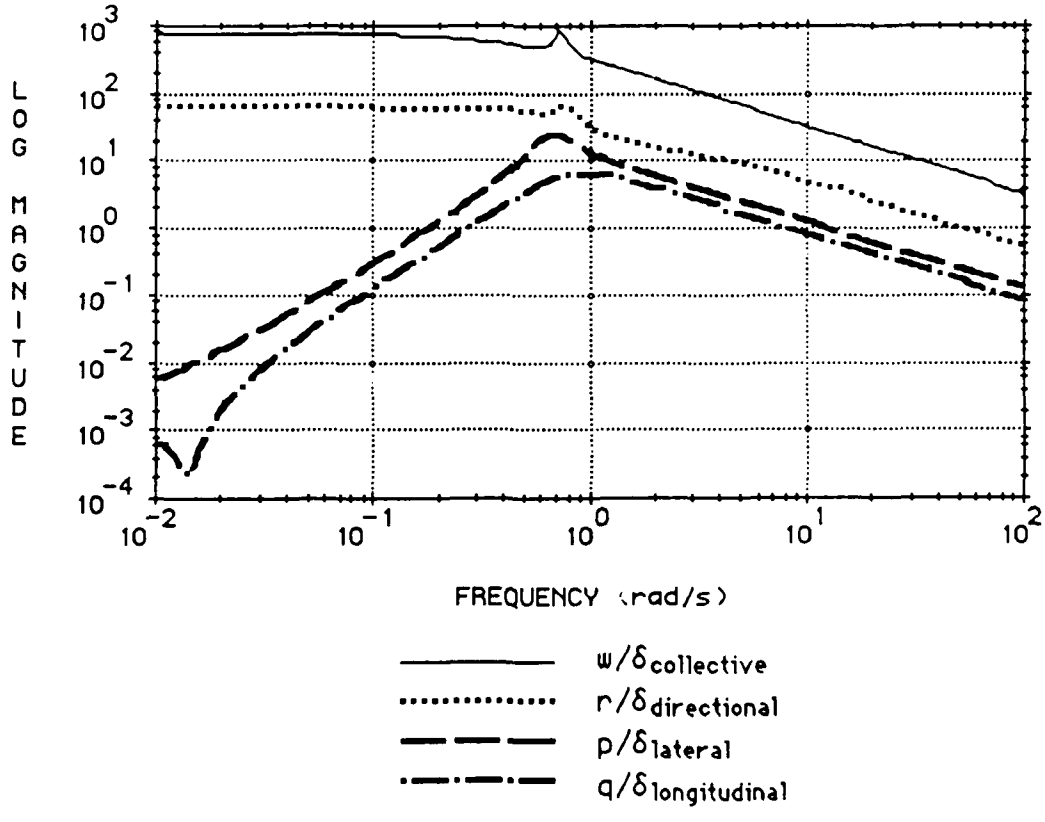

Fig. 5.1 Singular Value Plot of Open Loop Helicopter at Hover.

The open loop frequency response of the helicopter at hover is shown in Fig. 5.1. From this figure it can be seen that there are two channels, namely roll and pitch, with singular values of 0.0006 and 0.006 at frequency about 0.01 rad/s. This means that closed loop tracking and gust attenuation will be very poor in the roll and pitch channels since low frequency gains in these channels are so small. The difference in magnitude between the largest and the smallest singular value is about 122 dB, resulting in a condition number of $\sim 10^6$. Therefore the model is close to being singular at low frequency. This implies that any attempt to provide compensation at low frequency by inverting the plant will result in a very complicated and not very robust controller.

Regulated variables for the inner loop feedbacks are vertical velocity and yaw rates for heave and directional control and roll and pitch attitude rates for the lateral/longitudinal control. The control design was carried out to obtain desirable performance for the four regulated variable outputs and good stability robustness properties at the four control inputs. For good inner loop performance, it is necessary to have stable closed loop poles, decoupled closed loop responses and acceptable gust rejection properties. Gust rejection and command tracking are all improved with increasing bandwidth [17]. Eigenstructure assignment is used to design the inner loop control laws so that decoupled, first order rate responses are achieved about each axis. For a first order system, the bandwidth of the system is directly related to the position of the pole location. Therefore the pole location associated with each rate response is selected to have sufficiently high bandwidth so that crisp response to command is assured. The desired transfer functions between commands and inner loop regulated variables are given by

$$\frac{w}{w_c} = -\frac{\lambda_w}{(s + \lambda_w)} \tag{5.1}$$

$$\frac{\phi}{p_c} = \frac{\lambda_p}{s(s + \lambda_p)} \tag{5.2}$$

$$\frac{\theta}{q_c} = \frac{\lambda_q}{s(s + \lambda_q)} \tag{5.3}$$

$$\frac{r}{r_c} = \frac{\lambda_r}{(s + \lambda_r)} \tag{5.4}$$

The transfer functions between roll and pitch attitudes and lateral and longitudinal commands exhibit 1.0/s characteristics for frequencies below crossover and $\lambda_{p,q}/s^2$ characteristics above crossover frequency as shown in Figure 5.2.

Under the worst usable cue environment, Level 2 handling qualities are acceptable for the collective and directional loops. Since Level 1 handling qualities are not required under such a situation, Level 2 handling qualities will suffice. Level 2 handling qualities [17] require the response type [18] to be either RCDH (Rate Command Direction Hold) or RCHH (Rate Command Height Hold). These response types require open loop transfer functions between collective and directional commands and altitude and direction as shown in Fig. 5.2.

When the loop between the roll attitude and lateral command (given in Eq. 5.2) is closed with an external pilot command, ϕ_c, the response that the pilot sees will have integral characteristics as shown in Fig. 5.2. The control law and the kinematic relationship (between roll rate and roll angle) enable the lateral loop to have high gain at low frequency and low gain at high frequency. This satisfies the need for a k/s [9]-[13] attitude-to-stick frequency response in the region of pilot crossover. The high inner loop gain at low frequency provides good tracking of attitude commands and gust attenuation,

while roll off at high frequency helps to avoid potential instabilities due to high frequency rotor and structural dynamics. The same comments apply to the pitch attitude control loop.

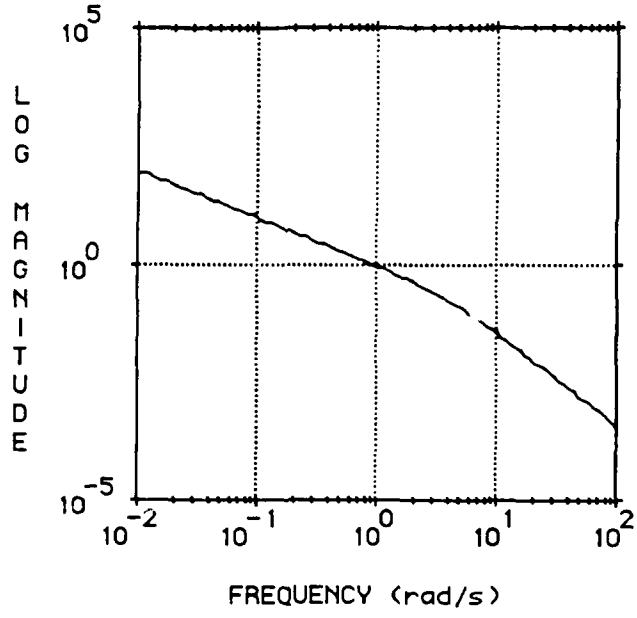

Fig. 5.2 Integral Characteristics of the Desired Transfer Functions.

The desired transfer functions between forward velocity and pitch command and side velocity and roll command are

$$\frac{u(s)}{q_c(s)} = \frac{\lambda_q}{s(s + \lambda_u)} \approx \frac{\lambda_q}{s^2} \tag{5.5}$$

$$\frac{v(s)}{p_c(s)} = \frac{\lambda_p}{s(s + \lambda_v)} \approx \frac{\lambda_p}{s^2} \tag{5.6}$$

The eigenvalues λ_u and λ_v are associated with the linearized drag forces in the forward and side directions. Since the values of λ_u and λ_v are small, the lateral and longitudinal velocities to roll and pitch commands are essentially $\lambda_{p,q}/s^2$. Equations 5.1-5.6 are then used to define the desired closed inner loop eigenstructure for the model.

B. Outer Loop

Once the inner loop system has been designed to approximate the desired transfer functions given in Eq. 5.1-5.6, various command response types can be achieved by simple single loop feedbacks or feedforwards.

The desired pitch and roll attitude transfer functions for ACAH are [2], [18]-[19]

$$\frac{\phi}{\phi_c} = \frac{\omega^2_\phi}{(s^2 + 2\zeta\omega_\phi s + \omega^2_\phi)} \tag{5.7}$$

$$\frac{\theta}{\theta_c} = \frac{\omega^2_\theta}{(s^2 + 2\zeta\omega_\theta s + \omega^2_\theta)} \tag{5.8}$$

Similar second order transfer functions are desired for TRCPH.

III. Inner Loops via Eigenstructure Assignment

A. Full State Feedback

1. Nominal Design

A full state regulator is developed using eigenstructure assignment techniques. Even though good decoupling of the closed loop eigenvectors is achieved, input distribution matrix coupling of the helicopter is so great that a feedforward gain matrix is required. Both the feedback control law and the feedforward gain matrix are designed assuming full state feedback. Since not all the states can be measured, the feedback control law cannot be implemented directly. Thus it is necessary to include a state estimator in the feedback loop in order to realize the control law. The state estimator is synthesized using eigenstructure assignment techniques so as to achieve loop transfer recovery in the crossover frequency range.

The theory of eigenstructure assignment by feedback control is discussed in Chapter 3. This section will be limited to a discussion of the design procedure and a presentation of the results.

The feedback control law is a linear function of the state vector

$$u = - K x \tag{5.9}$$

The feedback gain matrix, K is designed such that the implementation of this control law results in desired placement of the closed loop eigenvalues and shaping of the corresponding eigenvectors. The placement of the closed loop eigenvalues is necessary in order to obtain stability and set the time constants and natural frequencies for the rigid body modes. Eigenvector shaping is used to obtain modal decoupling needed to achieve handling quality specifications and reduce pilot workload. The values of the closed loop eigenvalues and eigenvectors must be specified by the designer. The ideal closed inner loop state equations for the helicopter model are derived from the desired transfer functions (Eqs. 5.1-5.6). The equation is given in state space form for the desired response as

$$\dot{x} = A^d x + B^d x_c \tag{5.10}$$

where

$$A^d = \begin{bmatrix} -\lambda_u & 0 & 0 & 0 & 1 & 0 & 0 & \lambda_q \\ 0 & -\lambda_v & 0 & 1 & 0 & 0 & \lambda_p & 0 \\ 0 & 0 & -\lambda_w & 0 & 0 & 0 & 0 & 0 \\ 0 & 0 & 0 & -\lambda_p & 0 & 0 & 0 & 0 \\ 0 & 0 & 0 & 0 & -\lambda_q & 0 & 0 & 0 \\ 0 & 0 & 0 & 0 & 0 & -\lambda_r & 0 & 0 \\ 0 & 0 & 0 & 1 & 0 & 0 & 0 & 0 \\ 0 & 0 & 0 & 0 & 1 & 0 & 0 & 0 \end{bmatrix}$$

$$B^d = \begin{bmatrix} 0 & 0 & 0 & 0 \\ 0 & 0 & 0 & 0 \\ \lambda_w & 0 & 0 & 0 \\ 0 & \lambda_p & 0 & 0 \\ 0 & 0 & \lambda_q & 0 \\ 0 & 0 & 0 & \lambda_r \\ 0 & 0 & 0 & 0 \\ 0 & 0 & 0 & 0 \end{bmatrix}$$

It can be seen that this state space representation gives the transfer functions in Eqs. 5.1-5.6. The values of $\lambda_{w,p,q,r}$ for the ideal A matrix are determined by the handling quality requirements. For a first order system, the bandwidth and the eigenvalue are identical. Bandwidths of 4 rad/s for vertical velocity, roll, pitch and yaw rate were chosen to assure Level 1 handling qualities. The values of λ_u and λ_v were set at 10% of their nominal values from the residualized A matrix since previous experience indicated that these values resulted in good steady state response [19]. The values of -.00199 and -.00526 for λ_u and λ_v are small enough so that $\lambda_{p,q}/s^2$ characteristics for lateral and longitudinal responses to roll and pitch commands are guaranteed.

Ed =

-.0020
-.0001
-.0053
-.0001
-4.0000
-4.0000
-4.0000
-4.0000

Table 5.1a Desired Closed Loop Eigenvalues

With the closed loop eigenvalues specified, this A^d is then used to define the desired eigenvalue/eigenvector configurations which are given in Table 5.1a.

Vd =

u	1.0000	.0000	.0000	1.0000	.0000	.0000	.0000	.0000
v	.0000	1.0000	1.0000	.0000	.0000	.0000	.0000	.0000
w	.0000	.0000	.0000	.0000	1.0000	.0000	.0000	.0000
p	.0000	.0000	.0000	.0000	.0000	.9701	.0000	.0000
q	.0000	.0000	.0000	.0000	.0000	.0000	.9701	.0000
r	.0000	.0000	.0000	.0000	.0000	.0000	.0000	1.0000
ϕ	.0000	.0013	.0000	.0000	.0000	-.2425	.0000	.0000
θ	.0000	.0000	.0000	.0005	.0000	.0000	-.2425	.0000

Table 5.1b Desired Closed Loop Eigenvectors

The desired eigenvectors associated with the closed loop eigenvalues are given in Table 5.1b. Kinematic constraints necessitate the coupling of pitch rate to pitch angle and pitch attitude to forward velocity for the longitudinal eigenvectors. These same conditions also apply to roll rate being coupled to roll angle and roll attitude to side velocity. This set of eigenvectors will achieve the required modal decoupling and therefore, are used as the desired eigenvectors for the regulator design procedure. The achievable non-dimensional eigenvectors are shown in Table 5.2a. The closed inner loop system exhibits substantially reduced modal decoupling when compared with the open loop system.

Va =

u	.9992	-.0007	-.0006	.9993	.0260	.0025	-.1063	0.0000
v	-.0006	.9998	.9998	-.0007	-.0339	.0467	-.0077	-.0244
w	-.0010	-.0002	.0001	-.0010	.9991	.0015	.0025	-.0008
p	-.0001	0.0000	0.0000	0.0000	.0015	.9691	.0006	.0020
q	0.0000	0.0000	-.0001	0.0000	.0025	.0006	.9646	-.0022
r	0.0000	0.0000	0.0000	0.0000	-.0008	.0011	-.0002	.9997
ϕ	.0360	.0138	.0061	.0360	-.0004	-.2423	-.0003	.0033
θ	.0148	.0168	.0168	.0120	-.0006	-.0002	-.2410	-.0080

Table 5.2a Achievable Non-Dimensional Regulator Eigenvectors

K =

.0248	.0239	-1.1628	-.0092	.0062	-.0133	-.0428	.0209
.0787	-.1040	.1210	.0735	.0760	.1779	.0028	.0036
-.0553	-.0355	.0976	-.0054	-.5350	.0112	.0096	-.0073
-.1162	-.0365	-.6114	-.0598	-.1664	-.3627	-.0205	.0085

Table 5.2b Non-Dimensional Regulator Feedback Gain Matrix

The extensive coupling of the control input matrix, B, requires a feedforward gain matrix to alleviate the problem of control cross-coupling. This requires the desired control distribution matrix be determined. The structure and the magnitude of the desired control matrix should be the same as that of the ideal B matrix in order to obtain the desired transfer functions. As can be seen from the desired control distribution matrix B^d in Eq. 5.8, the desired output to a collective input is a pure heave command. Similarly, pure roll rate and pitch rate are the desired commands to lateral and longitudinal stick pitch inputs. Also, a pure yaw rate command is desired for the pedal input. The feedforward gain matrix, H, was selected such that

$$B * H \approx B^d \tag{5.11}$$

Since the control distribution matrix B is non-square, it is necessary to solve for H using the optimal pseudo-inverse method [21], which is optimal in the sense that trace[($B*B^T$)($B*B^T$)] is minimized,

$$H = B^T * (B*B^T)^{-1} * B^d \tag{5.12}$$

The solution of this relation gives the feedforward gain matrix, H as shown in Table 5.3a.

H =

-1.2824	-.0007	-.0035	.0011
.1506	.2130	.1003	.1757
.0771	.0090	-.6223	.0111
-.6880	-.0489	-.1592	-.3990

Table 5.3a Non-Dimensional Feedforward Gain Matrix

B * H =

.0949	.0026	-.2950	.0044
-.1577	.0418	-.0346	-.0946
3.9915	.0016	.0057	-.0038
.0016	3.9996	.0006	.0010
.0057	.0006	3.9778	-.0005
-.0038	.0010	-.0005	3.9978
.0000	.0000	.0000	.0000
.0000	.0000	.0000	.0000

Table 5.3b Achievable Form of Non-Dimensional B^d

The achieved form for non-dimensional B^d is shown in Table 5.3b. This result achieves the decoupling desired for the four control inputs. It also includes some unwanted input

dynamics in forward and side velocities for heave command, forward velocity for longitudinal command, and side velocity for yaw rate command. Although the coupling terms in the achieved form of B^d are undesirable, they are tolerable due to the fact that the magnitude of these terms as compared to 4 of the command input is insignificant.

Full state step responses for the closed inner loop system were evaluated with the inclusion of the feedforward gain matrix. Using the dimensional regulator and feedforward gain matrix, the results of a simulation of the response of the full state model to a 5 deg/s step roll rate command are shown in Figs. 5.3 and 5.4. Both the open loop and closed inner loop responses are plotted on the same scale. Figs. 5.3 and 5.4 illustrate the unstable character of the open loop responses. The responses are extensively coupled. In contrast, the heave, the longitudinal, and the directional modes of the closed inner loop system were nicely decoupled from the lateral response. The full state closed inner loop responses are very similar to the ideal responses given in Eqs. 5.1 to 5.6. The roll rate response behaves like a first order system with a time constant of 1/4 second. The roll angle increases monotonically with time and the side velocity increases quadratically with time. The lack of cross coupling can be seen in the transfer function matrix in the appendix. The diagonal terms in the transfer matrix relating the outputs w(s), p(s), q(s), and r(s) to the inputs $w_c(s)$, $p_c(s)$, $q_c(s)$, and $r_c(s)$ are essentially $\frac{4}{(s+4)}$ while the off-diagonal terms are essentially zero. The non-zero vertical velocity, longitudinal and directional responses were very small compared with the lateral response.

The bode plot for the roll angle to lateral command transfer function can be seen in Fig. 5.5. When the loop between the roll angle and lateral command is closed with an external pilot command, Fig. 5.5 can be considered as the loop transfer function for the

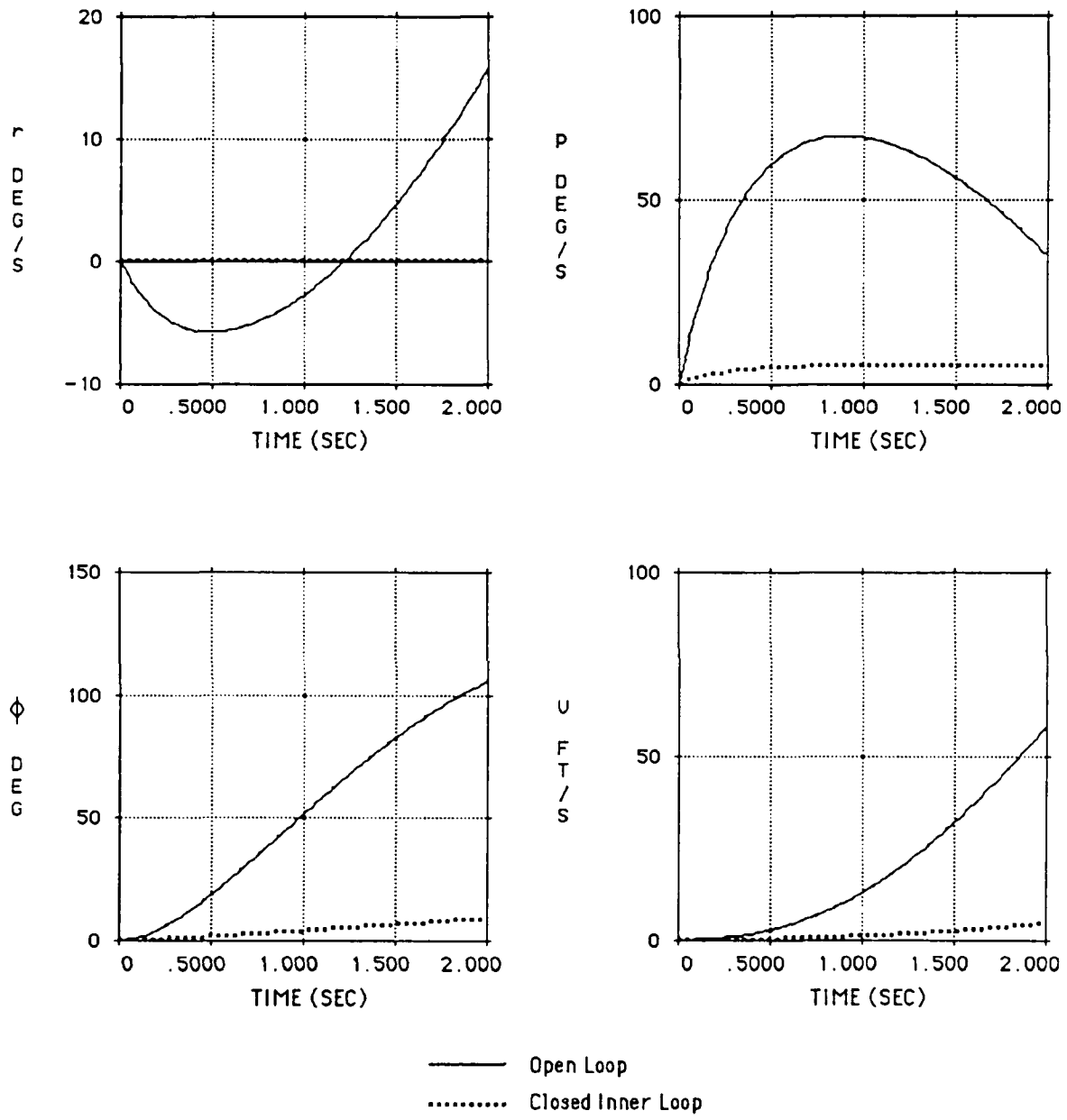

Fig. 5.3 Full State Open and Closed Inner Loop Time Responses to a Step Roll Rate Command.

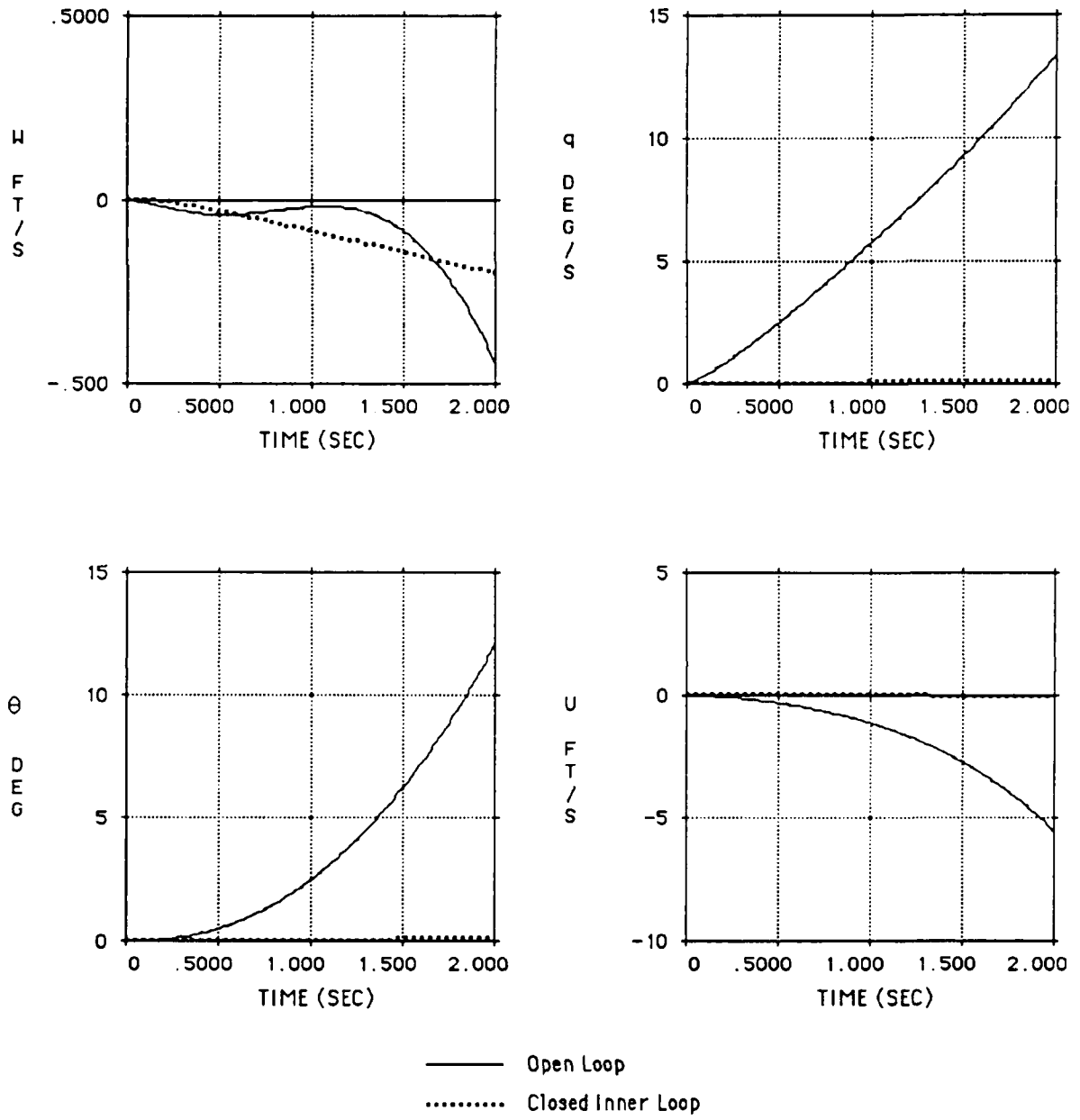

Fig. 5.4 Full State Open and Closed Inner Loop Time Responses to a Step Roll Rate Command.

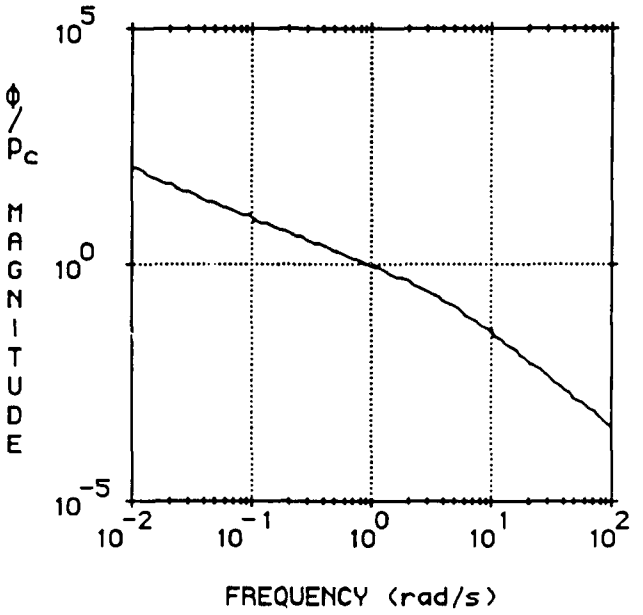

Fig. 5.5 Bode Magnitude of Roll Angle to Lateral Command.

inner loop control law. This plot shows high gain at low frequency for good tracking and low gain at high frequency for robustness. This also assures that good attenuation of gust can be achieved by the inner loop control law.

In addressing the handling qualities issues related to the disturbance response of the rotorcraft, the significant factors are the magnitude and the frequency content of the helicopter response to turbulence for which the pilot must compensate. The frequency range of pilot stabilization is approximately 0.5 rad/s to 5 rad/s [22].

Figure 5.6 shows the singular value plot of identity matrix minus the transfer function matrix of the closed inner loop system. In order to have a realistic plot, the units for the transfer functions from lateral, longitudinal, and directional commands to vertical velocity have to be properly scaled. Since the angular rate commands in the other channels are given in deg/s instead of rad/s, the units of the command had to be changed from rad/s to

deg/s. This was achieved by dividing the transfer functions from directional, lateral, and longitudinal commands to vertical velocity by a factor of 57.3.

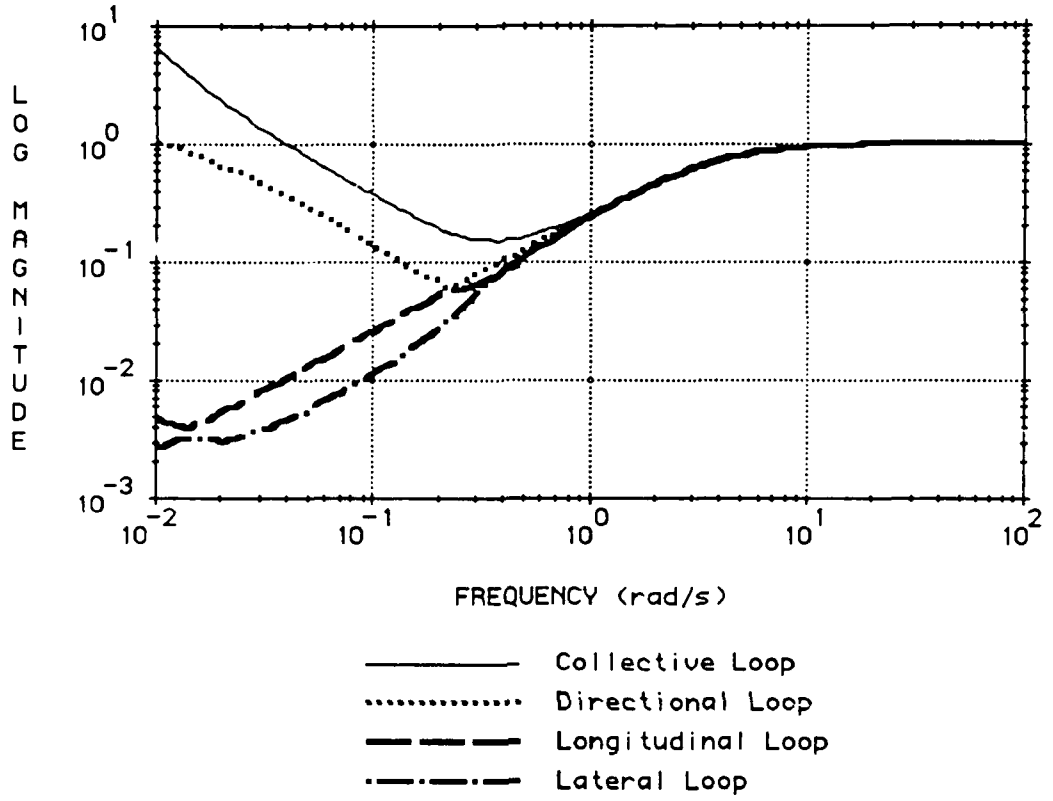

Fig. 5.6 Singular Values of [I - $G_{\text{Closed Inner Loop}}$].

For a system to have good decoupling characteristics, the $\bar{\sigma}$ [I - $G_{\text{closed loop}}$] must be smaller than unity in the frequency range of interest. As shown in Fig. 5.6, decoupling of the heave mode is not satisfied at low frequencies but the controller has been able to achieve small gains over the frequency range of interest, 0.1 to 10 rad/s, in each of the four control channels. This plot indicates that response in each channel is the same for frequencies greater than 1.0 rad/s as the singular values are essentially the same for each channel. Fig. 5.6 shows improvement, in terms of the decoupling and bandwidth criteria for each controlled loop compared with the open loop system. The responses in Fig. 5.6 exhibit decoupling. This is also shown by the transfer matrix given in the Appendix B. The

singular value plot illustrates essentially first order response with a bandwidth of 4 rad/s in each channel. At low frequencies, some coupling exists because it is impossible to achieve full pole/ zero cancellation. Since the coupling occurs below the frequency range of interest, it is tolerable.

$$\begin{bmatrix} w \\ \\ \dashv \\ r \end{bmatrix} = G_{\text{closed loop}} \begin{bmatrix} w_c \\ p_c \\ q_c \\ r_c \end{bmatrix} \qquad (5.13)$$

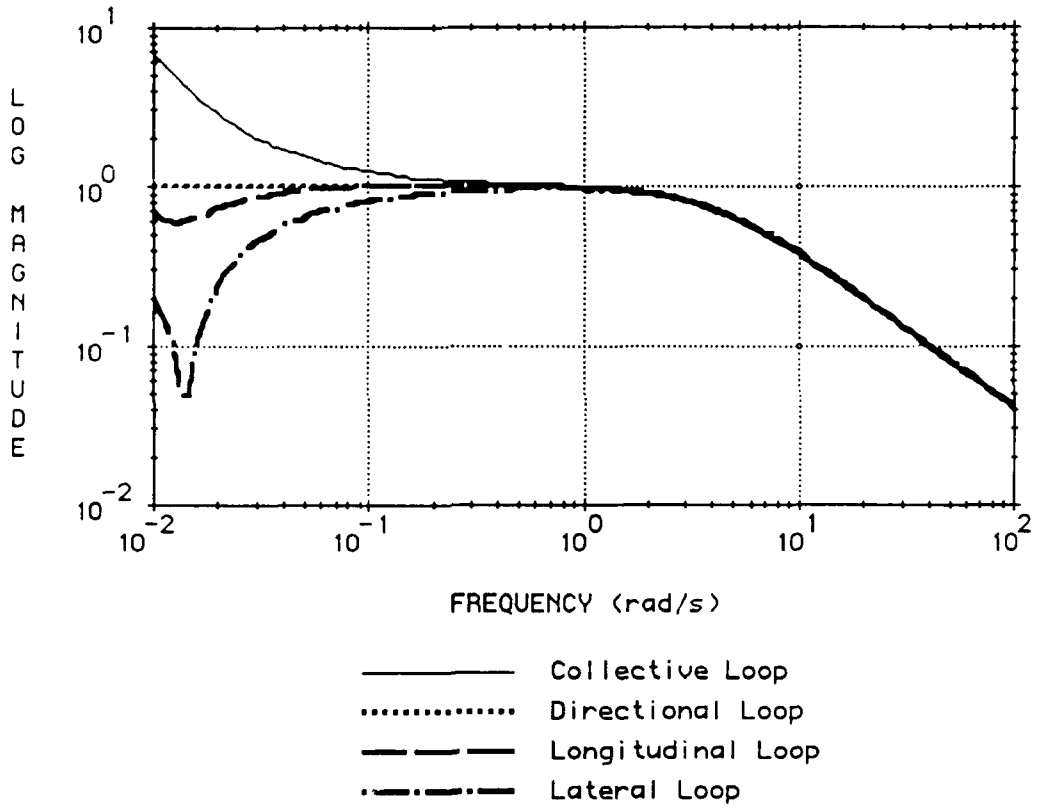

Fig. 5.7 Singular Values of $\bar{\sigma}$ [$G_{\text{Closed Inner Loop}}$].

Another mean to verify the inner loop control law is to look at the singular values of closed inner loop system, as given by $G_{\text{closed loop}}$ in Eq. 5.13. Fig. 5.7 shows the singular values plot of $G_{\text{closed loop}}$. The singular values are first order with a bandwidth of about 4 rad/s, except at frequencies below 0.1 rad/s. This plot indiactes that the achievable

transfer functions between w and w_c, p and p_c, q and q_c, and r and r_c are very close to the desired transfer functions. The singular values at low frequencies are not flat is because the achievable transfer functions do not have total pole and zero cancellation. These low frequency dynamics will not become a concern because they can be corrected by the pilot. Fig. 5.7 also shows that response in each channel is essentially the same for frequencies greater than 1.0 rad/s.

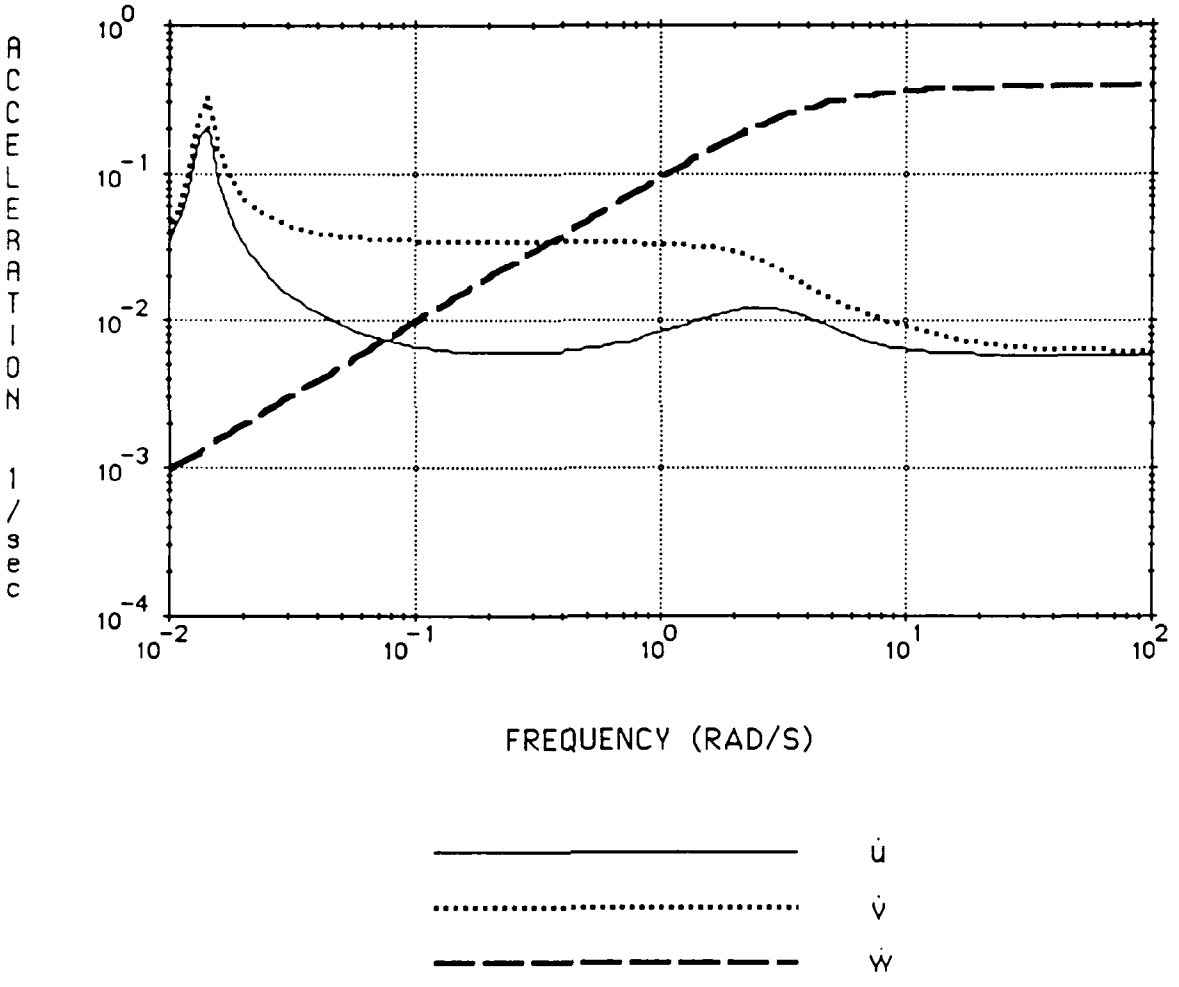

Fig. 5.8 Full State Closed Inner Loop Response of Accelerations to Vertical Gust.

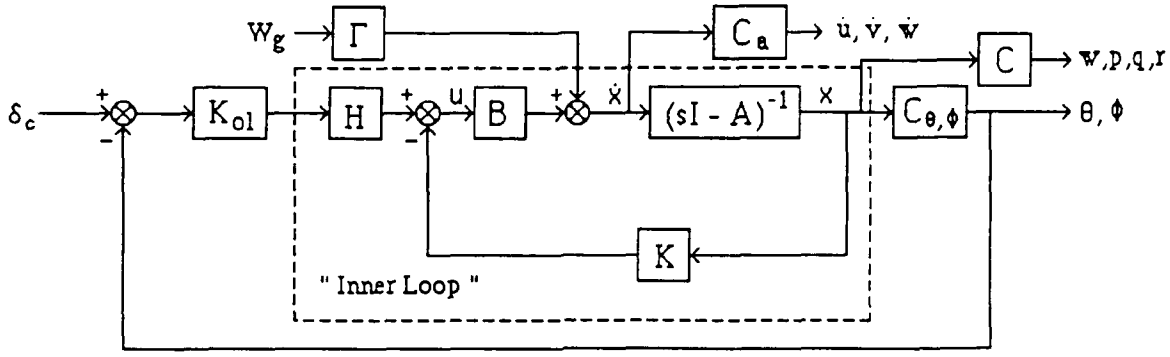

5.9a. Inner Loop Feedback system with Vertical Gust to Acceleration Response.

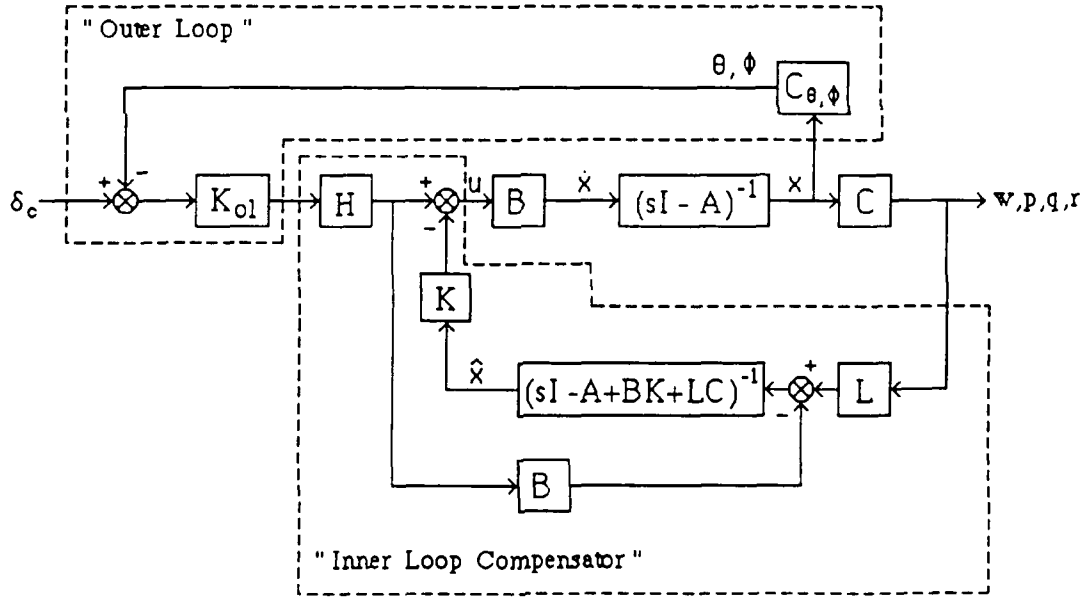

5.9b. Estimator in Feedback Loop.

Fig. 5.9 Block Diagram for Inner and Outer Loops Feedback Configuration.

A plot of the transfer function response of the three components of the linear acceleration of the center of gravity to a vertical gust is shown in Fig. 5.8. The block diagram of this closed loop configuration can be seen in Fig. 5.9a. As would be expected, longitudinal and lateral accelerations are insensitive to a vertical gust. In the case of the vertical acceleration, the small singular value at low frequencies [22] shows good attenuation of gust response. This plot also shows that the vertical acceleration has a bandwidth of 4 rad/s. Even at frequencies above the bandwidth, the gain between vertical acceleration and vertical gust is only 0.4. Although no specifications exist for gust response, Key [17] indicates that the bandwidth of the gust should be about the same as the bandwidth of command response to ensure adequate disturbance rejection. Fig. 5.8 shows that the closed inner loop system has very good gust attenuation for all frequencies.

B. Full State Estimator

The full state regulator in the inner loop requires that all states be fed back. Since only vertical velocity, pitch rate, roll rate and yaw rate are measured in the inner loop, it is necessary to include a state estimator in the feedback loop in order to implement the control law. The use of eigenstructure assignment techniques to achieve loop transfer recovery is discussed in Chapter 3. This section presents a brief discussion of the design procedures and the results of implementing the control law.

The control law with the estimator in the inner loop is given by

$$u = - K \hat{x} \tag{5.15}$$

where $\hat{x}$ is the estimate of the state vector given by the state estimator

$$\dot{\hat{x}} = A \hat{x} + B u + L(y - C \hat{x}) \tag{5.16}$$

The block diagram of the system with the estimator in the feedback loop is given in Fig. 5.9b. The estimator gain matrix L, is to be selected such that A - LC is stable and the frequency response of the system with the regulator/estimator in the feedback loop approximates the full state loop transfer matrix. That is

$$K_8(s)G_8(s) \approx [\, K\,(\, sI - A\,)^{-1}\, B\,](s) \qquad (5.17)$$

where $K_8(s) = [\, K\,(\, sI - A + BK + LC\,)^{-1}\, L\,](s)$ and

$$G_8(s) = [\, C\,(\, sI - A\,)^{-1}\, B\,](s)$$

This is called loop transfer recovery (LTR) [23]-[24].

The four finite open loop transmission zeroes of the transfer matrix relating the outputs w(s), p(s), q(s), and r(s) to the inputs $w_c(s)$, $p_c(s)$, $q_c(s)$, and $r_c(s)$ of the helicopter are

$$z_{1,2} = 0.0$$

$$z_{3,4} = -.000734 \pm .01398i$$

The four desired eigenvalues and eigenvectors of the estimator were placed at the four transmission zero positions and their respective left zero directions. The values of z_1 and z_2 were approximated by -.001 and -.0015 because of computational difficulties arising from multiple roots. The remaining four closed loop eigenvalues were placed at -10.0 rad/s (Table 5.4) and their corresponding eigenvectors were arbitrarily chosen. The desired and achievable estimator eigenvectors are given in Table 5.5. Figure 5.10 shows the full state and the combined regulator/estimator inverse closed loop transfer functions. This configuration achieves full LTR from 0.1 rad/s up to 5 rad/s. This frequency range is desirable because it includes the inverse closed loop transfer function characteristics of the

bandwidth of the regulator. Below and above this frequency range, the presence of the estimator in the feedback loop results in an additional 20 dB/decade of roll off. The high frequency roll off enhances robustness compared with the full state regulator.

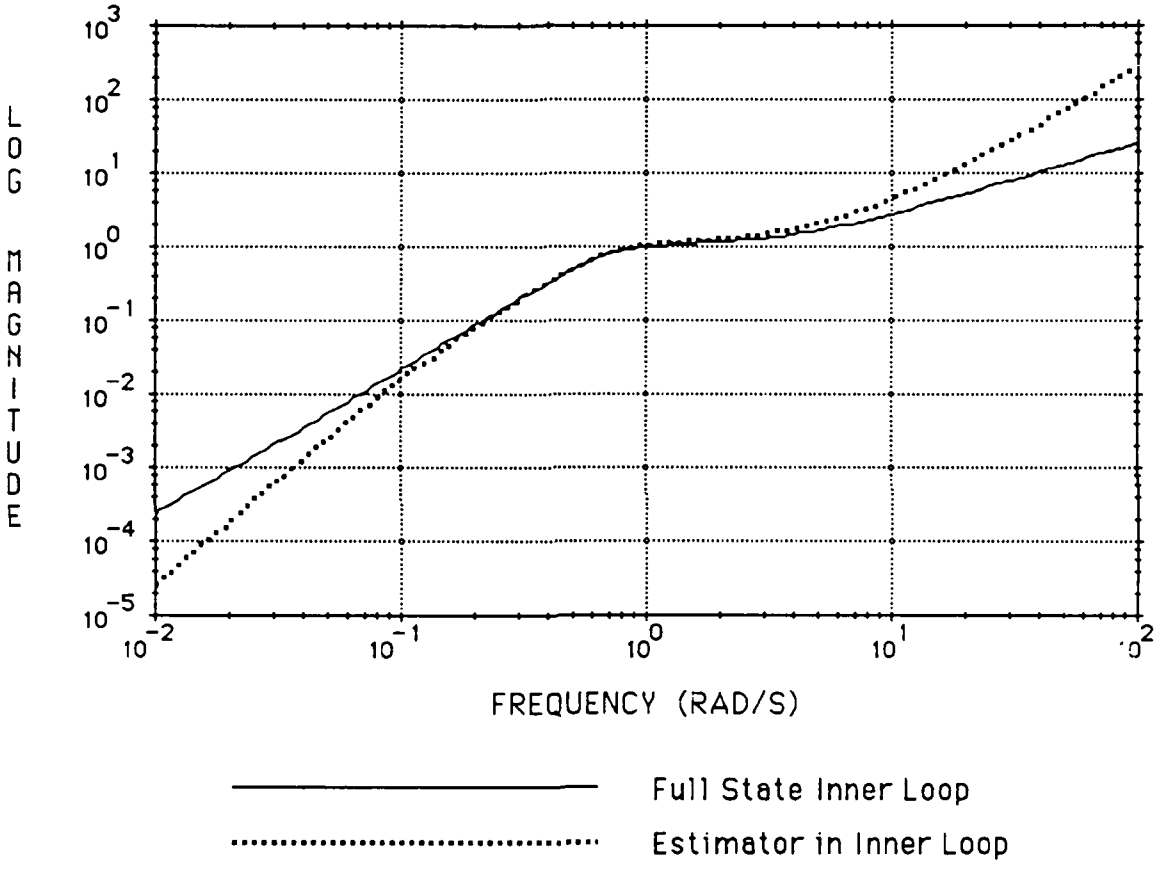

Fig. 5.10 $\underline{\sigma}[\, I + (K(s)G(s))^{-1} \,]$ Full State Inner Loop and Estimator in the Feedback Loop.

ED =

-.0007 ±	.0140i
-.0010 +	.0000i
-.0015 +	.0000i
-10.0000 +	.0000i
-10.0000 +	.0000i
-10.0000 +	.0000i
-10.0000 +	.0000i

Table 5.4 Desired Estimator Eigenvalues

VD = (Desired estimator eigenvectors)

u	.0083 ±	.0152i	0.0000	0.0000	.0000	.0000	.0000	.0000
v	.0119 ±	.0006i	0.0000	0.0000	.0000	0000	.0000	.0000
w	.0003 ±	.0003i	0.0000	0.0000	1.0000	.0000	.0000	.0000
p	-.0001 ±	0.0000i	0.0000	0.0000	.0000	1.0000	.0000	.0000
q	.0007 ±	.0011i	0.0000	0.0000	.0000	.0000	1.0000	.0000
r	.0003 ±	0.0000i	0.0000	0.0000	.0000	.0000	.0000	1.0000
ϕ	-.0006 ±	.5642i	.7690	.7761	.0000	.0000	.0000	.0000
θ	-.7032 ±	.4321i	-.6393	-.6307	.0000	.0000	.0000	.0000

VA = (Attainable estimator eigenvectors)

u	.0083 ±	.0152i	-.0010	-.0014	.0078	-.0446	-.0366	-.1094
v	.0119 ±	.0006i	-.0012	-.0018	.0070	.2510	-.0182	-.0693
w	.0003 ±	.0003i	0.0000	0.0000	.9999	-.0016	.0004	.0014
p	-.0001 ±	0.0000i	0.0000	0.0000	-.0015	.9667	.0031	.0133
q	.0007 ±	.0011i	0.0000	0.0000	.0004	.0032	.9991	-.0054
r	.0003 ±	0.0000i	-.0001	-.0001	.0014	.0136	-.0054	.9914
ϕ	-.0006 ±	.5642i	.7690	.7761	-.0027	-.0167	.0012	.0046
θ	-.7032 ±	.4321i	-.6393	-.6307	-.0005	-.0030	-.0024	-.0073

Table 5.5 Desired Estimator Eigenstructure

L =

.0139	-.0307	-2.0074	.0055
-.0212	-.0276	2.0934	-2.0215
.5700	.0018	-.0133	.1357
-.0045	20.0522	-2.1698	1.7284
-.0103	.2049	26.9162	-.0361
-.0021	1.1677	1.0953	27.0865
0.0000	2.8616	.0368	-.0648
0.0000	-.0043	2.9044	.0744

Table 5.6 Non-Dimensional Estimator Gain Matrix

The non-dimensional estimator gain matrix is given in Table 5.6. Improved LTR is obtained as the finite eigenvalues are moved closer to the transmission zeroes and as the infinite eigenvalues are moved to the left. It is important to place the infinite eigenvalues no further to the left than is required to achieve LTR necessary for stability robustness, since moving the infinite eigenvalues further to the left increases the estimator bandwidth and sensor noise may become a problem.

The frequency response of the inner loop compensator (regulator/ estimator), [K (sI - A + BK + LC)$^{-1}$ L](s) is shown in Fig. 5.11. It can be seen that the controller has a condition number which is of the same order as the plant. This seems reasonable because the open loop model has a large separation in the singular values at low frequency with the roll and pitch channels being very small and the vertical velocity and yaw rate channels very large. In order to achieve good tracking and gust rejection characteristics, it is necessary to increase the gain in each loop proportionally so that the loop gain of K(s)G(s) as defined in Eq. 5.17 has an integral characteristic at frequencies below crossover and $1/s^2$ characteristic above crossover frequency. Therefore the increases in the gains in the roll and pitch loops,

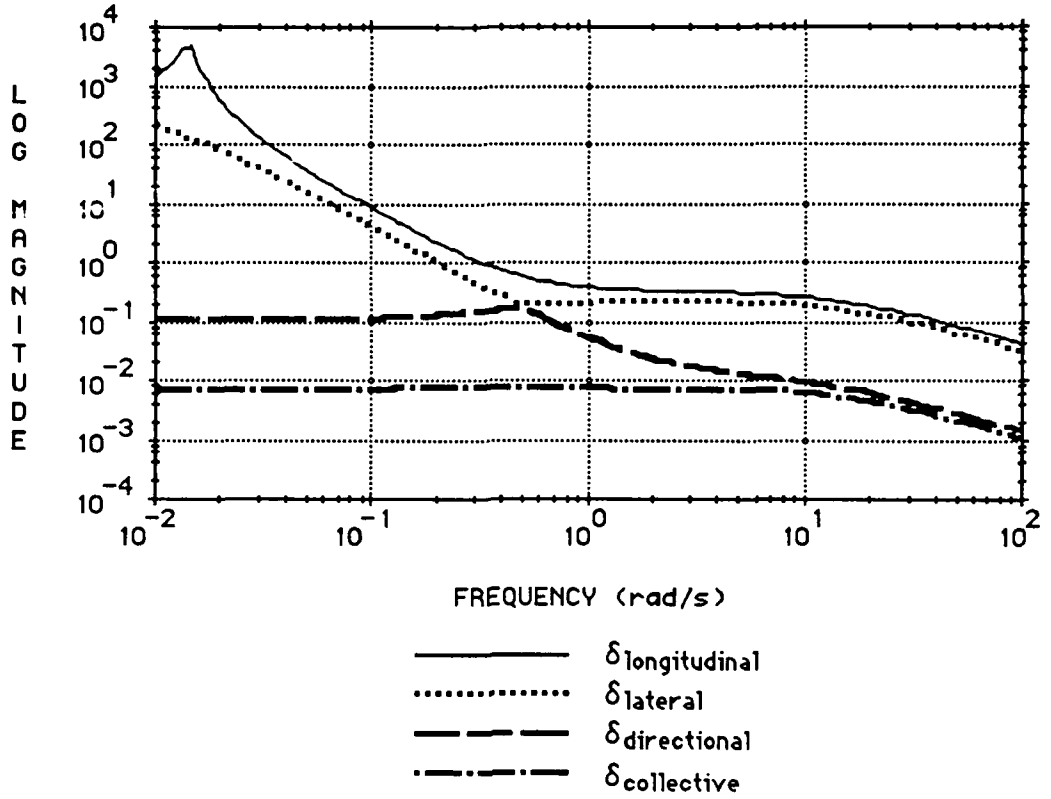

Fig. 5.11 Singular Value Plot of Compensator (Regulator/ Estimator).

which have a very low open loop DC gains, will have proportionally greater increases in gains than in the vertical velocity and yaw rate loops, which have higher open loop DC gains. This requirement is indicated by the singular value plot of the compensator, K(s) in Fig. 5.11.

IV. Outer Loop

Once the inner loop system has been design to approximate the desired transfer functions given in Equations 5.1-5.6, various command response types can be achieved by simple single loop feedbacks or feedforwards. The inner loop system already exhibits RC response, so only ACAH and TRCPH are discussed.

A. ACAH

For ACAH, the lateral and longitudinal angles, ϕ and θ, can be fed back by an outer loop with a proportional gain of K_ϕ and K_θ to achieve Attitude Command/ Attitude Hold type response about the roll and pitch axes. Thus only the roll and pitch angle measurements are needed for the outer loop design. If the outer loop sensors fail, the inner loop control controller will maintain stability of the helicopter, therefore multiple redundant sensors are not required in the outer loop.

The transfer functions between commanded and actual pitch and roll angle are given in Eq. 5.18-5.19. Both K_ϕ and K_θ were selected as 2. The transfer functions are second order with a natural frequency, $\omega_{n\phi,\theta} = 2.83$ rad/s and a damping ratio, $\zeta = 0.707$

$$\frac{\phi}{\phi_c} = \frac{K_\phi \lambda_p}{(s^2 + \lambda_p s + 2\lambda_p)} \tag{5.18}$$

$$\frac{\theta}{\theta_c} = \frac{K_\theta \lambda_q}{(s^2 + \lambda_q s + 2\lambda_q)} \tag{5.19}$$

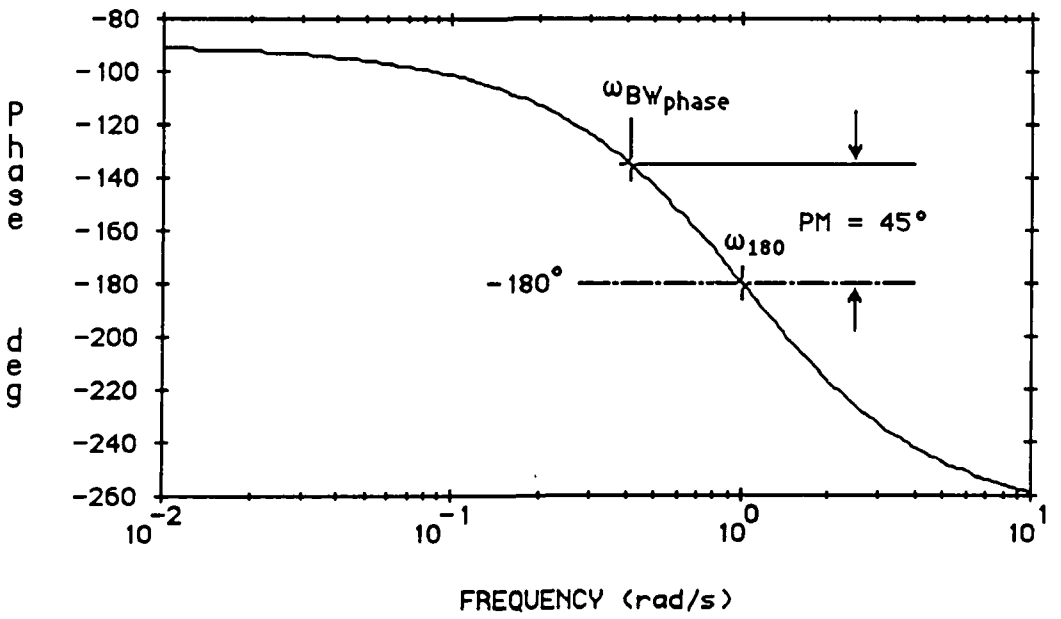

Fig. 5.12 Definition of Phase Margin Limited Bandwidth.

Using the handling quality specification for a second order system, the desired bandwidth is defined in terms of the natural frequency and damping ratio of the system as in Eq. 5.20. This type of bandwidth is phase margin limited and is defined as the frequency where the phase angle becomes -135 degrees as shown in Fig. 5.12. The roll and pitch attitude command response give a Level 1 handling quality with a bandwidth of 5.46 rad/s.

$$\omega_{bw} = \omega_n (\zeta + \sqrt{\zeta^2 + 1}) \tag{5.20}$$

Since direct force control is available only in the heave direction, the lateral and longitudinal velocities of the helicopter in hover must be controlled using roll and pitch moments about the aircraft center of gravity. The relationship between pilot commands a change in roll or pitch attitude and lateral or longitudinal velocities is shown by the following transfer functions

$$\frac{u(s)}{\theta_c(s)} = \frac{K_\theta \lambda_q (s + \lambda_q)}{(s + \lambda_u)(s^2 + \lambda_q s + 2\lambda_q)} \tag{5.21}$$

$$\frac{v(s)}{\phi_c(s)} = \frac{K_\phi \lambda_p (s + \lambda_p)}{(s + \lambda_v)(s^2 + \lambda_p s + 2\lambda_p)} \tag{5.22}$$

The resulting closed roll and pitch attitude outer loops eigenvalues are obtained as

-.0006 ± .0140i
-2.0107 ± 1.9866i
-1.9925 ± 2.0038i
-4.0000 + .0000i
-4.0000 + .0000i

As can be seen from the closed outer loop poles, the eigenvalues corresponding to vertical velocity mode, roll and pitch attitudes, and yaw rate were very much as specified. There is

a low frequency, oscillatory mode with a frequency of $\omega_n = 0.014$ rad/s and a damping ratio of $\zeta = 0.043$. This phugoid period mode might become unstable due to uncertainties in the aerodynamic coefficients. The amount of instability which can be tolerated can be estimated by examining the minimum allowable time to double amplitude for a particular mode. The equation for time to double amplitude is given as

$$t_{double} = \frac{0.69}{|\lambda|} \qquad \text{if } \lambda \text{ is real} \qquad (5.23)$$

or

$$t_{double} = \frac{0.69}{|\zeta\omega_n|} \qquad \text{if } \zeta\omega_n \text{ is the real part of the complex root} \qquad (5.24)$$

For ACAH response type, the specified minimum t_{double} is 6.8 seconds. Under the worst case perturbations in the A and B matrices, it can be shown [25] that this phugoid mode has a time to double amplitude of $t_{double} = 22.5$ seconds. This time is long enough that the pilot can instinctively correct for any instability with his normal control motions. There is some indication that many pilots prefer a slightly unstable phugoid mode.

The results of a simulation of the response of the helicopter to a step roll rate command of 5 deg/s with only the inner loop closed and to a step roll attitude command of 5 degrees with both the inner and outer loops closed are shown in Figs. 5.13 and 5.14. The actual helicopter responses shown in Figures 5.13 and 5.14 are very similar to the ideal responses given in Eqs. 5.1-5.6, Eqs. 5.18-5.19 and Eqs. 5.21-5.22. With only the inner loop closed, the roll rate response behaved like a first order system, and with both the inner and outer loops closed, the roll angle exhibited a second order response as desired. It can be seen from Figs. 5.13-5.14 that the inner loop gives rate response to pilot input and the outer loop gives attitude response. Also, the decoupling of the states is further improved when the outer loop is closed. An effect, called "rate cross-coupling", which holds for a

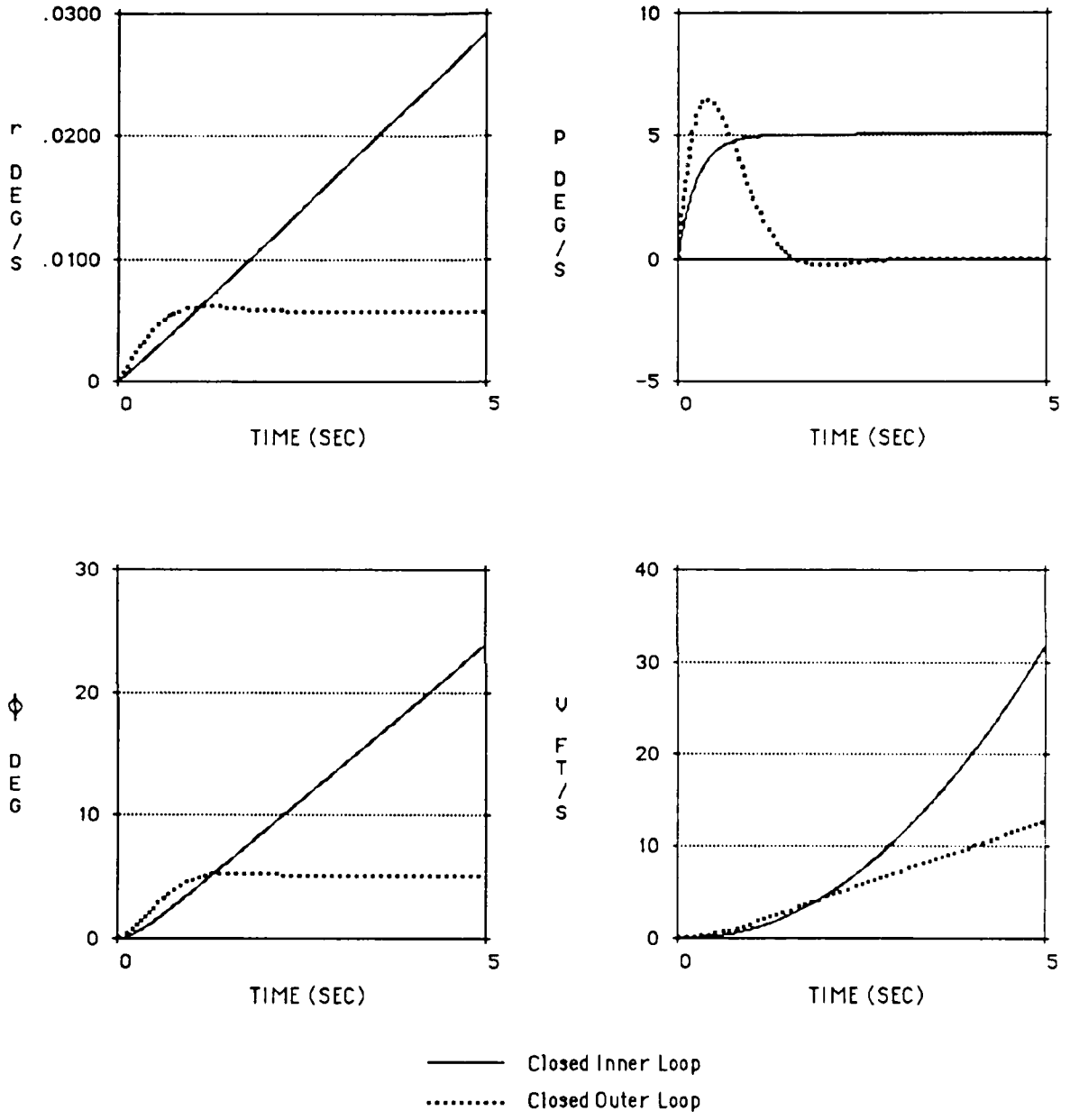

Fig. 5.13 Full State Closed Inner and Outer Loop Time Responses to a Step Roll Command.

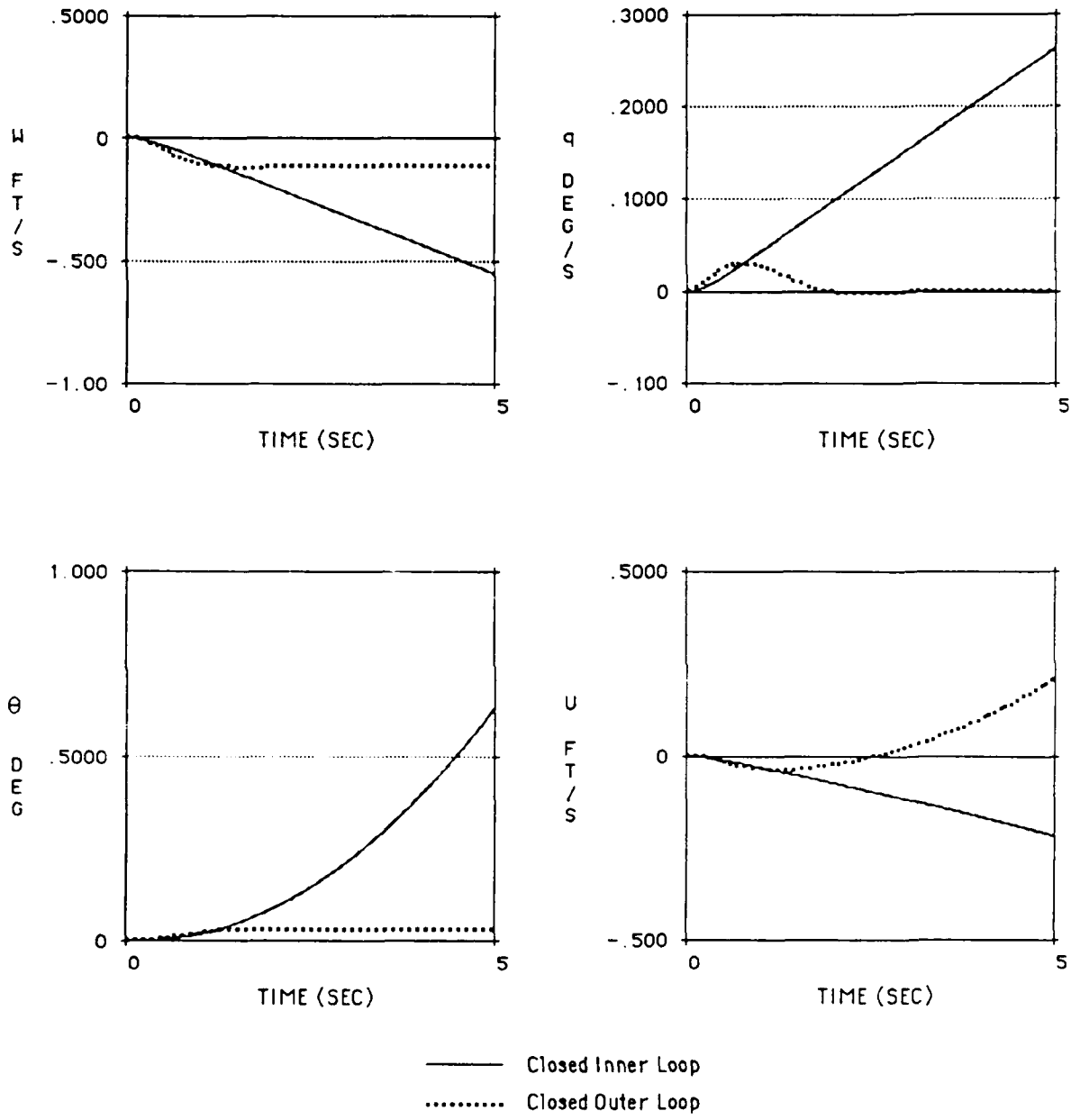

Fig. 5.14 Full State Closed Inner and Outer Loop Time Responses to a Step Roll Command.

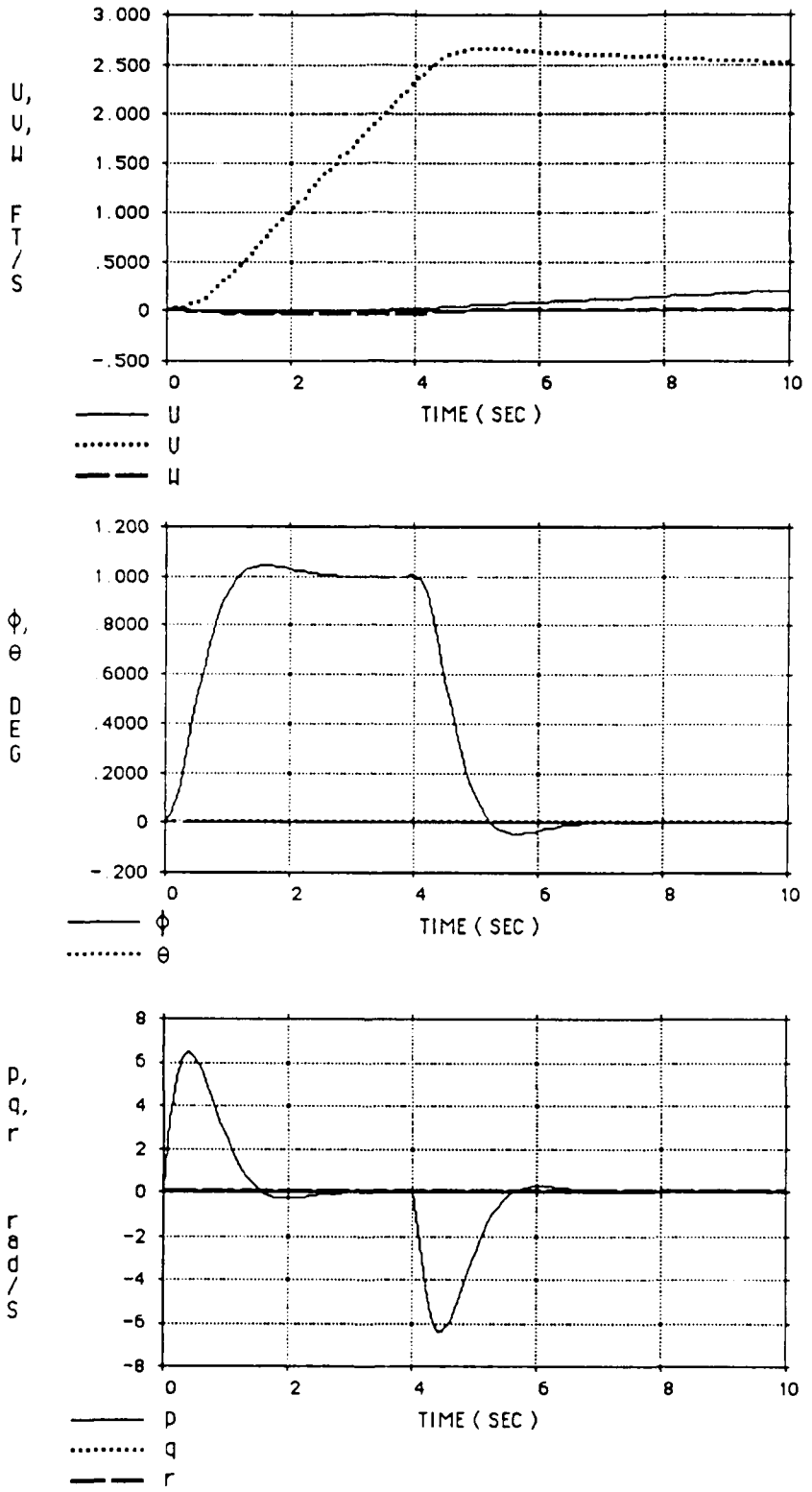

Fig. 5.15 Full State Closed Outer Loop Response to a 5 degrees Step Roll Command of Duration 4 seconds.

right (positive) roll, i.e. the helicopter will pitch-up when rolling right, is shown in the inner and outer loop responses. The reason why the outer loop pitch rate returns to zero is that once a steady roll attitude is established, there is no longer any rolling angular velocity and this particular effect disappears. Also, the side velocity for the outer loop is essentially linear after 1 second but the side velocity response for the inner loop crosses the side velocity response for the outer loop at about 2.5 seconds and increases quadratically. This implies that in order to keep a constant roll rate, higher side thrust force is required.

The decoupled character of the response is further illustrated in Fig. 5.15 which shows the response to a 5 deg roll angle command which is maintained for four seconds and then returned to zero. The results were plotted such that all linear velocities and angular displacements are on the same graphs to better illustrate the closed loop decoupling. The response of the side velocity to roll command results in an acceleration command/ velocity hold type of response. Once the attitude achieves its commanded value, the control is returned to the zero stick position. The attitude drops back to its original value within two seconds after the control is released, whereas, the side velocity remains almost constant. Fig. 5.15 also shows that after the stick has been released, there is a slight increase in the forward velocity. Pitch attitude remains unchanged at zero through out the 10 seconds indicating that the decoupling is good.

Control actuator deflections were shown in Fig. 5.16 for the maneuver illustrated in Figs. 5.13-5.14. It can be seen that the maneuver requires less than one degree deflection from collective, lateral, longitudinal, and tail rotor pitch. These values were very small compared to the maximum control input values of 9 degrees for collective, 8.75 degrees for lateral, 15 degrees for longitudinal, and 18.5 degrees for collective tail rotor. Hence the

inputs will not saturate the system with a aggressive maneuver that requires a ±30 deg. roll angle command. This would be a very large roll angle command for a helicopter in hover.

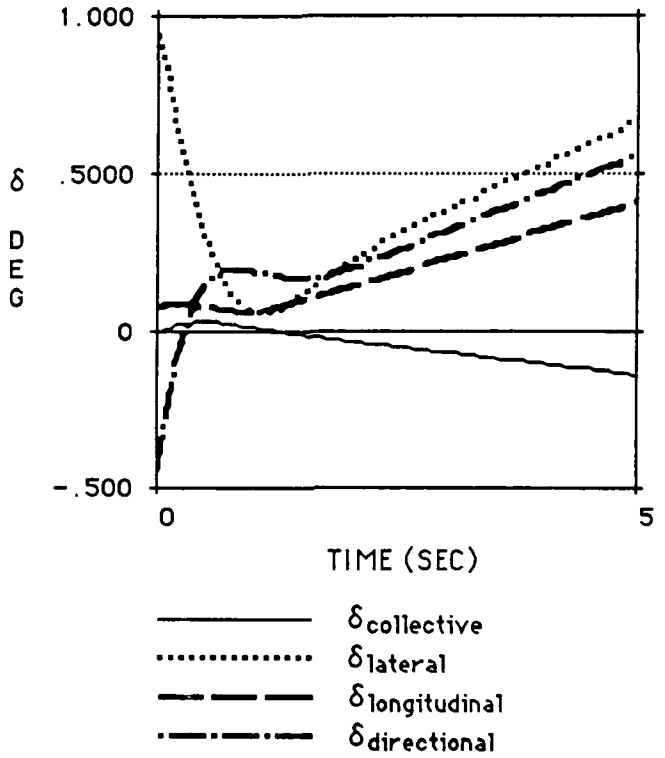

Fig. 5.16 Control Actuator Deflections.

Closed outer loop time responses were also calculated for a 5 ft/s step command in vertical velocity (Figs. 5.17 and 5.18) and a 5 deg/s command in yaw rate (Figs. 5.19 and 5.20). Pilot collective and pedal commands are of primary importance in maintaining hover. Considerable training and coordination are required for pilots to maintain a helicopter at a constant altitude during hover. Changes in collective result in changes in torque produced by the engine, this in turn produces yawing moments which must be compensated for by the changes in tail rotor collective pitch. These changes in tail rotor collective pitch effect the power supplied to the main rotor which requires changes in main

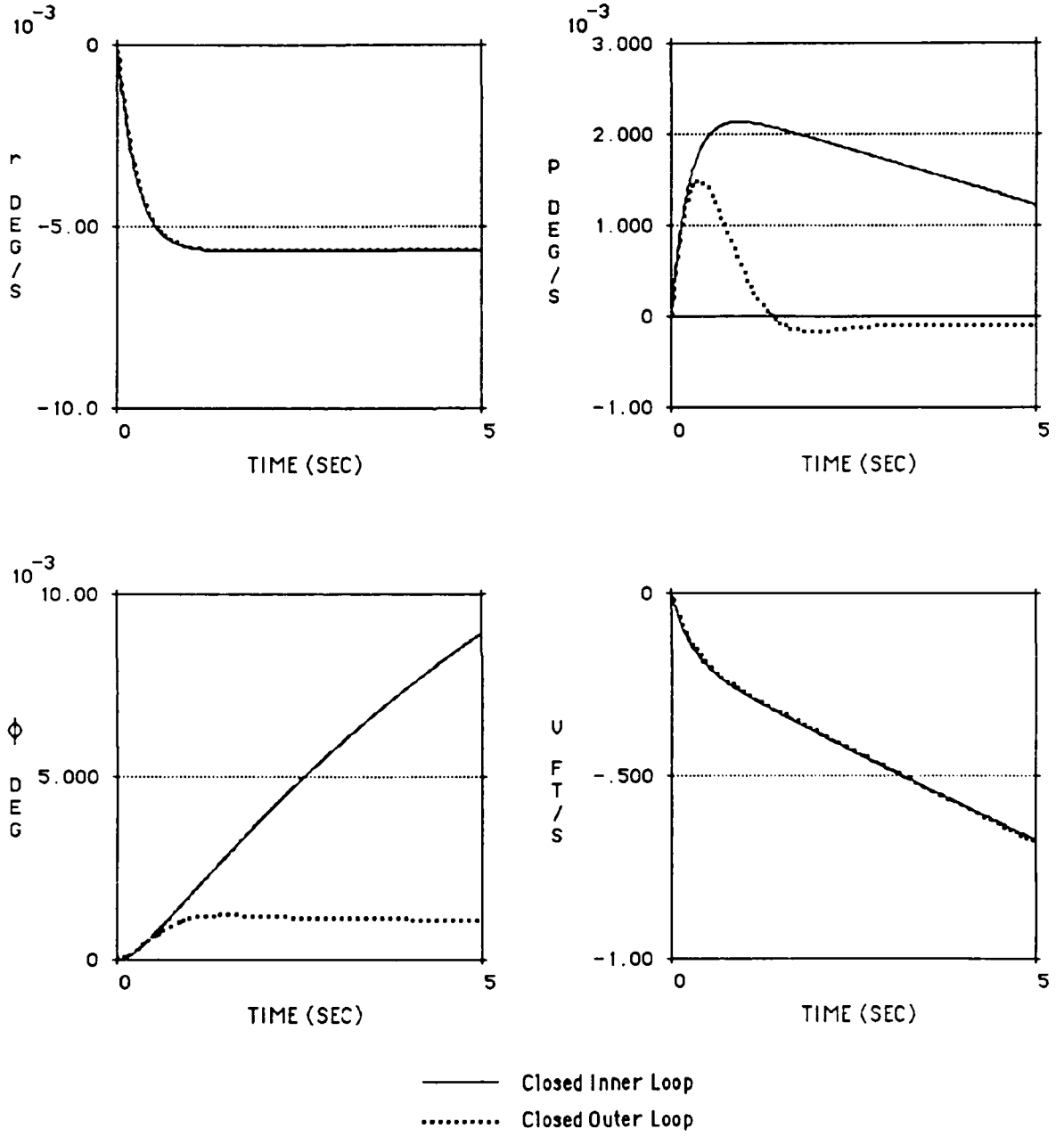

Fig. 5.17 Full State Closed Inner and Outer Loop Time Responses to a 5 ft./s Heave Command.

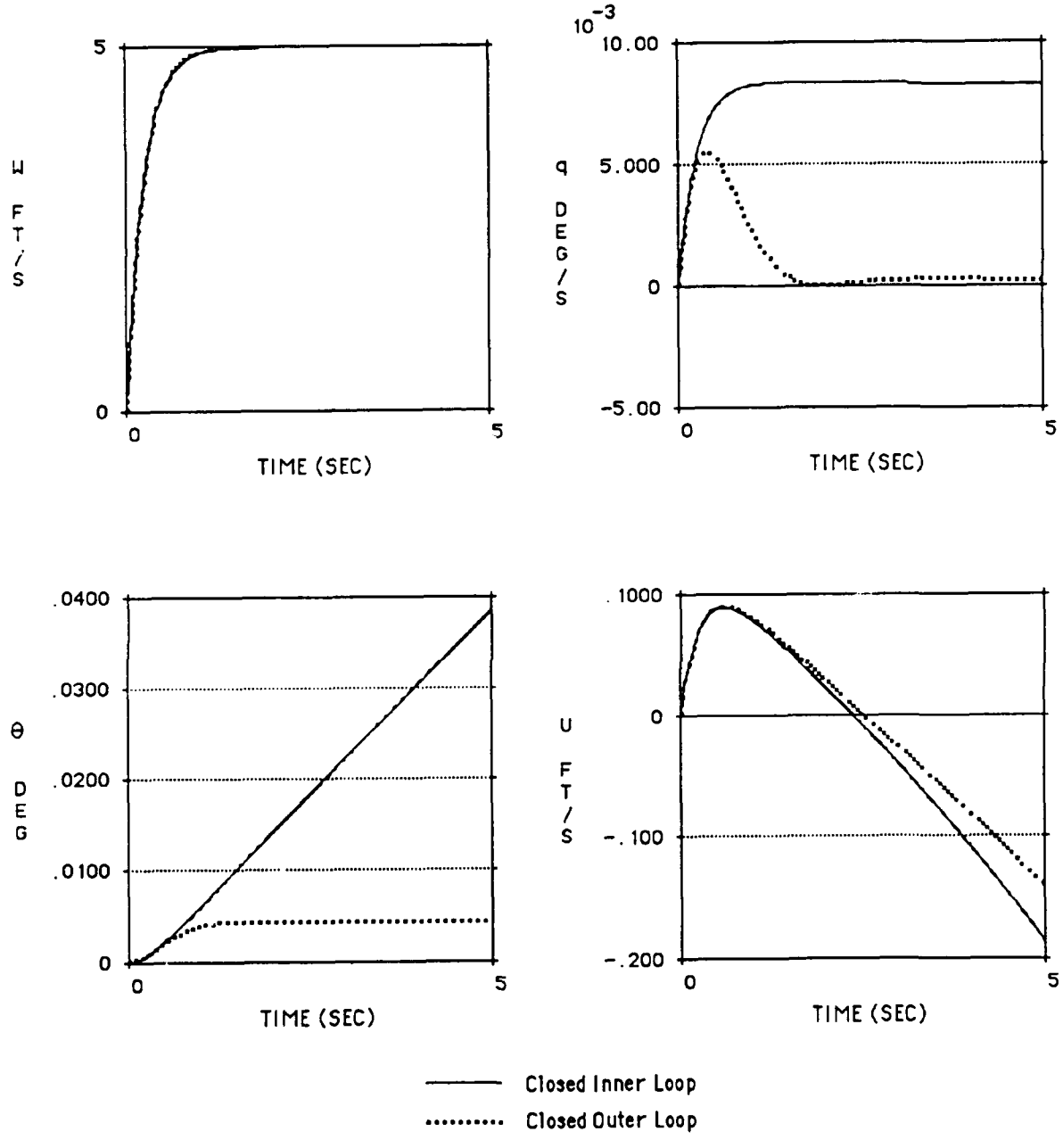

Fig. 5.18 Full State Closed Inner and Outer Loop Time Responses to a 5 ft./s Heave Command.

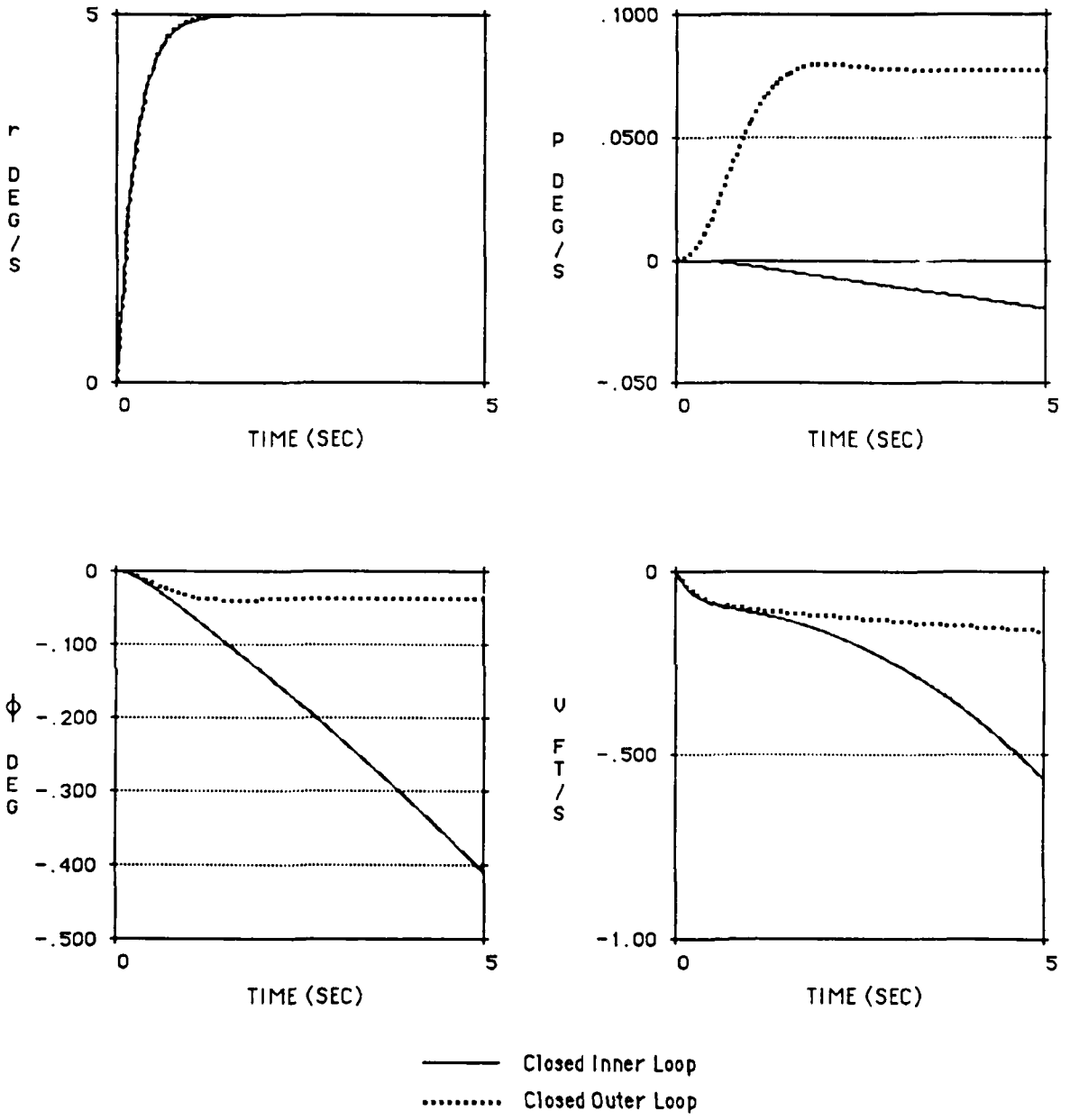

Fig. 5.19 Full State Closed Inner and Outer Loop Time Responses to a 5 deg./s Yaw Rate Command.

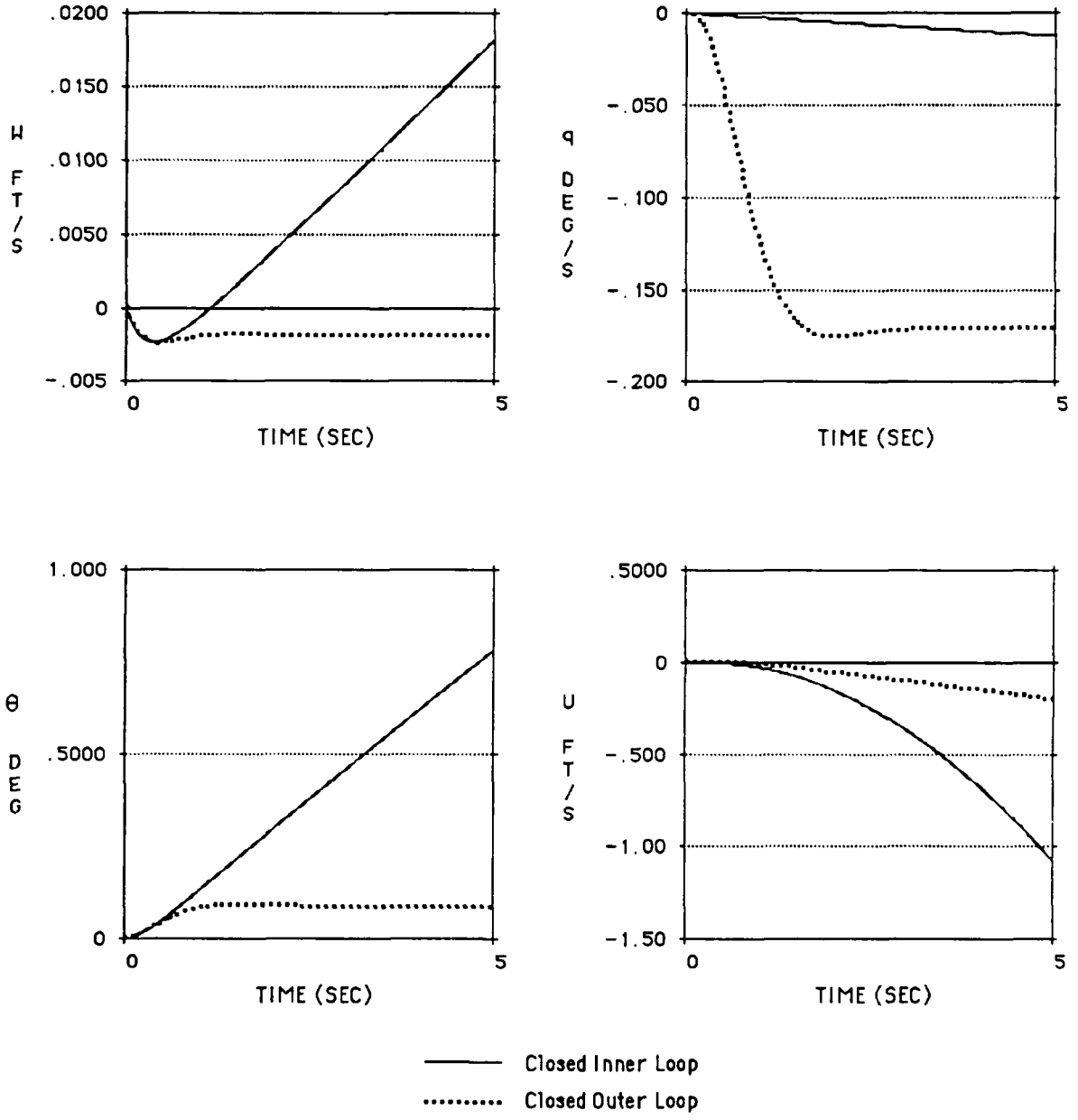

Fig. 5.20 Full State Closed Inner and Outer Loop Time Responses to a 5 deg./s Yaw Rate Command.

rotor collective pitch and so on. Decoupling response to collective and pedal inputs results in improved handling qualities. Figures 5.17 and 5.18 illustrate the response to a collective input from the pilot. A collective pitch change from the pilot input gives a change in the mean blade angle of attack, which produces a change in the thrust magnitude. The change in thrust magnitude increases the main rotor torque, which in term requires the increase in the tail rotor thrust power to provide the anti-torque forces to balance the helicopter. There is a non negligible side velocity which is caused by the change in tail rotor pitch required to balance the main rotor torque. Fig. 5.18 shows that the side velocity increases linearly in order to keep a constant yaw rate. Correction of this side velocity would require a small lateral stick input. It can be seen that the yaw rate, roll rate, pitch rate, roll angle and pitch angle are all negligible. The qualitative requirement given for collective control is to achieve vertical velocity response and shall not cause objectional response in yaw or more other axes [18]. Limits on this form of cross-coupling are specified in terms of yaw rate oscillation parameters per rate of climb. The values for $\left|\frac{r_1}{\dot{h}_3}\right|$ and $\left|\frac{r_3}{\dot{h}_3}\right|$ are 0.00111 and 0.00114 respectively. These values are much smaller than the values of 0.65 and 0.15 as required by Level 1 handling qualities.

Figures 5.19 and 5.20 show the effect of a 5 deg./s yaw rate command. The change in vertical velocity is negligible however the lateral and longitudinal responses are small but not negligible and would require both lateral and longitudinal stick inputs for stabilization. During yawing maneuvers, the drag force of a tail rotor must be countered by the main rotor. The decoupling of all states is improved when the outer loop is closed.

Since pilots are sensitive to the shape of the phase curve at frequencies above the bandwidth frequency, phase delay parameter, τ_p as defined in Eq. 5.25 is used for the evaluation of the design.

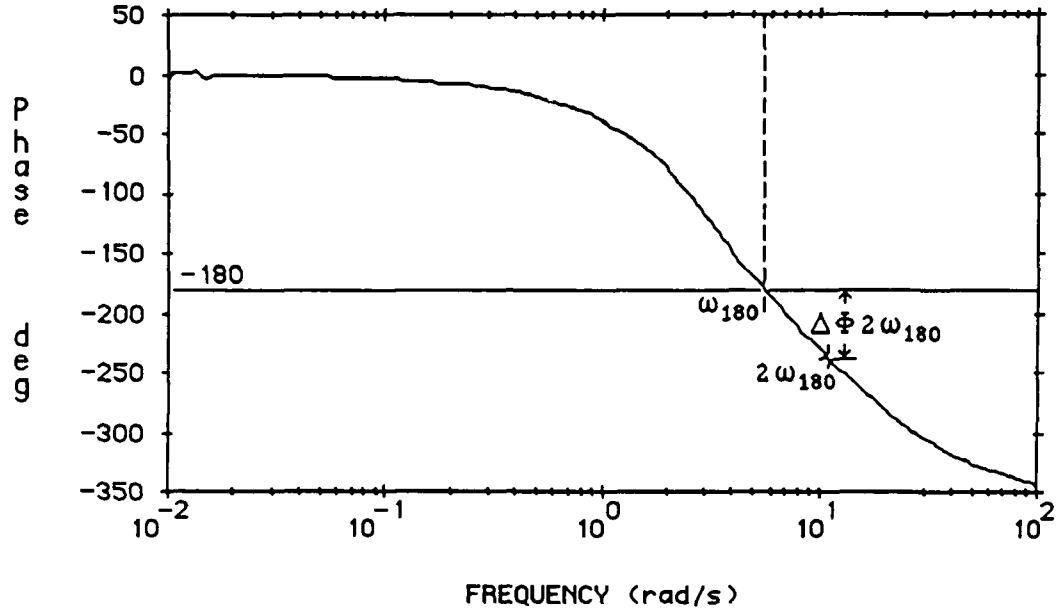

Fig. 5.21 Phase Delay of ACAH System plus Effective Time Delay.

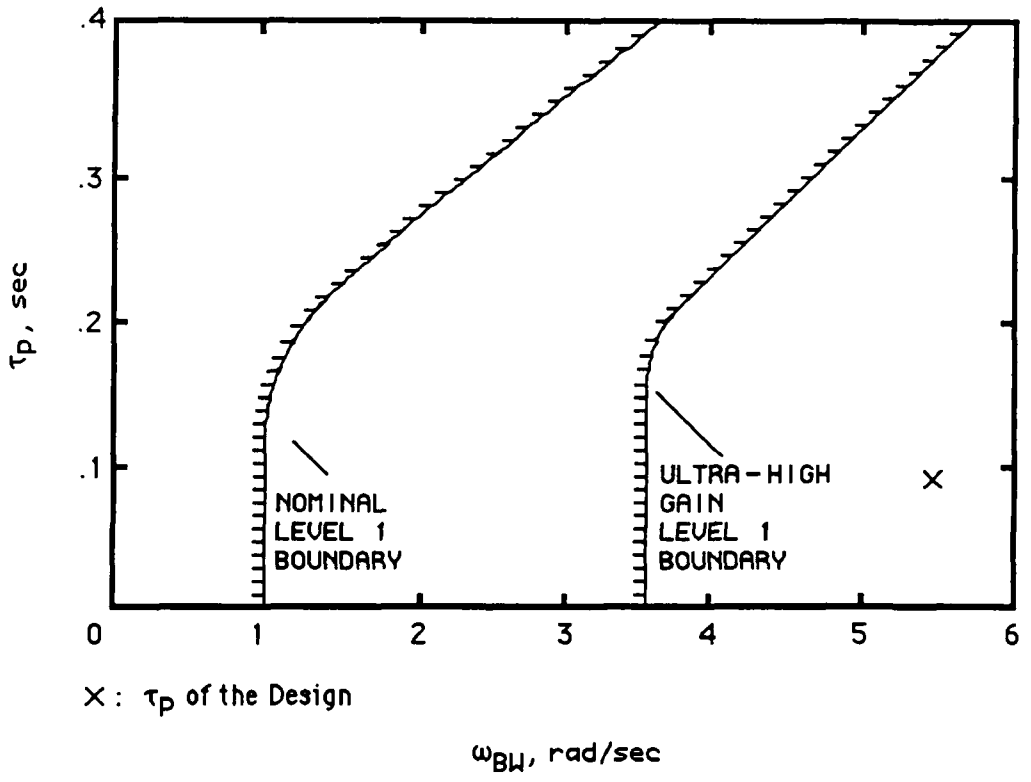

Fig. 5.22 Level 1 Small-Amplitude Requirements for Minimum and Maximum Gain Tasks.

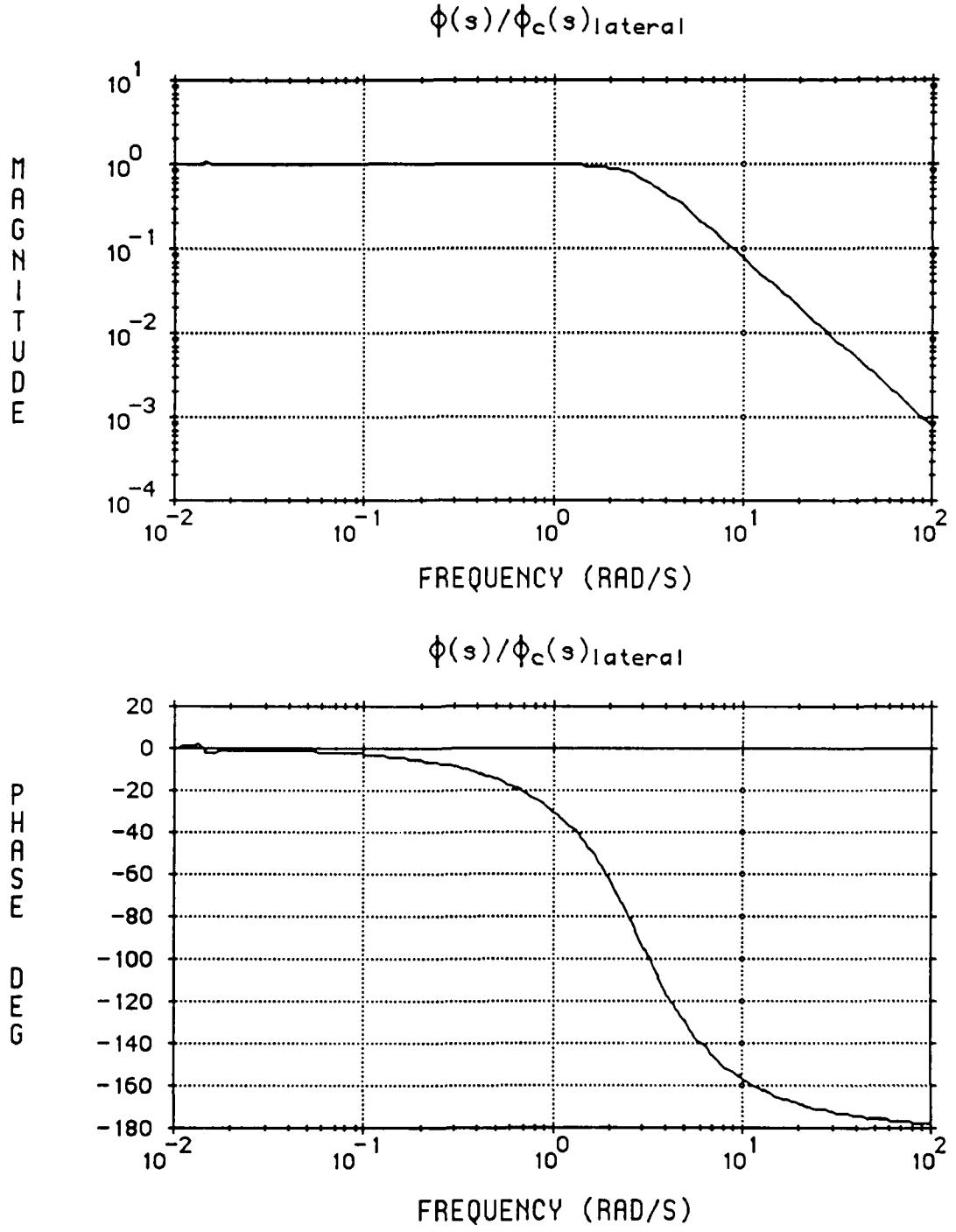

Fig. 5.23 Closed Outer Loop Full State Roll Attitude Bode Magnitude and Phase Plots.

$$\tau_p = \frac{\Delta\Phi 2\omega_{180}}{57.3\ (\ 2\omega_{180}\ )} \tag{5.25}$$

Hoh [19] indicates that for large values of phase delay, the phase curve drops off more rapidly than for small values. The evaluation of τ_p is based on the assumption that the ACAH system has a total effective time delay of 0.15 seconds in the roll axis. The resulting bode phase plot about the roll axis of the ACAH system plus total effective time delay is shown in Fig. 5.21. From figure 5.21, $\Delta\Phi 2\omega_{180}$ is determined to be 57.57 degrees and $2\omega_{180}$ is determined to be 10.98 rad/s. Using Eq. 5.25, the phase delay of the overall system is calculated to be $\tau_p = 0.092$ seconds. As shown in Fig. 5.22, this value satisfies Level 1 handling qualities requirements for ultra high gain tasks.

The bode magnitude plot in Fig. 5.23 shows that the roll attitude response to lateral input is flat until about 2.83 rad/s, it then rolls off at 40 dB/decade. The bandwidth is determined to be 5.46 rad/s from the phase plot in Fig. 5.23 using the phase margin limited criteria. Similar results are obtained for the pitch transfer function. The vertical velocity and yaw rate transfer functions are characterized by simple decoupled first order responses and are similar to each other.

B. TRCPH

With the inner rate loops closed, the transfer function between the forward velocity and the rate command is

$$\frac{u}{q_c} \approx \frac{\lambda_q}{s^2} \tag{5.26}$$

The desired transfer function for forward velocity TRCPH is

$$\frac{u}{u_c} = \frac{\omega^2_u}{s^2 + 2\zeta\omega_u s + \omega^2_u} \tag{5.27}$$

This transfer function can be obtained as shown below

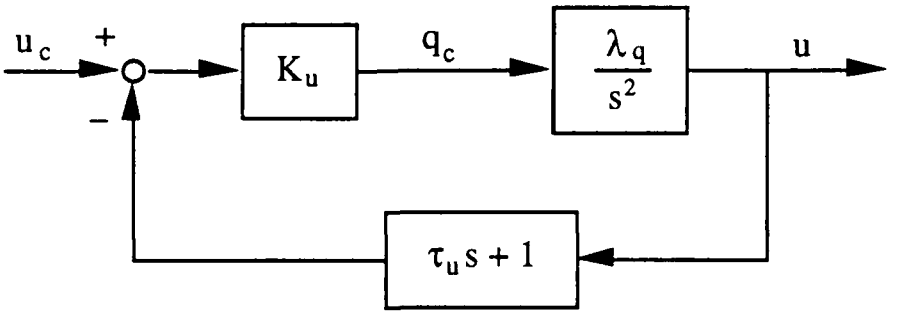

Fig. 5.24 Block Diagram for Forward Velocity TRCPH.

with the equivalent transfer function being

$$\frac{u}{u_c} = \frac{\lambda_q K_u}{s^2 + \tau_u \lambda_q K_u s + \lambda_q K_u} \tag{5.28}$$

From Eqs. 5.27 and 5.28 with λ_q fixed from the inner loop design, the gain K_u and time constant τ_u can be selected to give the desired damping ratio and natural frequency. This system will give a constant forward velocity output for a constant non-zero pilot input and zero velocity for zero input. If more precise position control is desired, it can be achieved by the addition of a positional feedback loop as shown

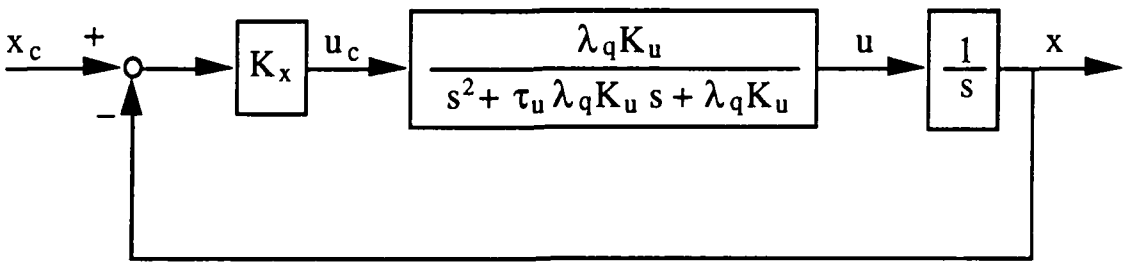

Fig. 5.25 Block Diagram for Position Control.

Similar result can be obtained for control of TRCPH of lateral velocity and position.

References

1. Tischler, Mark B., "Assessment of Digital Flight-Control Technology for Advanced Combat Rotorcraft," Presented at the American Helicopter Society National Specialists' Meeting on Rotorcraft Flight Controls and Avionics, Cherry Hill, N.J., Oct. 1987.

2. Miller, D. G. and White, F., "A Treatment of the Impact of Rotor-Fuselage Coupling on Helicopter Handling-Qualities," 43rd Annual National Forum of the American Helicopter Society, May 1987.

3. McRuer, D. T., Myers, T. T., Thompson, P. M., "Literal Singular-Value-Based Flight Control System Design Techniques," *Journal of Guidance, Control and Dynamics*, Vol. 12, No. 6, Nov.- Dec., 1989, pp 913-919.

4. Smith, Roger E., and Sarrafian, Shahan K., "Effect of Time Delay on Flying Qualities: An Update," *Journal of Guidance, Control and Dynamics*, Vol. 9, No. 5, Sept.-Oct. 1986, pp. 578-584.

5. Doyle, J. C., "Analysis of Feedback Systems with Structured Uncertainties," *Proc. IEE*, Vol. 129, Nov. 1982.

6. Doyle, J. C., Wall, J. E., and Stein, G., "Performance and Robustness Analysis for Structured Uncertainty," Proceedings of the 21st IEEE Conference on Decision and Control, Vol. 2, Dec. 1982.

7. Enns, Dale F., "Multivariable Flight Control for an Attack Helicopter," Proceedings of the 1986 American Control Conference, Seattle, Washington, June 1986, pp 858-863.

8. Enns, Dale F., "Analysis of Control Laws for an Unstable Flexible Aircraft," Proceedings of AIAA Guidance, Navigation, and Control Conference, Monterey, California, August 1987.

9. Miller, D. P. and Vinje, E. W., "Fixed-Base Flight Simulator Studies of VTOL Aircraft Handling Qualities in Hovering and Low-Speed Flight," Air Force Flight Dynamics Lab., Wright-Patterson AFB, OH, AFFDL-TR-67-152, Jan. 1966.

10. McRuer, D. T., and Krendel, E. S., "Mathematical Models of Human Pilot Behavior," AGARD-AG-188, Jan. 1974.

11. Smith, R. H., "A Unifying Theory for Pilot Opinion Rating," Proceedings of the 12th Annual Conference on Manual Control, NASA TM X-73, 170, May 1976, pp. 542-558.

12. Hess, Ronald A., and Sunyoto, Iwan, "Toward a Unifying Theory for Aircraft Handling Qualities," *Journal of Guidance, Control and Dynamics*, Vol. 8, No. 4, Jul.-Aug. 1985, pp. 440-446.

13. Hess, Ronald A., "Structural Model of the Adaptive Human Pilot," *Journal of Guidance, Control and Dynamics*, Vol. 3, No. 5, Sept.-Oct. 1980, pp. 416-423.

14. Hendrick, Russell C., "Flight Controls for Advanced Military Helicopters," *Scientific Honeyweller*, pp 144-152, Winter 1989.

15. Hoh, R. H., Mitchell, D. G., Aponso, B. L., Key, D. L., and Blanken, C. L., "Proposed specification for Handling Qualities of Military Rotorcraft, Vol. 1 - Requirements," U.S. Army Aviation Systems Command, Moffett Field, CA, TR-87-A-4, May 1988.

16. Aponso, Bimal L., Mitchell, David G. and Hoh, Roger H., "Simulation Investigation of the Effects of Helicopter Hovering Dynamics on Pilot Performance," *Journal of Guidance, Control and Dynamics*, Vol. 13, No. 1, Jan.- Feb. 1990, pp 8-15.

17. Key, David L., "A New Handling Qualities specification for U.S. Military Rotorcraft," Proceedings of Royal Aeronautical Society International Conference on Helicopter Handling Qualities and Control, London, Nov. 1988.

18. Hoh, Roger H., "Dynamics Requirements in the New Handling Qualities Specification for US Military Rotorcraft," Proceedings of Royal Aeronautical Society International Conference on Helicopter Handling Qualities and Control, London, Nov. 1988.

19. Tischler, Mark B., Fletcher, Jay W., Morris, Patrick M., and George, T. Tucker, "Application of Flight Control System Methods to an Advanced Combat Rotorcraft,"

Proceedings of Royal Aeronautical Society International Conference on Helicopter Handling Qualities and Control, London, Nov. 1988

20. Garrard, W. L., Low, E., and Prouty, S. J., "Design of Attitude and Rate Command System for Helicopters Using Eigenstructure Assignment," *AIAA Journal of Guidance, Control and Dynamics*, Vol. 12, No. 6, Nov.-Dec. 1989, pp. 783-791.

21. Strang, Gilbert, *Linear Algebra and its Applications*, 3rd Edition, Harcourt Brace Jovanovich, Publishers, San Diego, 1988.

22. Baillie, Stewart W., and Morgan, J. Murray, "Control Sensitivity, Bandwidth and Disturbance Rejection Concerns for Advanced Rotorcraft," Presented at the 45th Annual Forum of the American Helicopter Society, Boston, Massachusetts, 22-24 May, 1989.

23. Stein, G., and Athans, M., "The LQG/LTR Procedure for Multivariable Feedback Control Design," *IEEE Transactions on Automatics Control*, Vol. 32, 1987, pp 105-114.

24. Kazerooni, H., and Houpt, P. K., "On the Loop Transfer Recovery," *Int. Journal of Control*, Vol 43, 1986, pp 981-996.

25. Bidian, Peter A., "Robust Analysis for a Helicopter Controller Using a Stochastic Approach," Plan B Master's Project, Dept. of Aerospace Engr. and Mechanics, Univ. of Minnesota, Minneapolis, MN, June 1990.

Chapter 6

Robustness Analysis

I. Introduction

In control system design, the physical system to be controlled is represented by a nominal mathematical model derived from assumptions concerning the physics governing the system. The control system is then designed and evaluated using this model. Due to our inability to mathematically model any system exactly, the physical system upon which the control system actually operates responds differently to control inputs than its nominal mathematical model. Thus, no matter how well a control law may work when applied to the nominal model, it will work differently when applied to the actual system because of the presence of model uncertainties. The effects of these modeling errors must be evaluated before the control law can be considered for implementation. This evaluation is called robustness analysis. The robustness of SISO systems has been traditionally determined using the concepts of gain and phase margins. Robustness of MIMO systems requires more sophisticated concepts, and has been the area of intensive research for the last decade [1].

The purpose of this Chapter is to use several tools to analyze the robustness of the control laws designed in Chapter 5. The methods used are unstructured and structured singular value analyses and simulations using mathematical models which are more realistic than the nominal design model. The properties which are of most interest are : (1) nominal performance, that is how well the control system meets performance specifications when applied to the model used for control law design, (2) stability robustness, the ability of the control system to maintain stability despite the presence of model uncertainties, and (3)

robust performance, the ability of the control system to meet the performance specifications and maintain stability in the presence of model uncertainties [2]. Nominal performance was evaluated in Chapter 5 so this Chapter will concentrate primarily on the evaluation of stability and performance robustness.

II. Unstructured Singular Value Analysis

A. Stability Robustness

Since the inner loop system is flight critical, the stability robustness of this stabilization loop with respect to modeling errors and parameter variations is very important. A sufficient condition [3] for the closed inner loop system to be robustly stable with respect to the multiplicative error E(s) [4], is

$$\underline{\sigma}\,(\, I + [\, K(s)G(s)\,]^{-1}\,) > \bar{\sigma}\,(E(s)) \quad \text{for all } s = j\omega \tag{6.1}$$

where $0 < \omega < \infty$.

As discussed in Chapter 4, the multiplicative error is modeled as an effective time delay. The stability boundary is determined by varying the effective time delay in the closed inner loop system. Many components of the effective time delay such as delays due to rotor response and structural dynamics are essentially fixed; however, others such as computational delays and sampling times may be influenced by the design of the flight control system hardware and software. For example, a faster computer, more effective algorithms or a faster sampling rate may be used to reduce actuator delays.

Based on the data in Reference 5, a break down of the various delays is given in Table 6.1.

Element	Delay (ms)
Rotor	66
Actuators	31
Zero-order hold	17
Computations	22
Notch filter	11
Total delay	147

Table 6.1 Summary of Time Delay Contributors.

The total effective time delay is chosen to be 0.15 seconds. Since large relative modeling errors cannot be avoided as frequency increases, the modeling error is estimated to lie within the region shown in Fig. 6.1. If the modeling error is indeed within this region, stability of the closed loop system is assured if $\underline{\sigma}$ (I + [K(s)G(s)]$^{-1}$) does not enter this region. The time delay is modeled by a first order Pade approximation. The error is then

$$E(s) = \left(\frac{-2\Delta\tau s}{\Delta\tau s + 2}\right) I \qquad (6.2)$$

The maximum bandwidth that the closed loop system can achieve results when the error model has a magnitude of one, i.e. $\left|\frac{-2\Delta\tau s}{\Delta\tau s + 2}\right| = 1$. Letting $s = j\omega$, the maximum bandwidth of the first order closed loop system (i.e. a loop transfer function of $L = \frac{\omega_{bw}}{s}$) can be related to total effective time delay of the uncertainty model as follows

$$\omega_{max\ bw} = \frac{2}{\sqrt{3}\,\Delta\tau} \qquad (6.3)$$

The above equation provides a simple quantitative relationship useful in preliminary design studies as it allows the designer to trade off various hardware and/or software options versus bandwidth. As shown in Eq. 6.3, the achievable closed loop crossover

frequency depends inversely on the effective time delay $\Delta\tau$ in the stabilization loop. Using this equation, the maximum achievable crossover frequency is estimated to be 7.7 rad/s, which is substantially higher than the design bandwidth of 4 rad/s. However, it would not be prudent to try and achieve the maximum achievable bandwidth, because the error model is itself only an estimate and approximation of the actual unknown error.

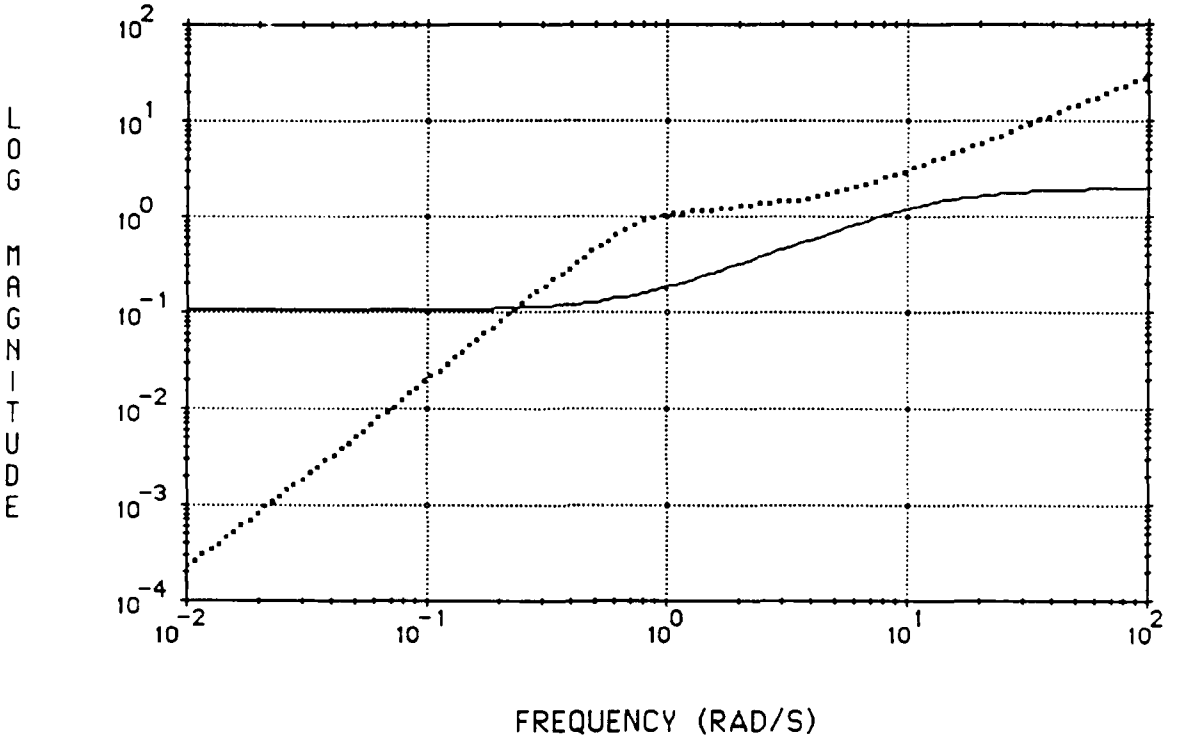

Fig. 6.1 $\underline{\sigma}$ [I + (K(s)G(s))$^{-1}$] Full State Inner Loop and Estimator in the Feedback Loop.

As can be seen in Fig. 6.1, the stability condition given in Eq. 6.1 is violated below 0.01 rad/s. Condition 6.1 is conservative so that the helicopter may not be unstable; however, this is expected because of the high condition number at low frequency. The

frequency of 0.01 rad/s is much lower than the closed loop bandwidth of 4 rad/s so even if the helicopter exhibits low frequency instabilities, it should not have any significant effect on the handling qualities.

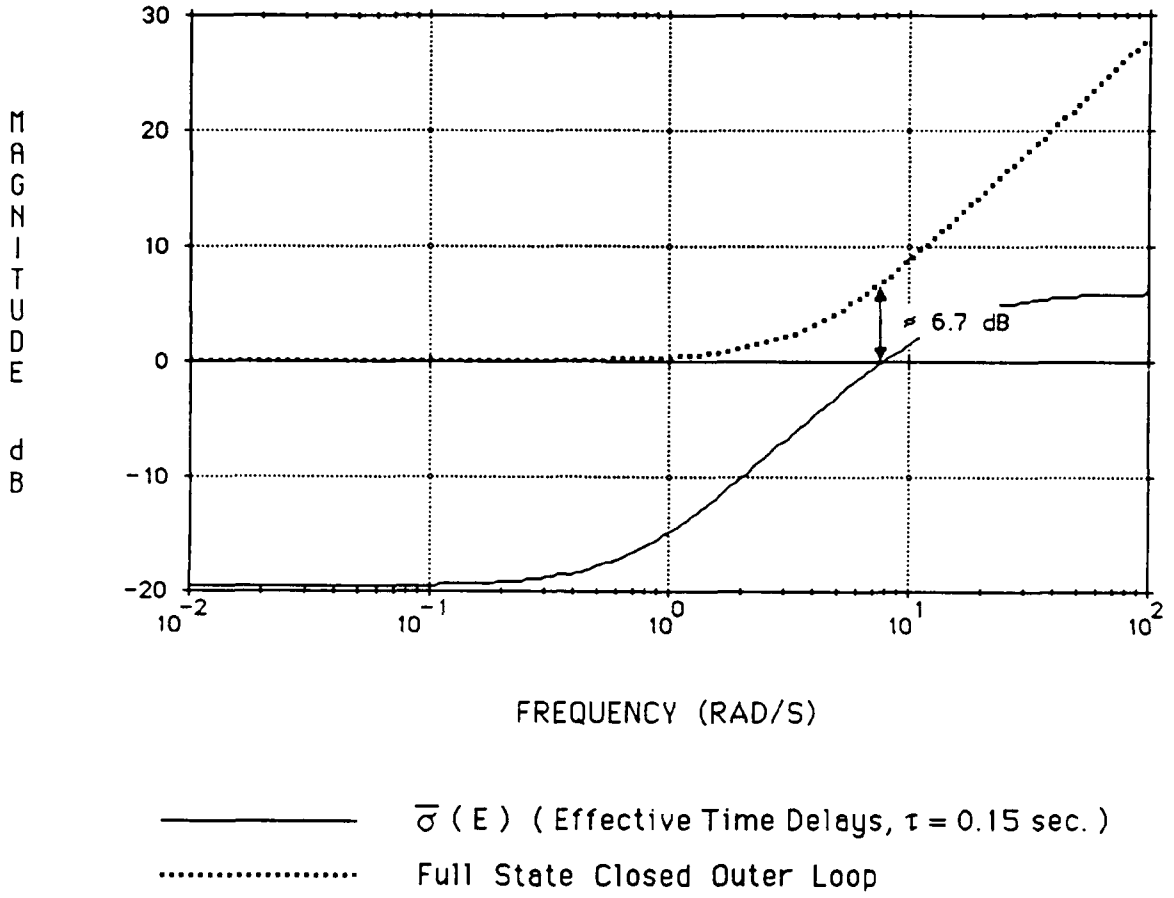

Fig. 6.2 Minimum Singular Value for Full State Closed Outer Loop and Maximum Singular Value of Error Matrix vs. Frequency.

Figure 6.2 illustrates that the stability robustness of the helicopter is further improved when the outer loop is closed. With the outer loop closed, the roll and pitch attitude responses become a second order. Closing the outer loop improves the stability robustness of the system at frequencies below 0.01 rad/s. A measure of the robustness of a MIMO system is the minimum difference between the minimum singular value of

$[\, I + (K(s)G(s))^{-1} \,]$ and the maximum singular value of the multiplicative error, E(s). This can be regarded as a MIMO gain margin. As shown in Fig. 6.2, the minimum difference between the two curves is 6.7 dB at about 7.39 rad/s.

B. Nominal Performance

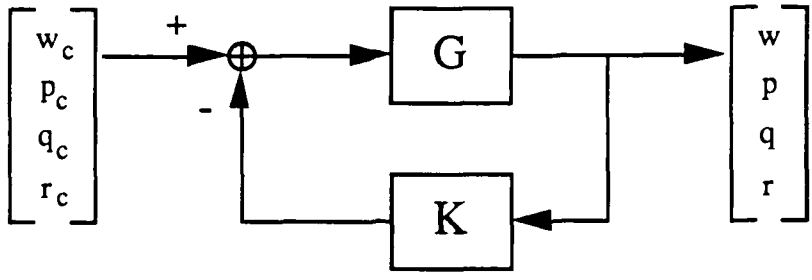

Fig. 6.3 Performance Test for Closed Inner Loop System.

The plot of the maximum singular value of a closed loop frequency response matrix can be used to test performance requirements for disturbance rejection and command following. For the closed inner loop system shown in Fig. 6.3, it is desired to achieve $\frac{4}{s+4}$ type of response from the input $\begin{bmatrix} w_c \\ p_c \\ q_c \\ r_c \end{bmatrix}$ to the output $\begin{bmatrix} w \\ p \\ q \\ r \end{bmatrix}$. The performance specification can then be represented by a Bode magnitude plot of $r(s) = \frac{4}{s+4}$. If the closed inner loop gain $\bar{\sigma}[\, G(I + K G)^{-1} \,]$ from the inputs to the outputs remains near the curve r(s) at all frequencies, the system meets its specification. A sufficient test [3] is to require that

$$\frac{1}{| r(j\omega) |}\, \bar{\sigma} [\, G(j\omega) (I + K(j\omega) G(j\omega))^{-1} \,] \leq 1 \qquad \text{for all } \omega \in \Re \tag{6.4}$$

A plot of the maximum singular value of the closed inner loop system multiplied by the inverse of the performance specification is shown in Fig. 6.4. The plot shows that the

system does not achieve the desired $\frac{4}{s+4}$ transfer function requirement at frequencies below 1 rad/s, however, the deviation from 1 is not large for frequencies greater than 0.1 rad/s. This further verifies the results obtained in Chap. 5 that the closed inner loop system does not have total poles/ zero cancellation at low frequencies. However, the time histories given in Chapter 5 show that the response of the system to commands is excellent.

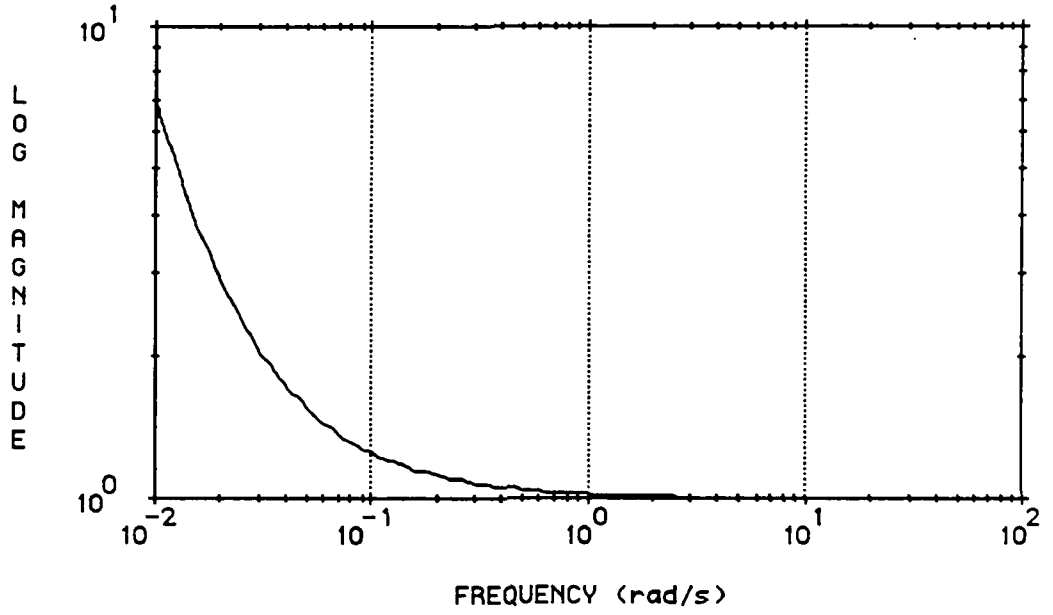

Fig. 6.4 $\frac{1}{|\, r(j\omega)\,|}\, \bar{\sigma}\,[\, G(j\omega)\,(\,I + K(j\omega)\,G(j\omega)\,)^{-1}\,]$.

III. Structured Singular Value Analysis

A. Theory

Unstructured singular value analyses are sometimes overly conservative because they do not take into account any information which may be available on the structure of the uncertainties. Structured singular value analyses methods have been developed to provide less conservative estimates of robustness properties than can be obtained from unstructured singular value analyses.

This section gives a fairly brief introduction to structured singular value, or μ-based methods. The μ-based methods discussed here have proven to be useful for analyzing the performance and robustness properties of linear feedback systems. The general robust performance framework used was developed by Doyle [7]-[12] in the early 1980's. Doyle uses the general interconnection structure illustrated in Fig. 6.5

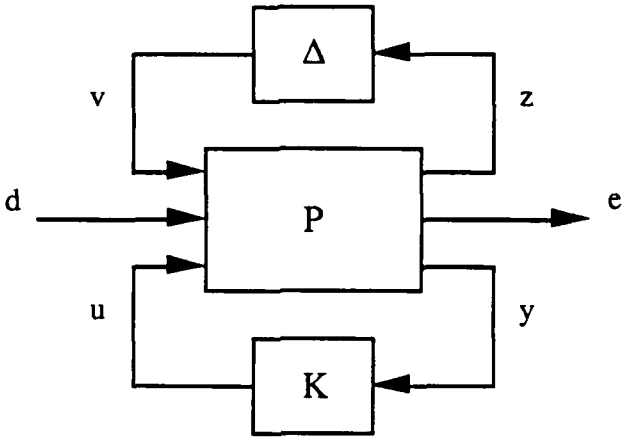

Fig. 6.5 General Interconnection Structure.

Any linear interconnection of inputs, outputs, commands, perturbations and a controller can be rearranged in the form of Fig. 6.5. The nominal model P(s), a 3x3 partitioned matrix, the controller K(s) and the perturbations Δ(s) are assumed throughout to be linear and time invariant. Four of the signals are familiar from standard control system literature. These are external inputs (disturbances), d, errors, e, measured plant outputs y, and control commands u. These four signals form four pairs of terminals, one being the $\frac{y}{u}$ pair across which the control law is connected, one being $\frac{e}{d}$, representing errors due to inputs or disturbances, one being $\frac{y}{d}$, representing sensor outputs due to inputs, and the other is the $\frac{e}{u}$ pair which represents the errors due to command inputs. The remaining terminals are connected to a bounded perturbation model (Δ) representing various uncertainties in the system.

The robust performance problem for helicopter control is defined in the block diagram shown in Fig. 6.6. The eighth order rigid body dynamic equations are in the helicopter equations block, which is equivalent to the nominal model P(s) in Fig. 6.5. Sensors measure linear velocities, body angular rates, and roll and pitch attitudes. Model uncertainty is parameterized with a multiplicative perturbation at the control inputs. The controller K(s) consists of full state feedback, feed forward, and outer loop feedback gain matrices.

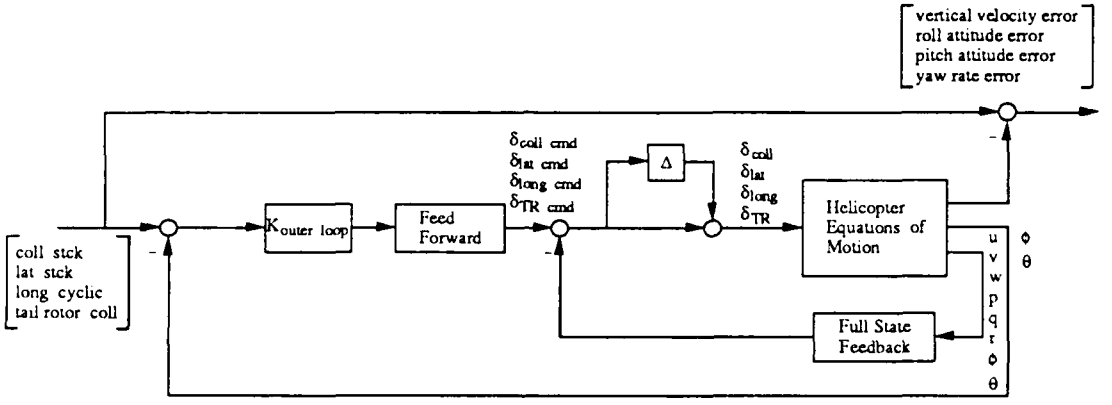

Fig. 6.6 Robust Performance Block Diagram Description.

The interconnection structure shown in Fig. 6.6 has four inputs and four outputs. The four inputs correspond to the pilot's collective, lateral cyclic, longitudinal cyclic and tail rotor collective inputs. The four outputs correspond to vertical velocity error, roll and pitch attitude errors, and yaw rate error.

For the purpose of analysis, the diagram of Fig. 6.6 reduces to that of Fig. 6.7 which is analogous to closing the lower loop of P with K in Fig. 6.5. The feedback control law can be thought of as another system component and which is incorporated into the model to yield a stable closed loop system, M. This forms the closed loop response interconnection

structure suitable for μ analysis. The closed loop system has a frequency response M(jω) that depends on P(jω) and K(jω).

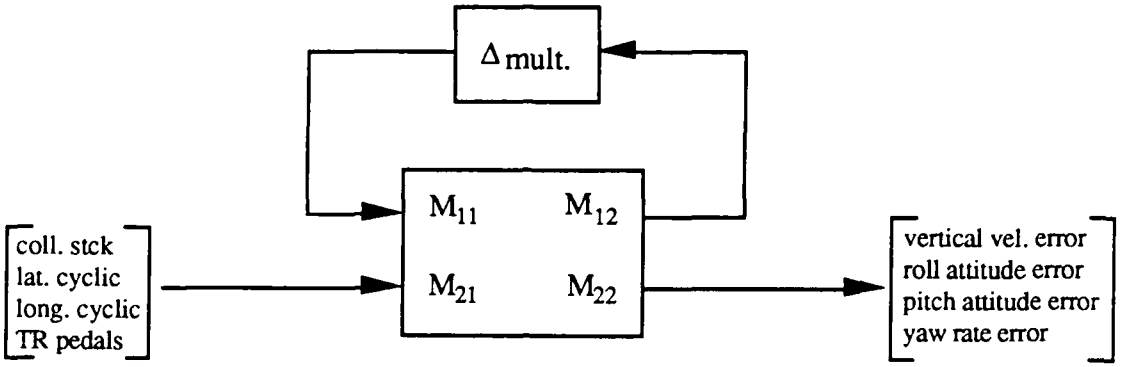

Fig. 6.7 Perturbed Pilot Stick Inputs to Errors.

B. Mathematical Formulation

This section begins with an explanation of the matrix and block diagram notation that will be used throughout this Chapter. $\Re^{nxk}$ is a real n x k matrix. Let $M \in \Re^{nxk}$, a real rational matrix function of the Laplace operator, s, whose elements can be represented by rational transfer functions, u and v are real vectors, with $u \in \Re^k$, $v \in \Re^n$, and $v = M u$ as given below

Fig. 6.8 Matrix-Vector Multiplication.

The block diagram for the standard feedback loop is illustrated in Fig. 6.9 where G is the plant and K is the controller. It is conventional to absorb any scalings, weights, or coloring filters into G to form P as given in Fig. 6.5. Since G is unweighted for the analysis purpose, it is the same as P in Fig. 6.5. If the eighth order dynamic equations of the helicopter in Fig. 6.6 are defined to be G, and the full state feedback, feed forward, and

outer loop feedback gain matrices are defined to be the controller K, then Fig. 6.6 is equivalent to the standard feedback loop.

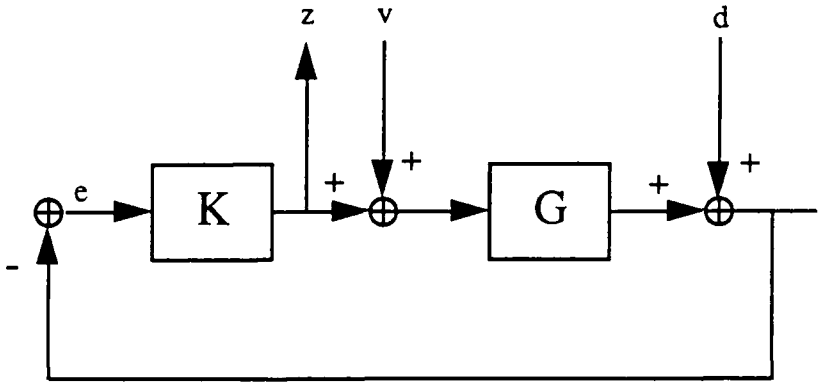

Fig. 6.9 Block Diagram for the Standard Feedback Loop.

In order to introduce a class of general linear feedback loops called the Linear Fractional Transformation, the matrix M is partitioned in 2 x 2 fashion as

$$M = \begin{bmatrix} M_{11} & M_{12} \\ M_{21} & M_{22} \end{bmatrix} \tag{6.5}$$

and furthermore $\begin{bmatrix} z \\ e \end{bmatrix} = M \begin{bmatrix} v \\ d \end{bmatrix}$. This can be represented as shown in Fig. 6.10

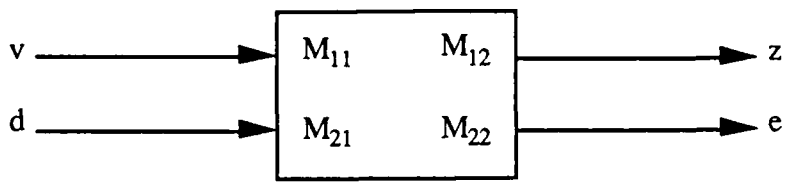

Fig. 6.10 Partitioned Matrix-Vector Multiplication.

Now, consider the analysis model which isolates the nominal part of the system M from the perturbations Δ as shown in Fig. 6.10. Suppose there is a defined block structure Δ which is compatible in size with M_{11}. Let $\Delta = \text{diag}\ (\Delta_1, \ldots, \Delta_n)$ be a block diagonal matrix. Let $\underline{\Delta}$ be the set of all matrices with a given, fixed block diagonal structure. The

individual i blocks may be either scalars or matrices. Assume that $\Delta_i \in C^{k_i x k_i}$; that is, each Δ_i is a square k_i x k_i complex matrix. The total matrix dimension of Δ is $m = \sum_{i=1}^{n} k_i$.

It is known that for a block diagonal $\Delta \in \underline{\Delta}$, $\bar{\sigma}(\Delta) = \max_i \bar{\sigma}(\Delta_i)$ [12]. That is, the overall gain of Δ is equal to the gain of its largest diagonal block.

For $\Delta \in \underline{\Delta}$, consider the following loop equations

$$\begin{aligned} z &= M_{11} v + M_{12} d \\ e &= M_{21} v + M_{22} d \\ v &= \Delta z \end{aligned} \tag{6.6}$$

The elements of M can be defined for the standard feedback loop shown in Fig. 6.9 with performance and plant perturbations specified at output and input respectively, as

$$M_{11} = K G (I + K G)^{-1} \tag{6.7}$$

$$M_{12} = K (I + G K)^{-1} \tag{6.8}$$

$$M_{21} = G (I + K G)^{-1} \tag{6.9}$$

$$M_{22} = (I + G K)^{-1} \tag{6.10}$$

The set of equations (6.6) is well posed, if for any vector d, there exist unique vectors v, z, and e satisfying the loop equations. Substituting v into the equation for e, it is obvious that the set of equations is well posed if and only if the inverse of $[I - M_{11} \Delta]$ exists. If not, then depending on d and M, there is either no solution to the loop equations, or there are an infinite number of solutions. If the inverse of $(I - M_{11} \Delta)$ does exist, the transfer function from d to e can be expressed as $e = F_u(M,\Delta)\, d$ where

$$F_u(M,\Delta) = M_{22} + M_{21} \Delta (I - M_{11} \Delta)^{-1} M_{12} \tag{6.11}$$

F_u (M,Δ) is called a Linear Fractional Transformation on M by Δ, and in a feedback diagram appears as

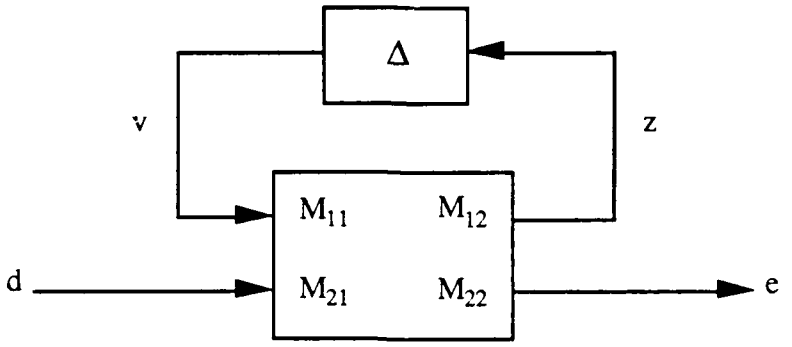

Fig. 6.11 Linear Fractional Transformation.

As can be seen from Fig. 6.11, M_{22} is the nominal map between the disturbance and error, and Δ represents perturbations, which affect the map through M_{11}, M_{12}, and M_{21}. The subscript u on F means that the "upper" loop of M is closed by Δ. An analogous "lower" linear fractional transformation F_l (P,K), describes the resulting matrix M obtained by closing the "lower" loop of P in Fig. 6.5.

The structured singular value of the matrix $M \in C^{mxm}$ denoted μ [M] is defined by

$$\mu [M] := \frac{1}{\min\limits_{\Delta \in \underline{\Delta}} \{ \bar{\sigma} (\Delta) : \det (I + M \Delta) = 0 \}} \qquad (6.12)$$

If no $\Delta \in \underline{\Delta}$ makes I + M Δ singular, and then μ [M] = 0. In addition, the structured singular value has the following properties

$$\rho [M] \leq \mu [M] \leq \bar{\sigma} [M] \qquad (6.13)$$

where ρ [M] is the spectral radius (largest eigenvalue) of M [8].

C. Robust Stability

The robust stability question is cast in terms of the closed loop response $M = F_l(P,K)$ shown in Fig. 6.6 and it involves determining whether the error remains in a desired set for the sets of inputs and perturbations Δ of size 1 or less. The robust stability question is answered by computing the structured singular value of M_{11} for block diagonal Δ. Since Δ has only one block in this case, the structured and unstructured singular values are the same. In general, this is not true. If this structured singular value is less than one for all frequencies, then stability is guaranteed for all possible uncertainties. That is, stability is robust if and only if

$$\bar{\sigma}[M_{11}(j\omega)] < 1 \qquad \forall\, \omega \qquad (6.14)$$

or

$$\mu[M_{11}(j\omega)] < 1 \qquad \forall\, \omega \qquad \text{for block diagonal } \Delta \qquad (6.15)$$

D. Nominal Performance

In the helicopter control problem, the nominal performance is acceptable if the responses meet the handling qualities specifications. The Level 1 handling qualities for an ACAH system require the following transfer functions. Bandwidth must be 2 rad/s or greater

$$\frac{w}{w_c} = \frac{\lambda_w}{(s + \lambda_w)}$$

$$\frac{\phi}{\phi_c} = \frac{\omega^2_\phi}{(s^2 + 2\zeta\omega_\phi s + \omega^2_\phi)}$$

$$\frac{\theta}{\theta_c} = \frac{\omega^2_\theta}{(s^2 + 2\zeta\omega_\theta s + \omega^2_\theta)}$$

$$\frac{r}{r_c} = \frac{\lambda_r}{(s + \lambda_r)}$$

Nominal performance means that with no model uncertainty as illustrated in Fig. 6.12, the system satisfies the above transfer functions from inputs d, to outputs e. If M_{22} achieves nominal performance, the closed outer and inner loop system will satisfy the handling qualities specifications. The nominal performance question is answered by computing the maximum singular value of M_{22}. If this maximum singular value is less than one for all frequencies then nominal performance has been achieved.

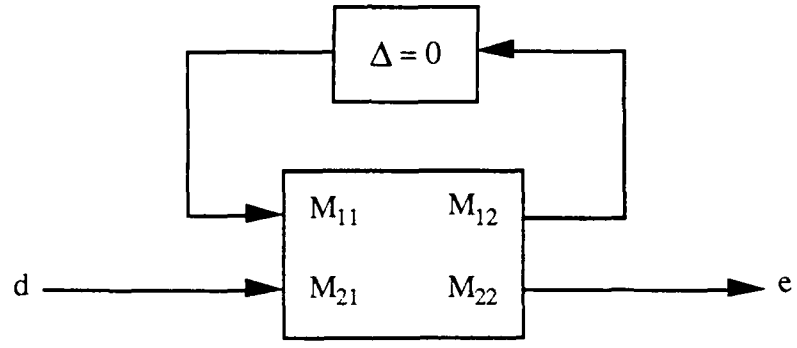

Fig. 6.12 Linear Fractional Transformation for Nominal Performance.

The nominal performance specification is satisfied if and only if

$$\bar{\sigma} [M_{22} (j\omega)] < 1 \qquad \forall \omega \qquad (6.16)$$

E. Robust Performance

The performance is robust if the desired response meets the handling qualities specifications (performance) in the presence of nonzero model uncertainty. The robust performance question is answered by computing the structured singular value of M for a block diagonal perturbation structure. If the structured singular value of M is less than one

for all frequencies, then robust performance has been achieved. That is performance is robust if and only if

$$\mu [M (j\omega)] < 1 \qquad \forall \omega \qquad (6.17)$$

F. Weighting Functions

The structured singular value analysis will be discussed with reference to the equivalent block diagrams shown in Figs. 6.6 and 6.7. The frequency response of the perturbation is used to model the effective time delay, $e^{-s\Delta\tau}$. Using a first order Pade approximation for the total effective time delay, the error can be expressed as

$$\Delta(s) = [\frac{- 2s}{s + \frac{2}{\Delta\tau}}] I \qquad (6.18)$$

The uncertainty is formulated in such a way that the perturbations enters the system in a feedback form, or a linear fractional way. For the uncertainty model to be more realistic, a 10% error at low frequencies is included in the error model. In the case of the multiplicative model uncertainty parameterized at the control inputs, the formalism for robust stability analysis requires $| \Delta_{mult} (j\omega) | \leq 1$ for all ω. For $\Delta\tau = 0.15$ seconds., the unweighted transfer function of Δ_{mult} is

$$\Delta_{mult} (s) = (\frac{s + 0.7}{s + 0.001}) (\frac{2s}{s + \frac{2}{0.15}}) \qquad (6.19)$$

This transfer function will have magnitude greater than one at frequencies greater than 7.7 rad/s. Therefore, a weighting function for the multiplicative uncertainty is required to make $| \Delta_{mult} (j\omega) | \leq 1$ for all ω. This weighting transfer function, $w_\Delta (s)$, is selected such that

$$\Delta_{mult} (j\omega) = \Delta'_{mult} (j\omega) \; w_\Delta (j\omega) \qquad (6.20)$$

where

$$| \Delta'_{mult} (j\omega) | \leq 1 \qquad \forall \omega \qquad (6.21)$$

Hence the weighting transfer function for the multiplicative uncertainty is given by

$$w_{\Delta}(s) = \left(\frac{s + 0.7}{s + 0.001} \right) \left(\frac{2s}{s + \frac{2}{0.15}} \right) = \Delta_{mult} (j\omega)$$

The weighting function for the inputs was chosen such that maximum pilot input to each channel satisfies the ACAH handling qualities specifications [13]-[14] for small amplitude inputs. The mathematical model [15]-[17] of the human pilot's central nervous and neuromuscular systems is very complicated. Therefore, a simple pilot model of a pure gain with a representative transport delay is used (high frequency pilot neuromuscular dynamics are included in the time delay) [18]-[19]. The addition of pilot lead is also studied by Aponso [18]. References 14 to 18 show that a first order low frequency phase lag characteristics are expected when pure gain dynamics are being controlled. The nominal design in Chapter 5 can be considered as a unity gain system. For simplicity, the pilot is modeled as a unity gain low pass filter of the form $\frac{a}{s + a}$. Based on experimental results [20], a bandwidth of 0.1 rad/s was chosen for this filter.

From Reference 13, a maximum input of 15 ft./s in vertical velocity, ± 10° in roll attitude, ± 5° in pitch attitude and ± 10 deg./s in yaw rate are required for small amplitude maneuvers. The resulting input weighting function is

$$w_d^{-1} = \begin{bmatrix} \frac{15(0.1)}{s+0.1} & 0 & 0 & 0 \\ 0 & \frac{10(0.1)}{s+0.1} & 0 & 0 \\ 0 & 0 & \frac{5(0.1)}{s+0.1} & 0 \\ 0 & 0 & 0 & \frac{10(0.1)}{s+0.1} \end{bmatrix} \begin{bmatrix} \text{ft./s} \\ \text{deg.} \\ \text{deg.} \\ \text{deg./s} \end{bmatrix}$$

According to Reference 14, the desired performance for precision hover is to maintain altitude within ± 1 meter (3.28 ft.) and heading within ± 2 degrees. Similar requirements are apply to roll attitude and pitch attitude. We will assume that errors must be reduced to zero in one second or less. Therefore, the output weighting function is selected so that vertical velocity is within ± 3.28 ft./s, yaw rate is within ± 2 deg./s, and roll and pitch attitude angles are within ± 2 degrees. The resulting output weighting matrix is given as

$$w_e = \begin{bmatrix} \frac{1}{3.28} & 0 & 0 & 0 \\ 0 & \frac{1}{2} & 0 & 0 \\ 0 & 0 & \frac{1}{2} & 0 \\ 0 & 0 & 0 & \frac{1}{2} \end{bmatrix} \begin{bmatrix} \text{s/ft} \\ \text{1/deg} \\ \text{1/deg} \\ \text{s/deg} \end{bmatrix}$$

When the multiplicative uncertainty, input and output weighting matrices are included in $M = F_l(P,K)$, the interconnection structure M' is

$$M' = \begin{bmatrix} w_\Delta KG(I+KG)^{-1} & w_\Delta K(I+GK)^{-1} w_d^{-1} \\ -w_e G(I+KG)^{-1} & w_e (I+GK)^{-1} w_d^{-1} \end{bmatrix} \qquad (6.22)$$

Therefore, the **robust stability** test is

$$\bar{\sigma}[M'_{11}] < 1 \qquad \forall \omega \qquad (6.23)$$

or

$$\bar{\sigma}\,[\, w_\Delta\, KG\,(\, I + KG\,)^{-1}\,] \;<\; 1 \qquad \forall\, \omega$$

The **nominal performance** test is

$$\bar{\sigma}\,[\, M'_{22}\,] \;<\; 1 \qquad \forall\, \omega \qquad (6.24)$$

or

$$\bar{\sigma}\,[\, w_e\,(\, I + GK\,)^{-1}\, w_d^{-1}\,] \;<\; 1 \qquad \forall\, \omega$$

and the **robust performance** test is

$$\mu\,[\, M'\,] \;<\; 1 \qquad \forall\, \omega \qquad (6.25)$$

G. Results

A plot of the maximum singular value of M'_{11} is shown in Figure 6.13. This indicates whether stability is guaranteed for model uncertainty discussed in the previous section. The maximum singular value has a value of greater than one at frequencies lower than 0.1 rad/s. Since this is in the frequency range in which instabilities will still result in Level 1 or 2 handling qualities, the robust stability test is considered satisfactory even though there is potential for low frequency instabilities.

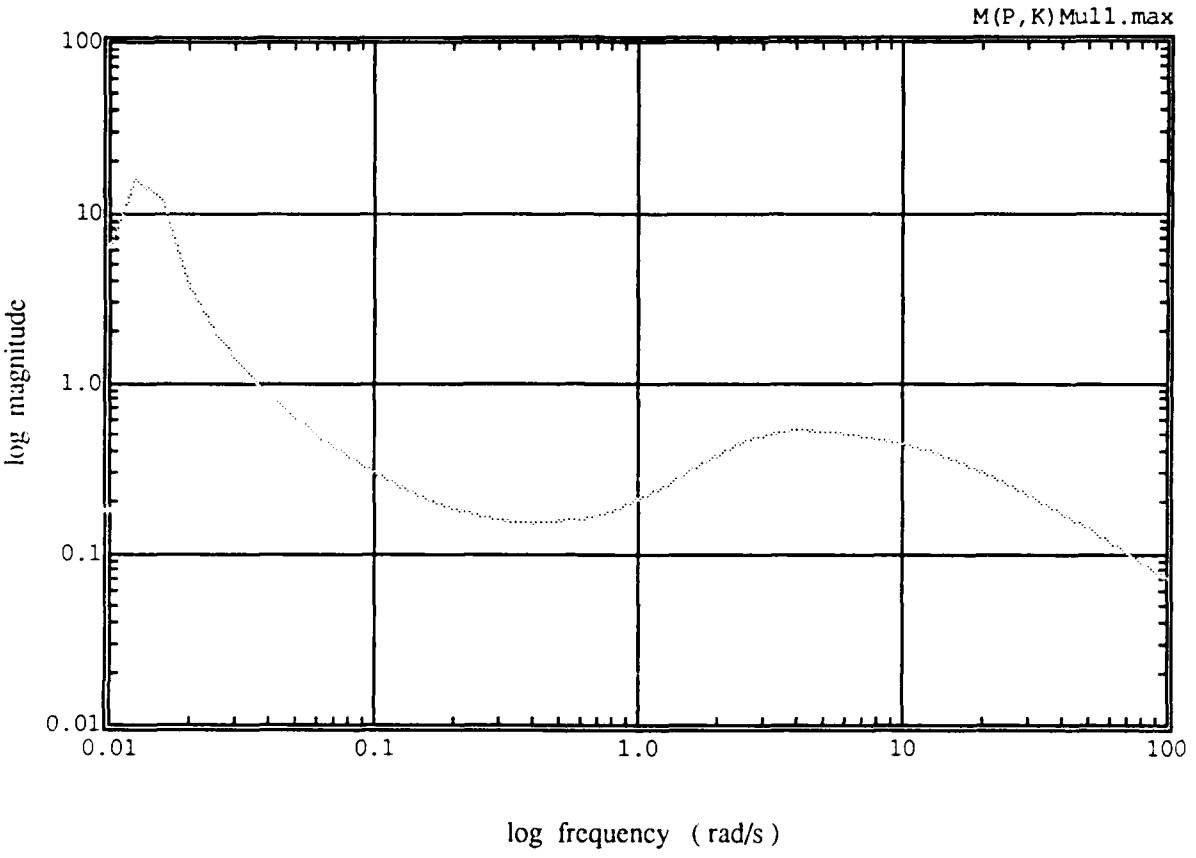

Fig. 6.13 $\bar{\sigma}$ [M'_{11}], Maximum Singular Value for Robust Stability.

The maximum singular value plot of M'_{22} is shown in Fig. 6.14. Since it is less than one for all frequencies, the vertical velocity, roll and pitch attitudes, and yaw rate deviations from desired are within the errors admitted by the weighting, w_e, discussed in Part E of this section. Thus nominal performance is guaranteed. This result also agrees with the time history responses obtained in Chapter 5.

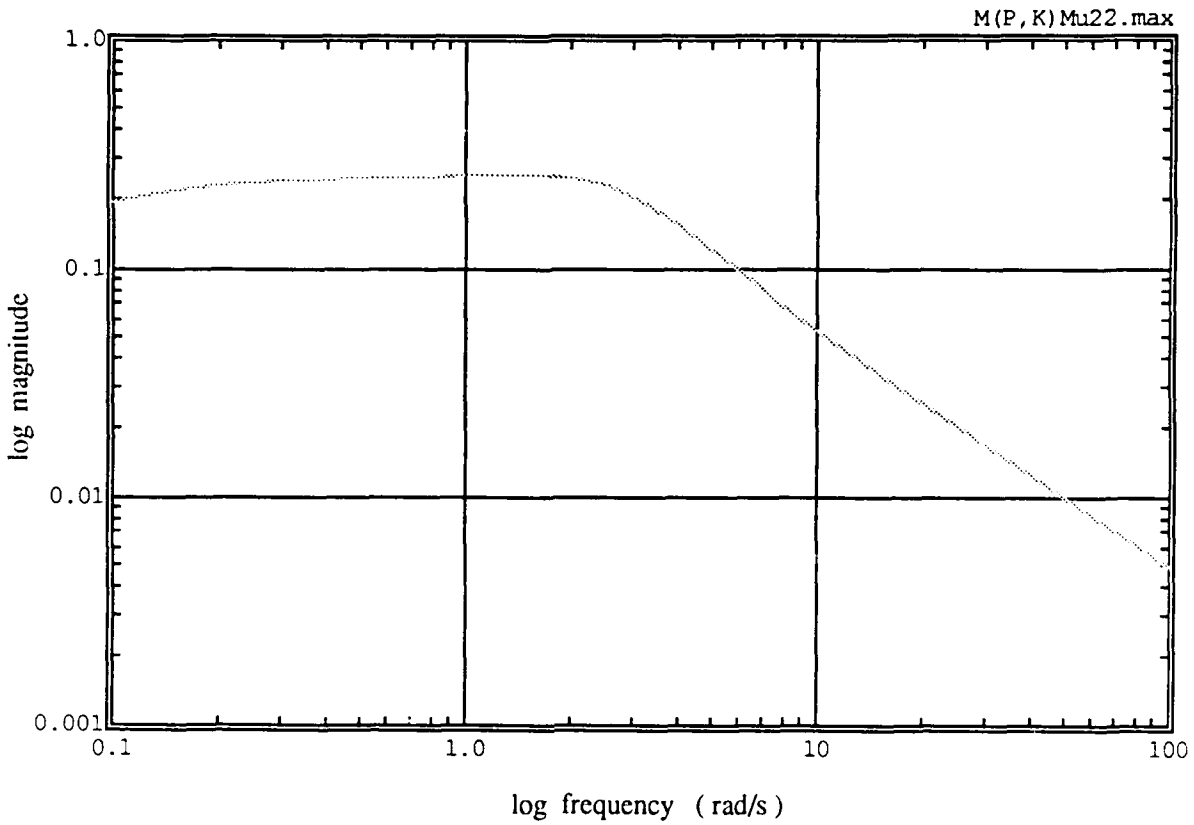

Fig. 6.14 $\bar{\sigma}$ [M'_{22}], Maximum Singular Value for Nominal Performance.

The robust performance question is answered by computing the structured singular value of M' for a two block structure. One block of this two block structures is Δ_{mult} and one block is "unit sized" Δ_o (nominal performance) [11]. A plot of this structured singular value is shown in Figure 6.15. The structured singular value is greater than one at frequencies lower than 0.15 rad/s. The robust performance is considered acceptable because frequencies lower than 0.15 rad/s are associated to the low frequency "phugoid" modes. This will be discussed in detail the following section. The vertical velocity, roll and pitch attitude, and yaw rate responses deviations from desired are within the errors, w_e, in the presence of model uncertainty.

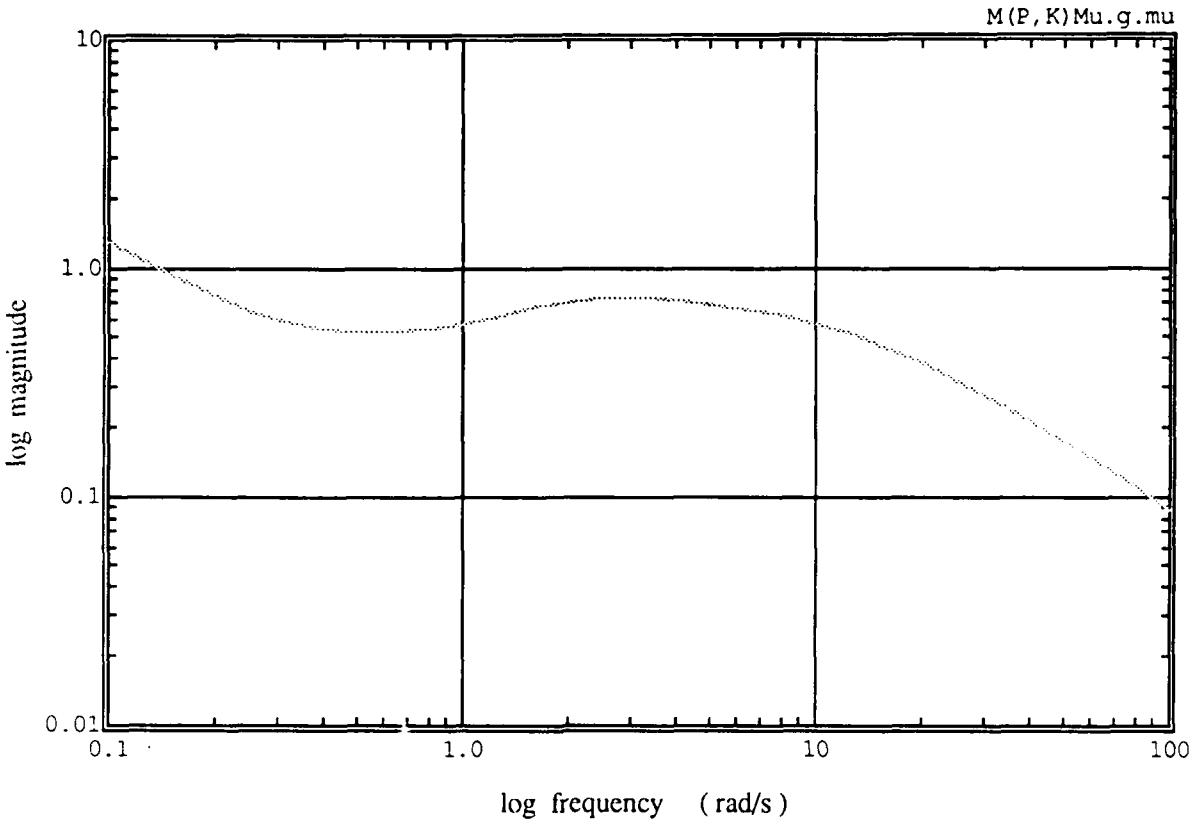

Fig. 6.15 μ [M'], Structured Singular Value for Robust Performance.

IV. Simulations

A. Analysis of Worst Case Perturbation

A different stability robustness test was used to examine the effect of variations of parameters in the nominal model. This is due mainly to the difficulty of determining the aerocoefficients of the rotorcraft accurately and results in low frequency uncertainties. Reference 21 used the stochastic root locus method to determine the influence of the simultaneous variations of between ± 20% the nominal values of all the elements of the A and B matrices on the closed inner loop eigenvalues. It was determined that varying the

element $A_{4,2}$ of the state matrix by - 20% and the element $B_{4,2}$ of the control matrix by + 20% resulted in the largest positive eigenvalue of any combination of variations. Therefore, the goal of this section is to determine whether the controller is able to maintain acceptable Level 1 handling qualities for the closed inner and outer loops system with this a worst case variation of the elements of the state and control matrices.

No Variation	Varying $A_{4,2}$	Varying $B_{4,2}$	Varying $A_{4,2}$ & $B_{4,2}$
-.0053	.2801	.2481	.3635
-.0020	-.3107	-.2716	-.4093
-.0001	-.0001	-.0001	-.0001
-.0001	-.0020	-.0020	-.0020
-4.0001	-3.9749	-4.2882	-4.2659
-4.0000	-4.0001	-4.0001	-4.0001
-4.0001	-4.0000	-4.0000	-4.0000
-4.0000	-4.0000	-4.0000	-4.0000

Table 6.2 Comparison of Closed Inner Loop Eigenvalues of the Nominal Design with Parameter Variations.

Table 6.2 shows the eigenvalues obtained from three different case studies and compares them to the eigenvalues of the nominal design. The maximum eigenvalue on the right half plane that will satisfy Level 2 mid-term handling qualities is 0.139, therefore, with the worst case parameter variation of the state and control matrices, the closed inner loop system mid-term response will be degraded to Level 3.

Table 6.3 shows the variations in eigenvalues when the outer loops are closed with gains in the roll and pitch attitude loops. The phugoid mode, though unstable is low frequency and can be stabilized with little effort by the pilot. These eigenvalues do not satisfy Level 1 limit on roll (pitch) oscillation. As given in Chapter 4, Level 1 limits for

tasks which do not require significant division of attention requires a minimum time to double amplitude of 6.76 seconds and a damping ratio ζ of -0.2. The above three cases have t_{double} of 38.3 seconds (varying $A_{4,2}$), 55.6 seconds (varying $B_{4,2}$) and 25.2 seconds (varying $A_{4,2}$ & $B_{4,2}$ simultaneously) which satisfy the doubling time requirement, but their damping ratios ζ of -0.8, -0.51 and -0.96 are beyond the limit of Level 1. However, these values are adequate for Level 2 handling qualities.

No Variation	Varying $A_{4,2}$	Varying $B_{4,2}$	Varying $A_{4,2}$ & $B_{4,2}$
-.0006 ± .0140i	.0180 ± .0121i	.0124 ± .0211i	.0274 ± .0084i
-2.0107 ± 1.9866i	-2.0118 ± 2.0191i	-2.1602 ± 2.2786i	-2.1754 ± 2.2958i
-1.9925 ± 2.0038i	-2.0101 ± 1.9933i	-2.0094 ± 1.9932i	-2.0091 ± 1.9932i
-4.0000	-4.0000	-4.0000	-4.0000
-4.0000	-4.0000	-3.9997	-3.9996

Table 6.3 Comparison of Closed Outer Loop Eigenvalues of the Nominal Design with Parameter Variations.

The results of a simulation of the response of the helicopter to a step roll attitude command of 5 degrees with both the inner and outer loops closed, which includes a - 20% variation of $A_{4,2}$ in the state matrix are shown in Figs. 6.16 and 6.17. The responses of the system that includes - 20% variation of $A_{4,2}$ are very similar to the responses with no variation in $A_{4,2}$ for the first two seconds. After two seconds, the responses in vertical velocity, roll and pitch attitudes, and yaw rate diverge, however, cross coupling is still small and performance acceptable. As given by the doubling time and also shown in Figs. 6.16 and 6.17, the rate of divergence is slow and should be able to be stabilized by the pilot with little effort. Similar responses are shown in Figs. 6.18 to 6.21 for the case with 20% variation of $B_{4,2}$ of the control matrix and varying $A_{4,2}$ and $B_{4,2}$ simultaneously. Again, performance is satisfactory even with these variations.

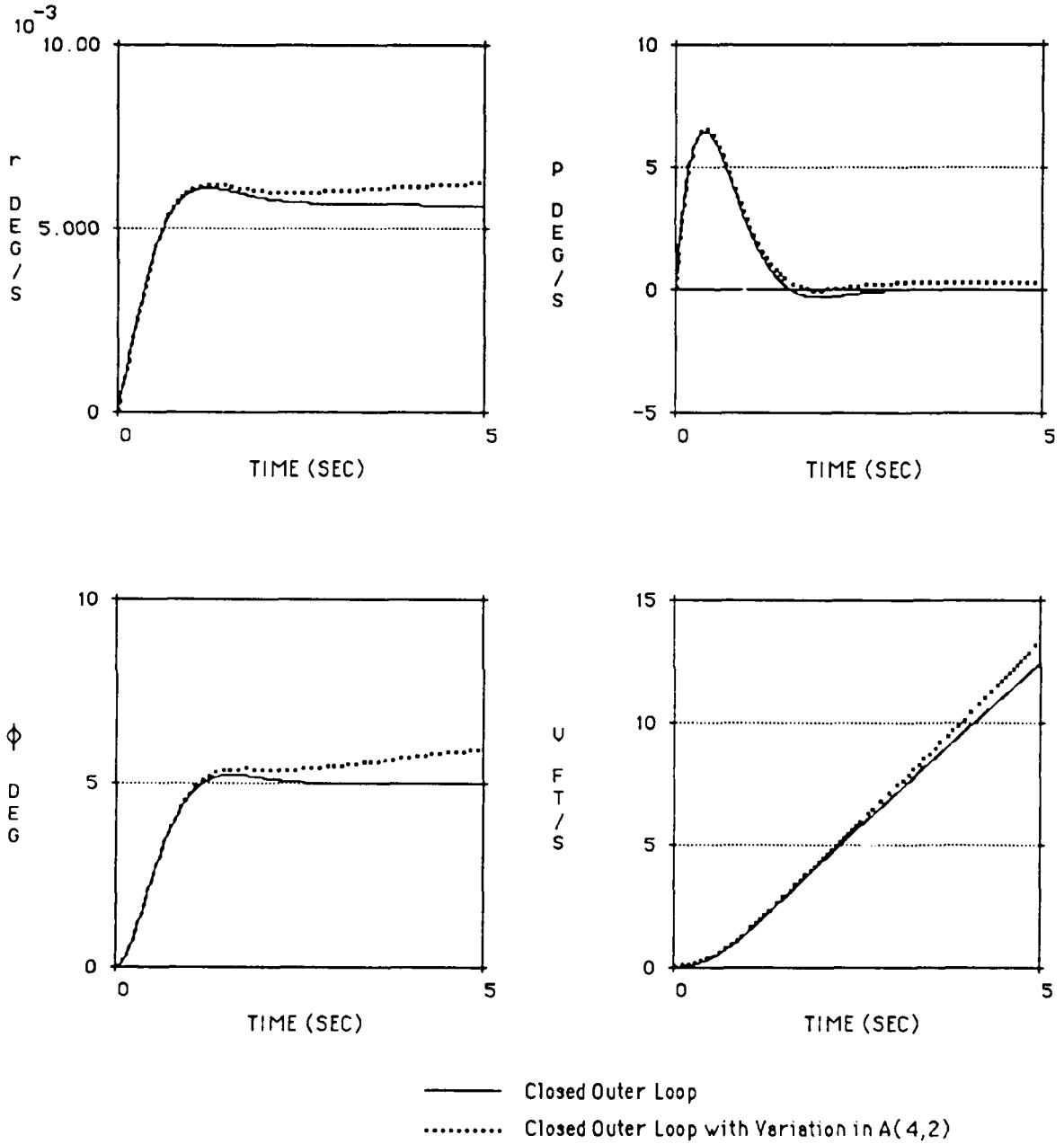

Fig. 6.16 Full State Closed Inner and Outer Loop Time Responses to a 5 Degrees Step Roll Command with Parameter Variation of - 20% in $A_{4,2}$.

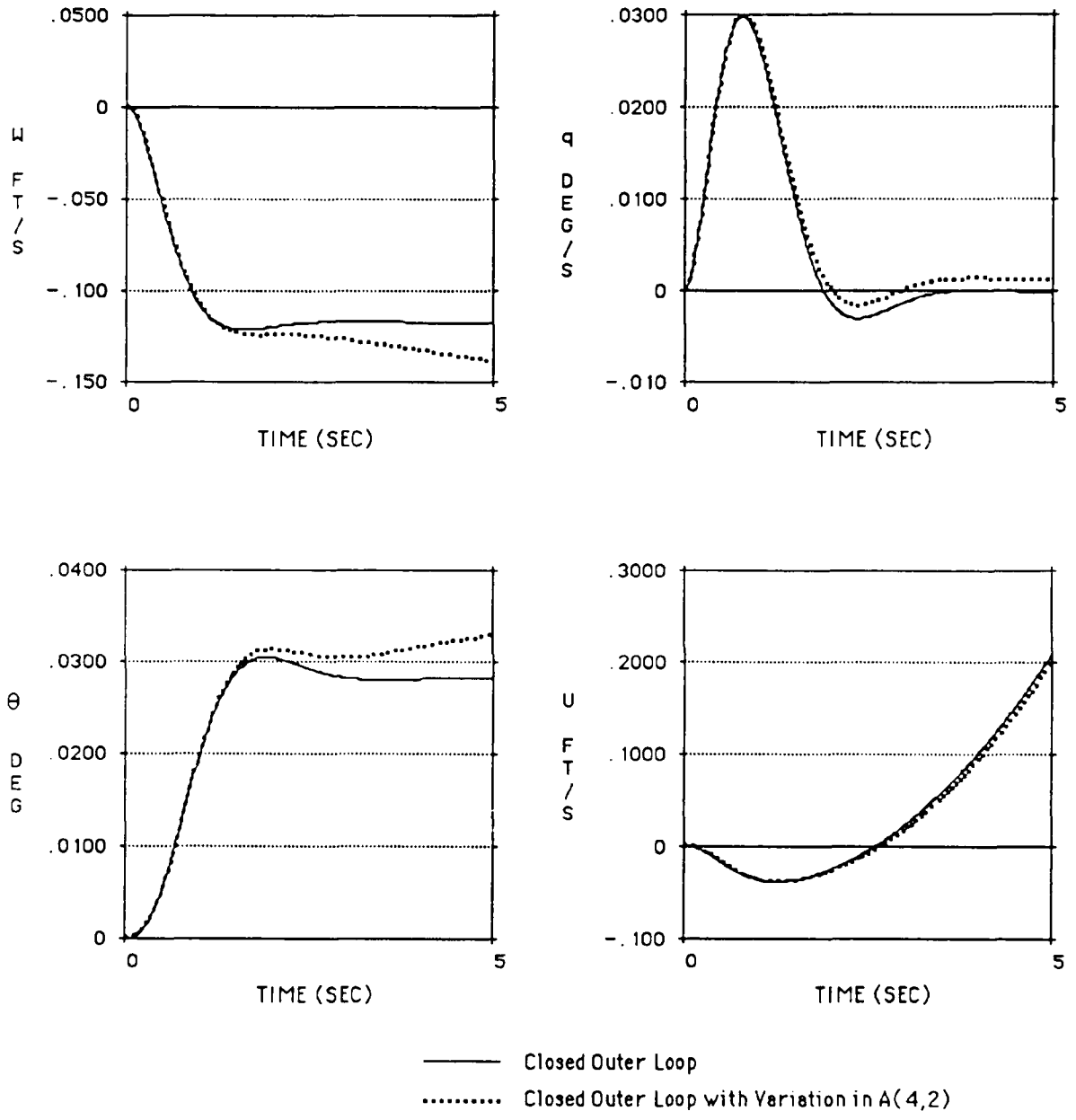

Fig. 6.17 Full State Closed Inner and Outer Loop Time Responses to a 5 Degrees Step Roll Command with Parameter Variation of - 20% in $A_{4,2}$.

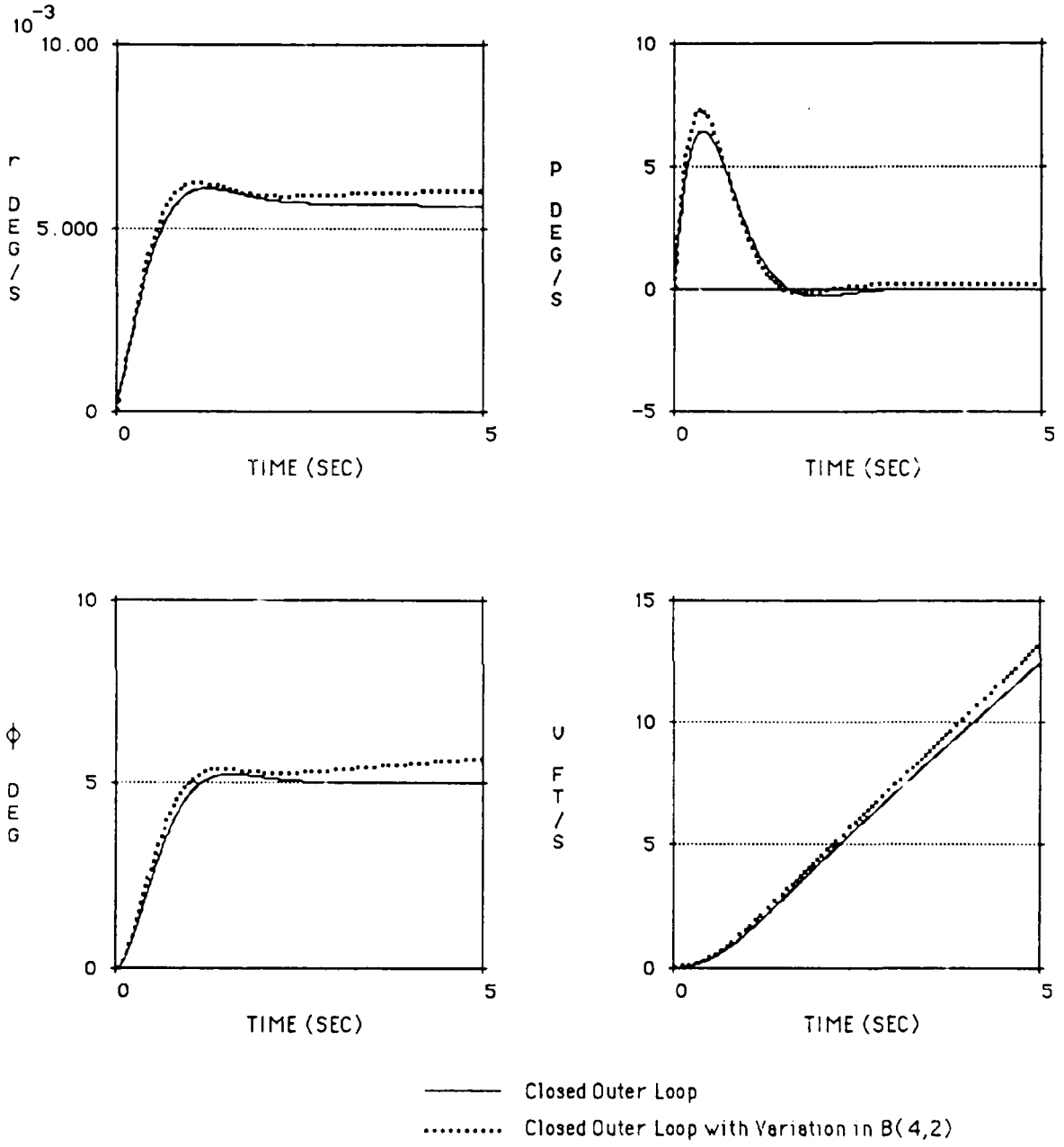

Fig. 6.18 Full State Closed Inner and Outer Loop Time Responses to a 5 Degrees Step Roll Command with Parameter Variation of + 20% in $B_{4,2}$.

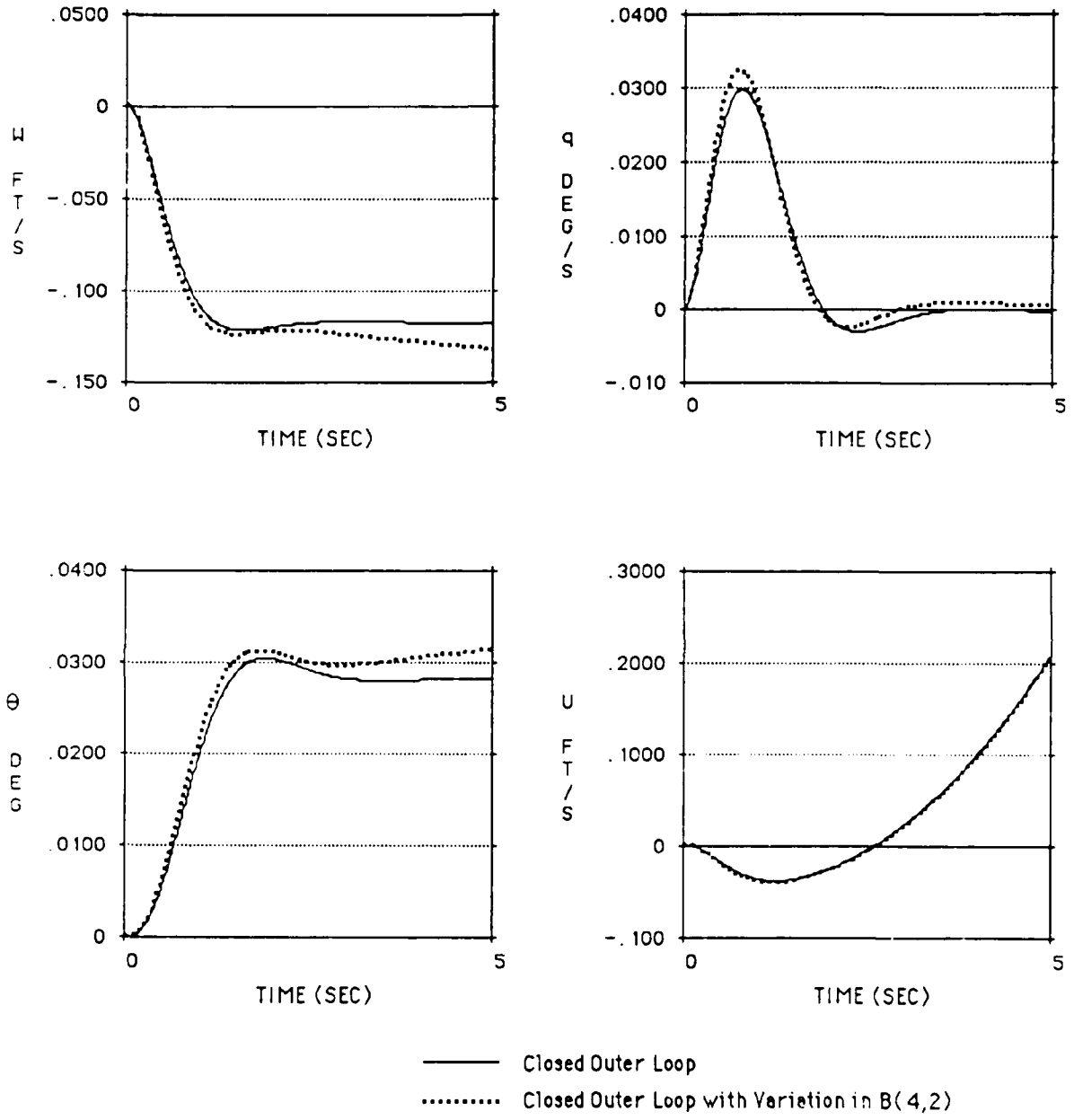

Fig. 6.19 Full State Closed Inner and Outer Loop Time Responses to a 5 Degrees Step Roll Command with Parameter Variation of + 20% in $B_{4,2}$.

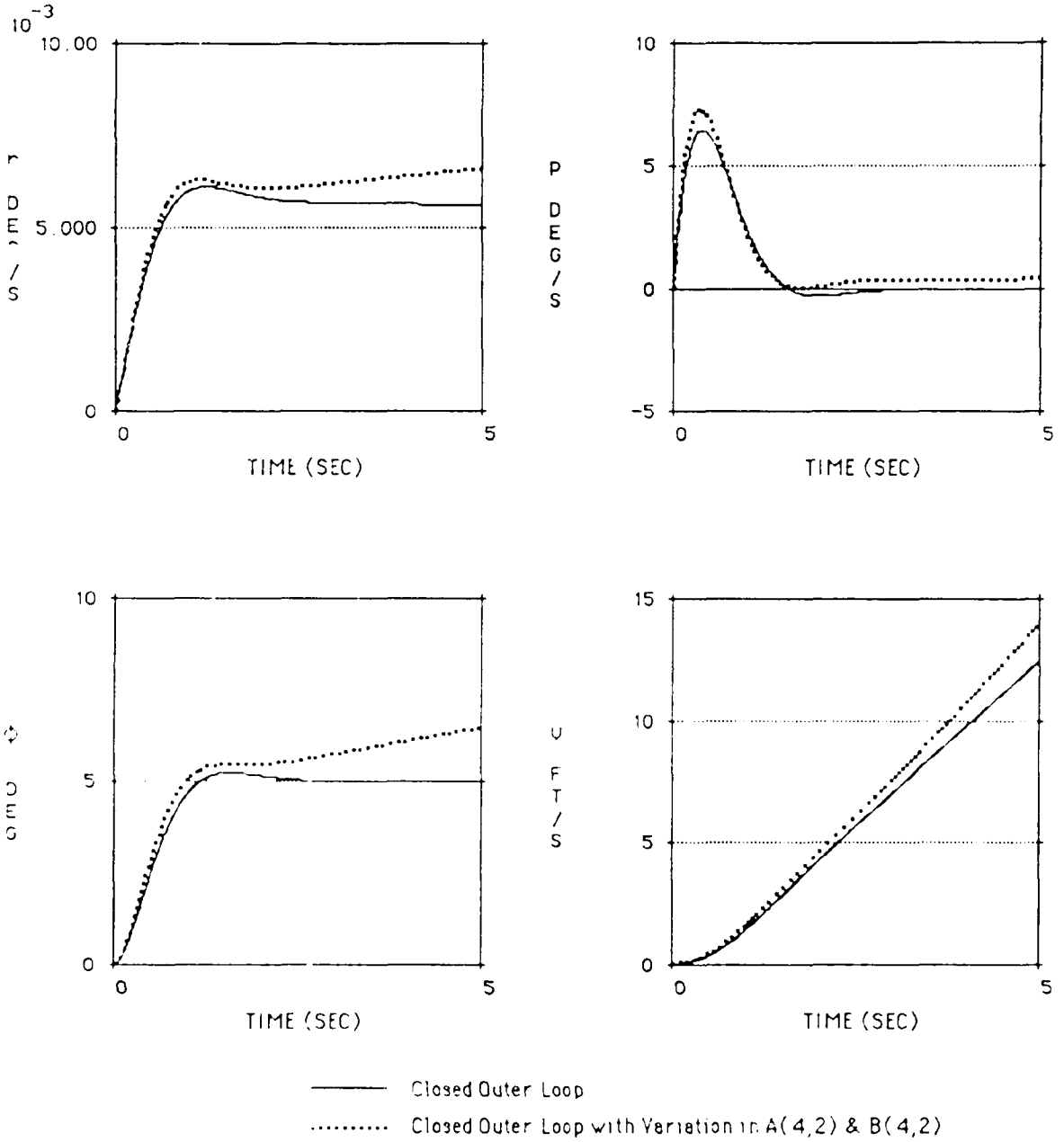

Fig. 6.20 Full State Closed Inner and Outer Loop Time Responses to a 5 Degrees Step Roll Command with Parameter Variation of - 20% in $A_{4,2}$ and + 20% in $B_{4,2}$.

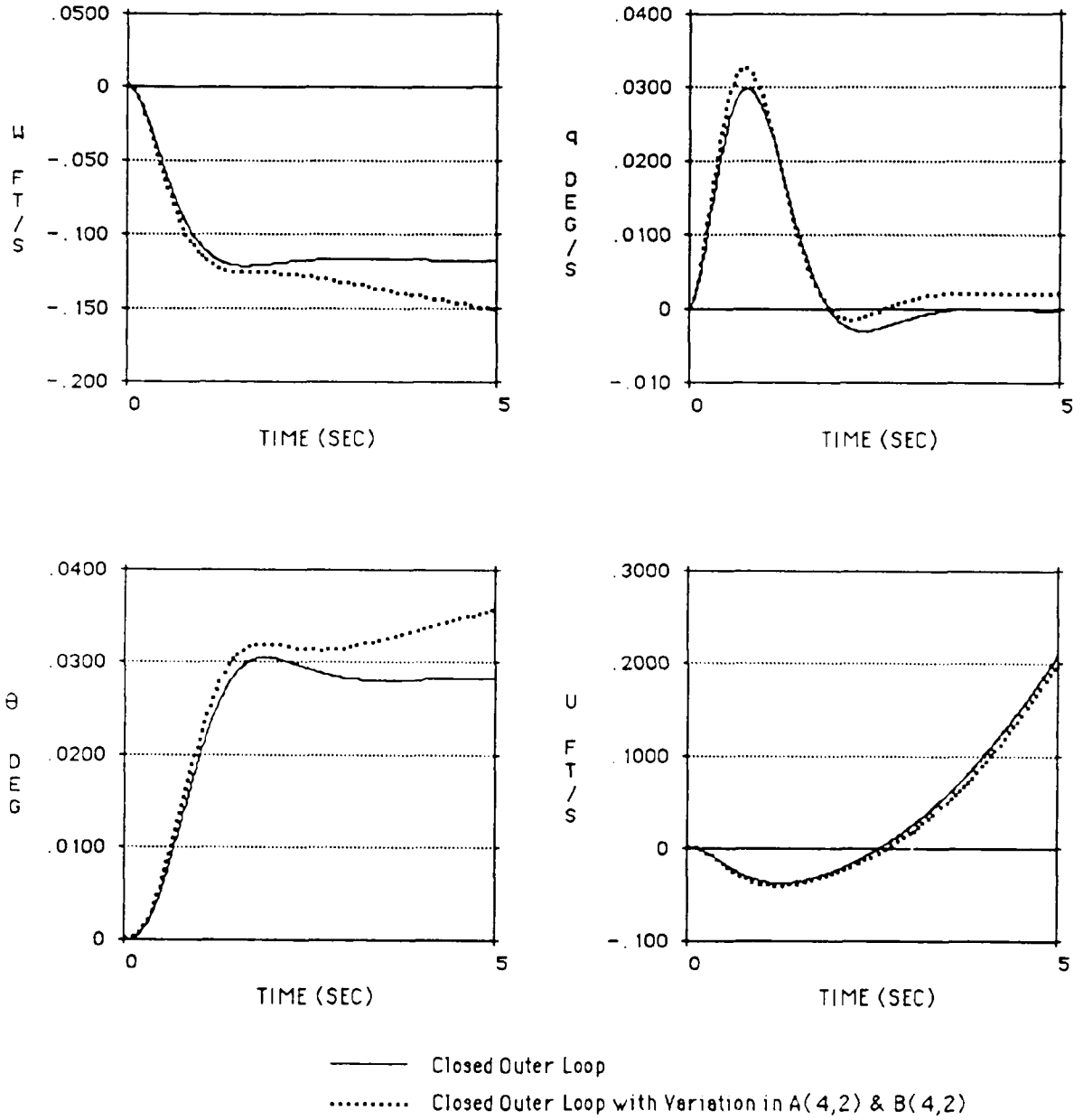

Fig. 6.21 Full State Closed Inner and Outer Loop Time Responses to a 5 Degrees Step Roll Command with Parameter Variation of - 20% in $A_{4,2}$ and + 20% in $B_{4,2}$.

B. Time Histories with High Order Model

Mode	12th Order Model		8th Order Model	
Phugoid	-.0006 ±	.0139i	-.0006 ±	.0140i
Pitch Attitude	-2.4448 ±	2.4231i	-2.0107 ±	1.9866i
Roll Attitude	-2.2628 ±	2.3004i	-1.9925 ±	2.0038i
Yaw Rate	-3.8038 +	.0000i	-4.0000 +	.0000i
Vertical Velocity	-3.9995 +	.0000i	-4.0000 +	.0000i
Advancing Rotor	-13.7551 ±	71.7906i		
Regressing Rotor	-10.2323 ±	3.6497i		

Table 6.4 Comparison of Closed Inner and Outer Loop Eigenvalues of 12th Order and 8th Order Models Using the Same Full State Regulator.

The full state regulator designed for the eighth order nominal system, was evaluated using the 12th order model which includes rotor dynamics. The closed inner and outer loop eigenvalues are shown in Table 6.4. The eigenvalues corresponding to the tip path plane flapping dynamics are essentially the same as the open loop system since there is no compensation for these two modes from the full state regulator. The remaining eigenvalues for the 12th order system are very close to the 8th order system, therefore, similar time responses are expected for the 12th and 8th order models.

The 12th order closed inner and outer loop time responses were also calculated for a 5 ft./s step command in vertical velocity (Figures 6.22 to 6.23), a 5 degree step command in roll and pitch attitude (Figures 6.25 and 6.26, and Figures 6.28 and 6.29), and a 5 deg./s step command in yaw rate (Figures 6.31 to 6.32). The longitudinal and lateral rotor flapping angles and angular velocities for the four maneuvers are shown in Figs. 6.24, 6.27, 6.30, and 6.33.

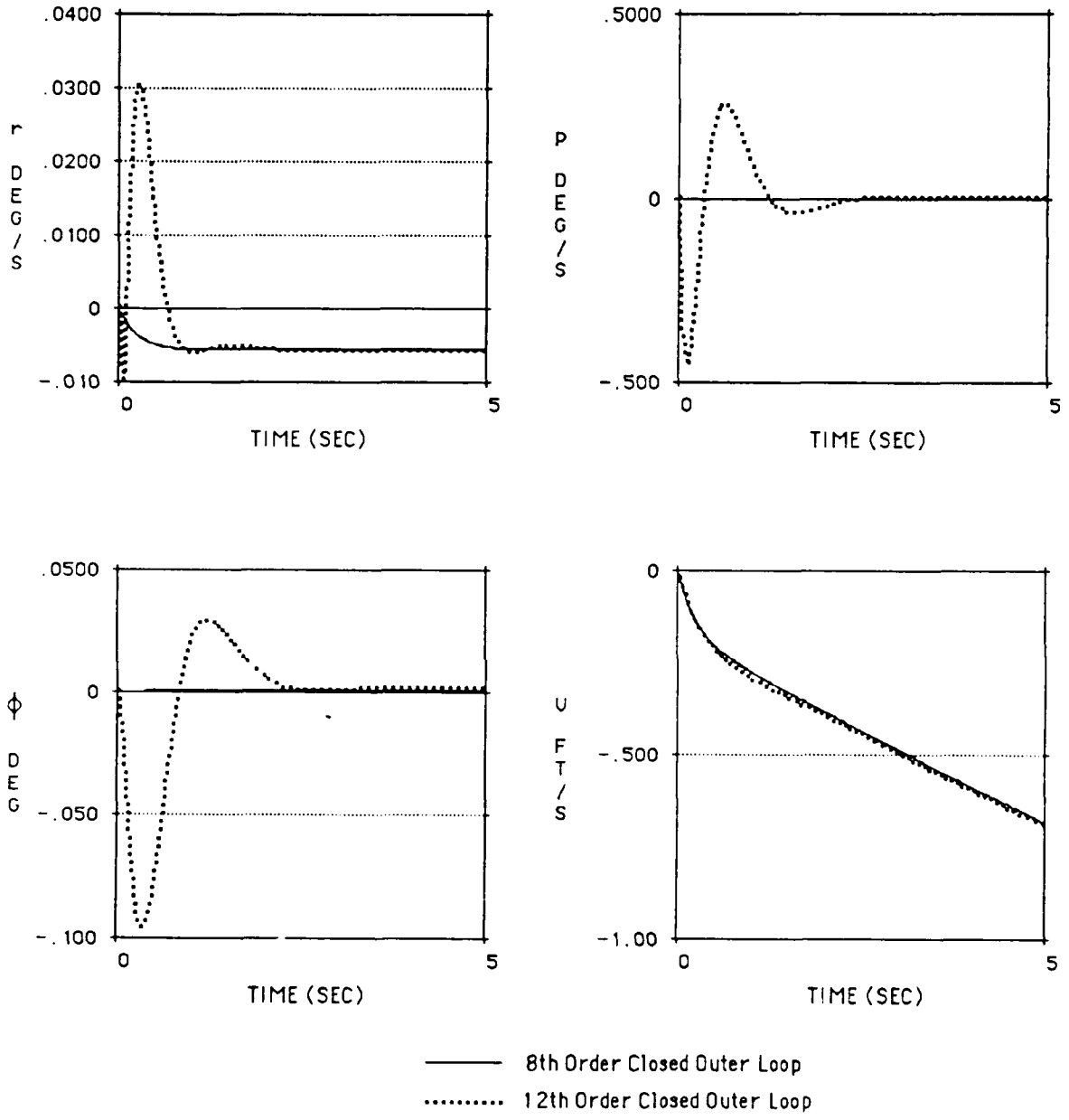

Fig. 6.22 12th Order and 8th Order Closed Loop Responses to a 5 ft./s Step Vertical Velocity Command.

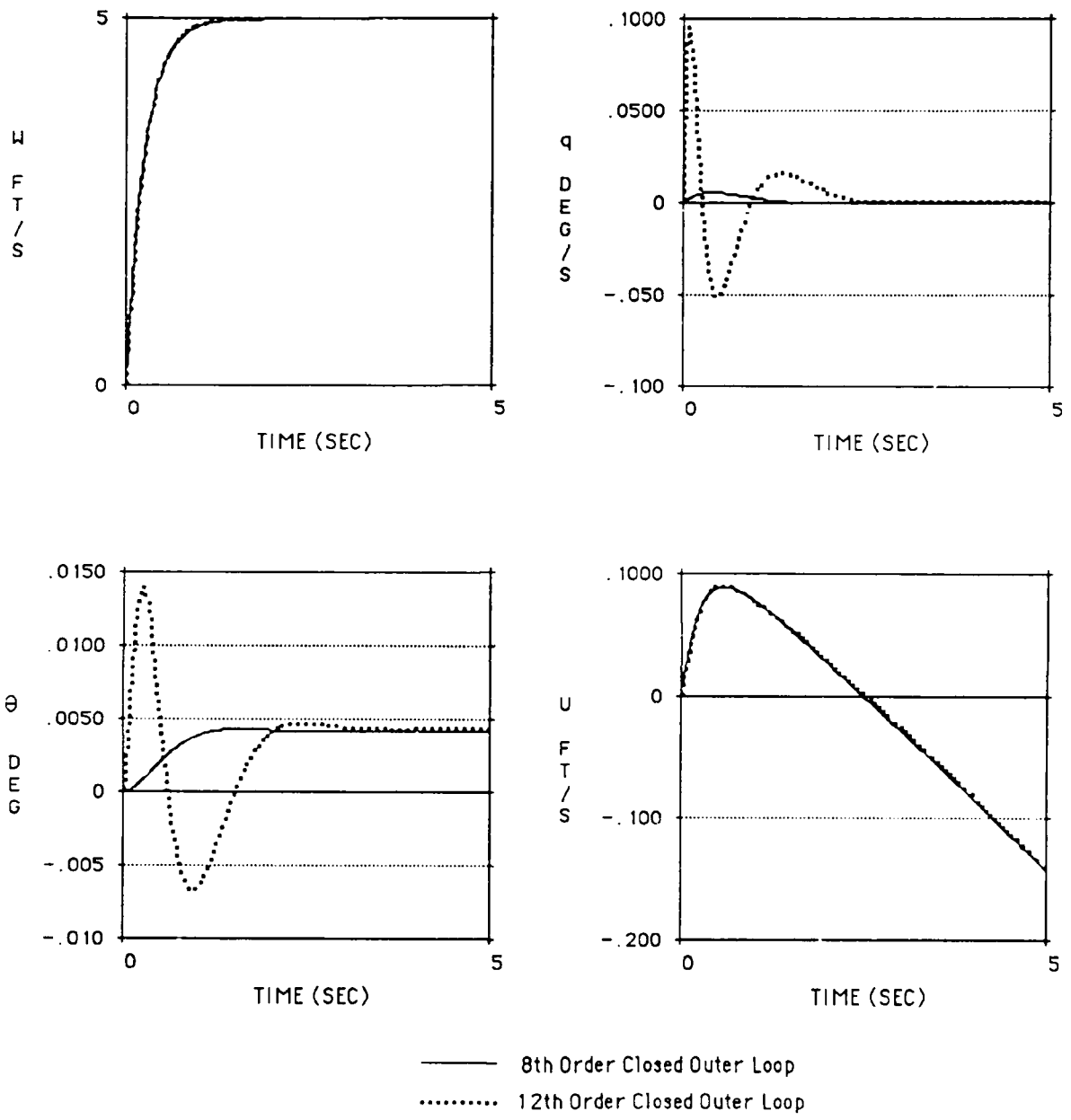

Fig. 6.23 12th Order and 8th Order Closed Loop Responses to a 5 ft./s Step Vertical Velocity Command.

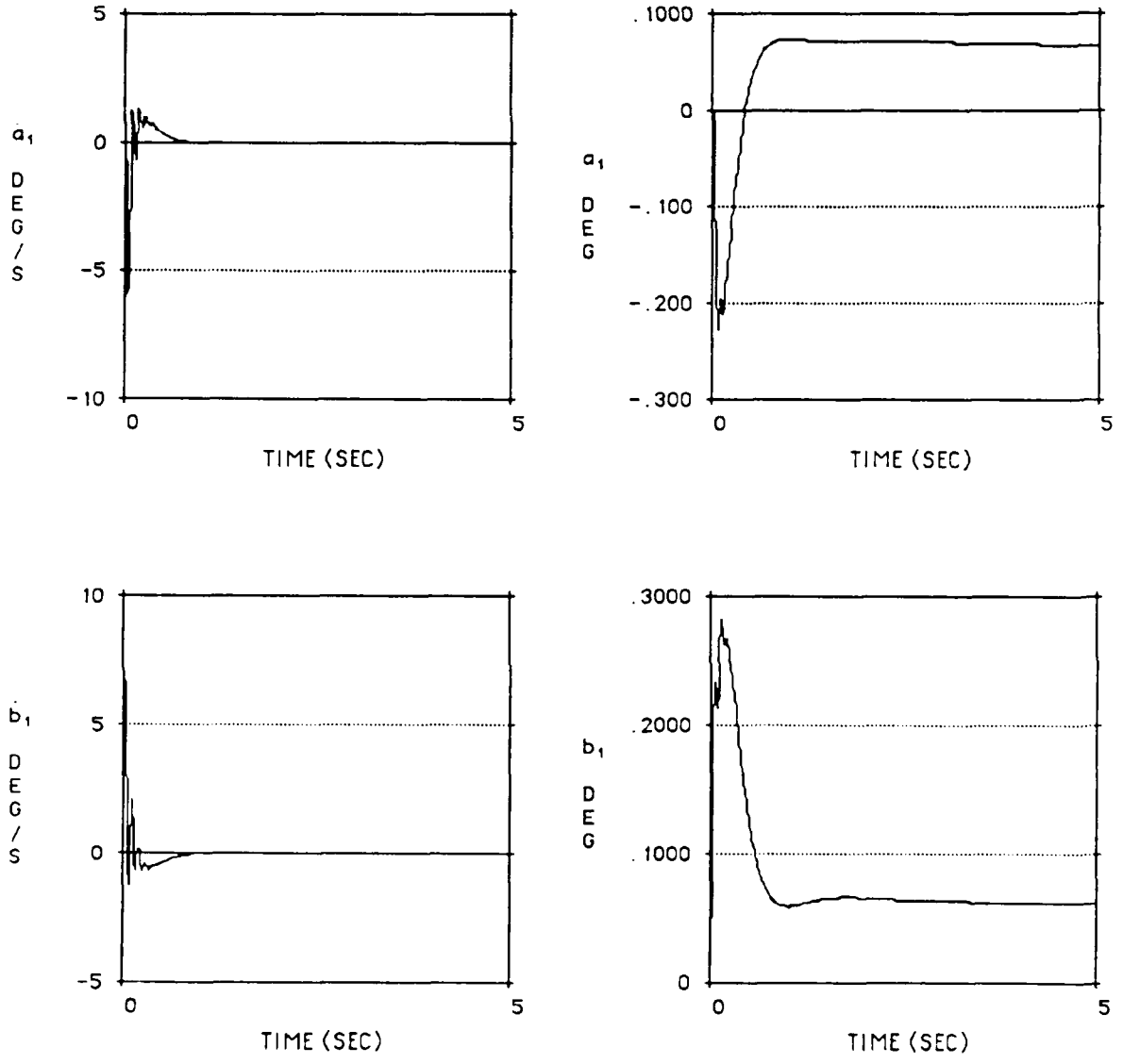

Fig. 6.24 12th Order and 8th Order Closed Loop Responses to a 5 ft./s Step Vertical Velocity Command.

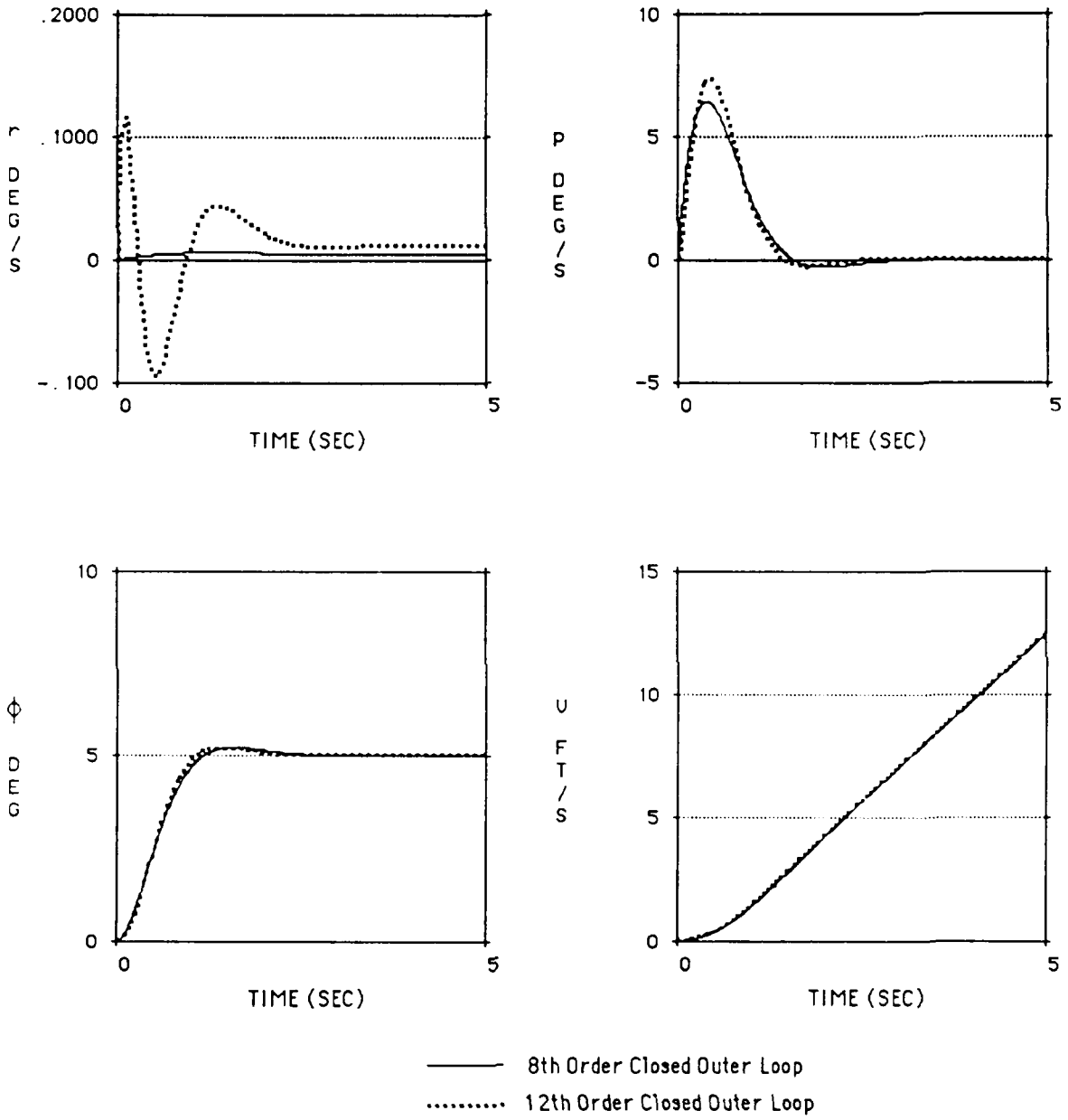

Fig. 6.25 12th Order and 8th Order Closed Loop Responses to a 5 Degrees Step Roll Attitude Command.

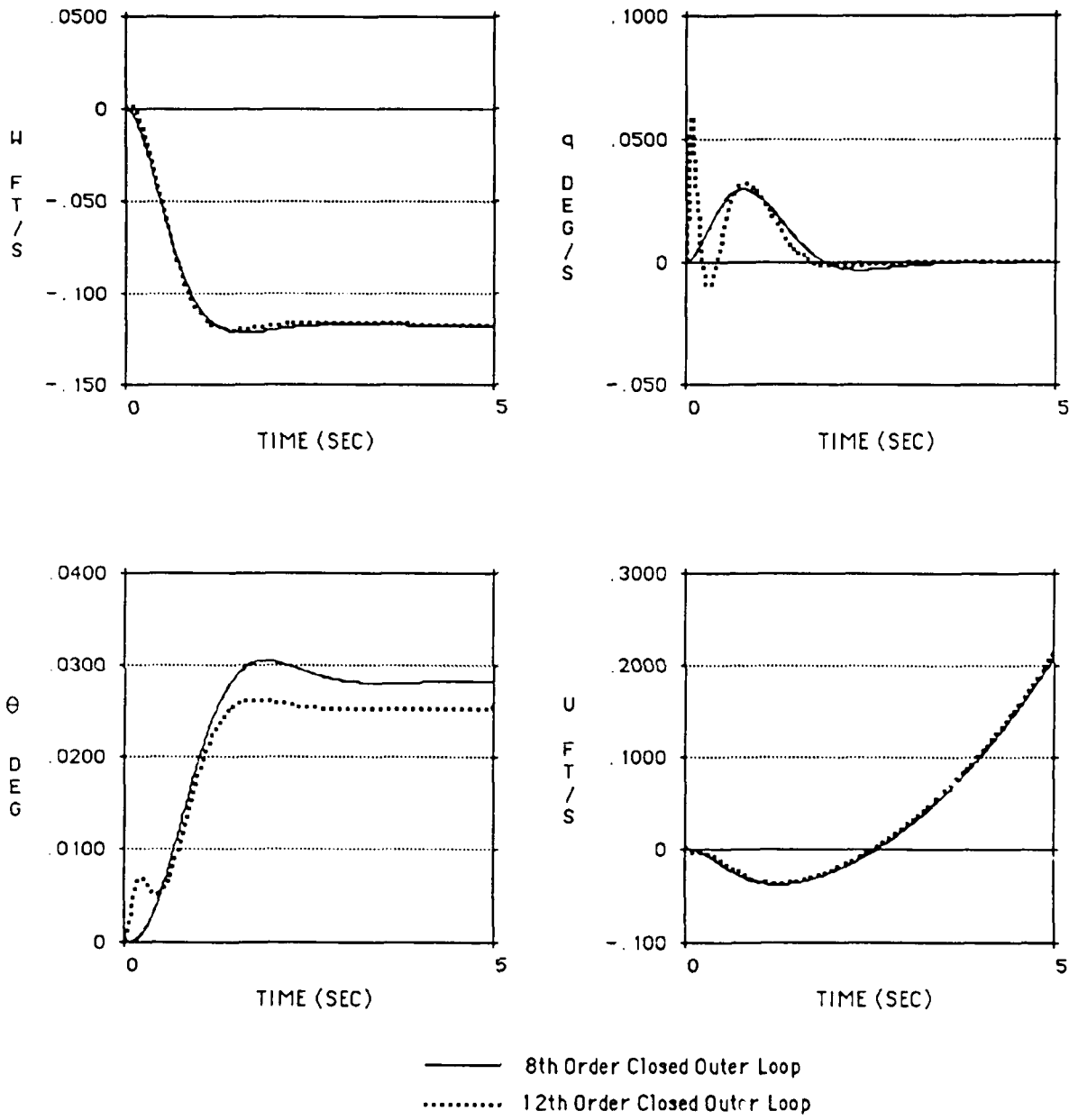

Fig. 6.26 12th Order and 8th Order Closed Loop Responses to a 5 Degrees Step Roll Attitude Command.

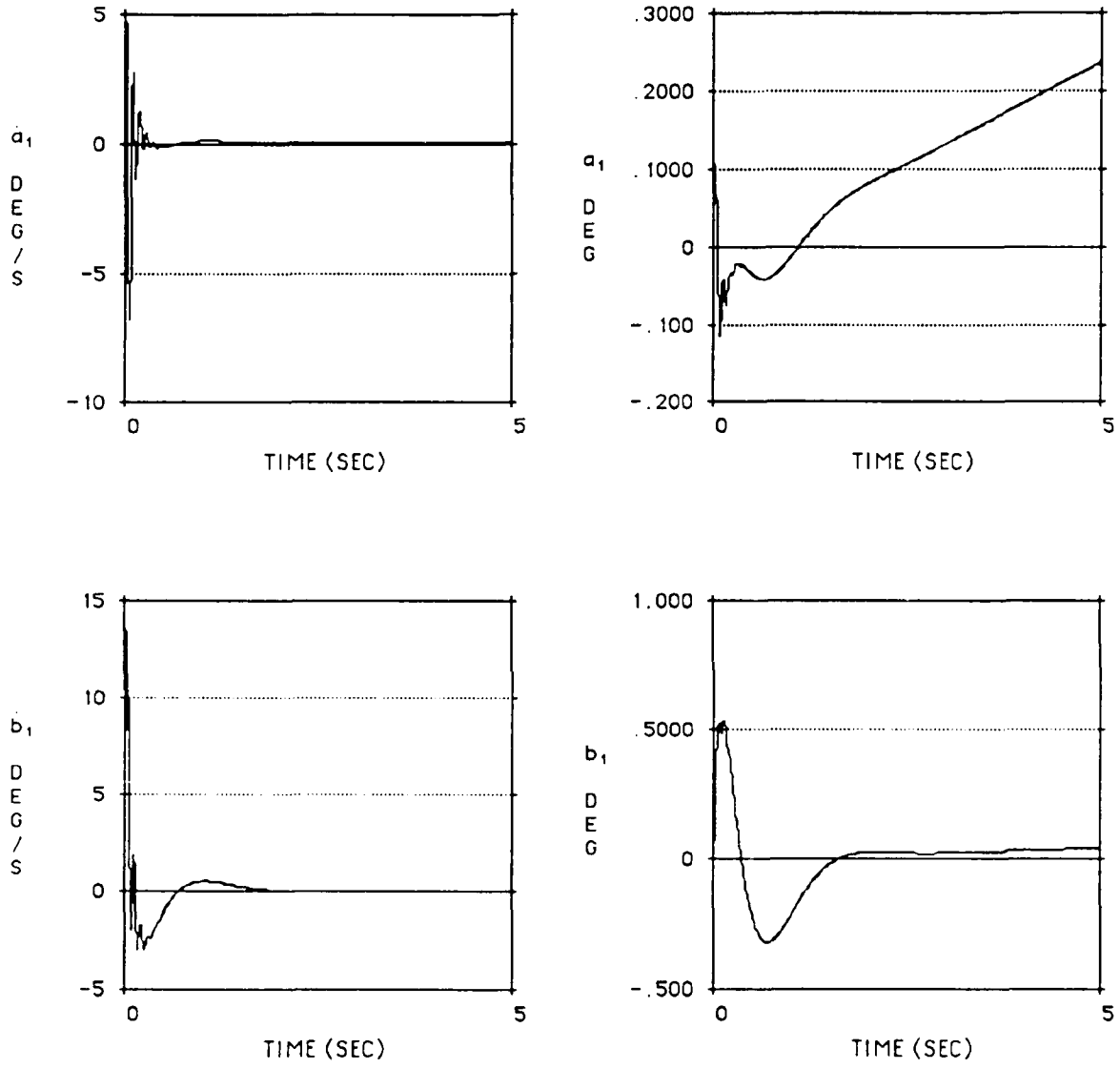

Fig. 6.27 12th Order and 8th Order Closed Loop Responses to a 5 Degrees Step Roll Attitude Command.

Figures 6.22 and 6.23 illustrate the response to a collective command of 5 ft./s from the pilot. It can be seen that the vertical velocity response is first order with little coupling in the other seven states. In general, the responses of the 12th order model in Figures 6.22 and 6.23 are very close to the 8th order full state responses with the exception of the overshoot for the first two seconds in pitch angle, pitch rate, roll angle, roll rate and yaw rate. This is expected because one of the flapping modes has very small damping effects and the full state regulator does not have any effect on these modes. Fig. 6.23 shows the responses of the lateral and longitudinal tip path plane tilting angles and angular velocities. These include the motions of the blades which have very low damping. The angular velocities settled down to zero after one second, the tilting angles are small and should not affect the performance of the helicopter.

Figures 6.25 to 6.26 show the roll attitude response resulting from pilot lateral command of 5 degrees. The response of roll angle to roll attitude command was second order and settled out to approximately 5 degrees in three seconds. The responses of the 12th order model in Figures 6.25 and 6.26 are close to the 8th order responses with overshoot in pitch angle, pitch rate and yaw rate for the first two seconds. The coupling between the pitch attitude and roll attitude command is smaller than the full state model. The responses of the three linear velocities are identical up to 5 seconds for both full state and 12th order models. Figure 6.27 shows that the flapping angular velocities settle down to approximately zero after one second. The longitudinal tilting angle is essentially linear after two seconds and is increasing at a rate of 0.47 deg./s. Since the 12th order model with the full state regulator is a stable system, this linear response will eventually reach a steady state value.

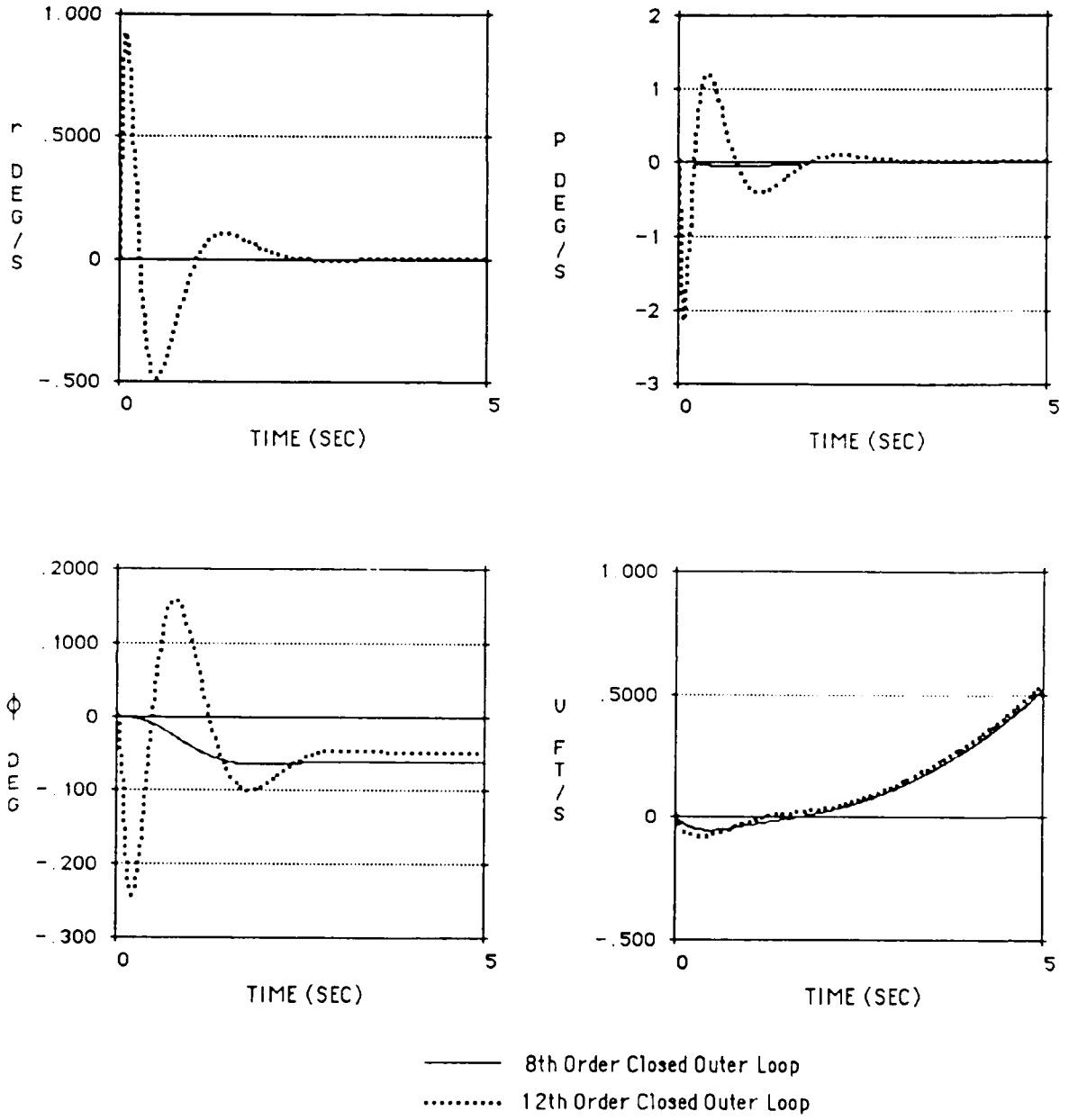

Fig. 6.28 12th Order and 8th Order Closed Loop Responses to a 5 Degrees Step Pitch Attitude Command.

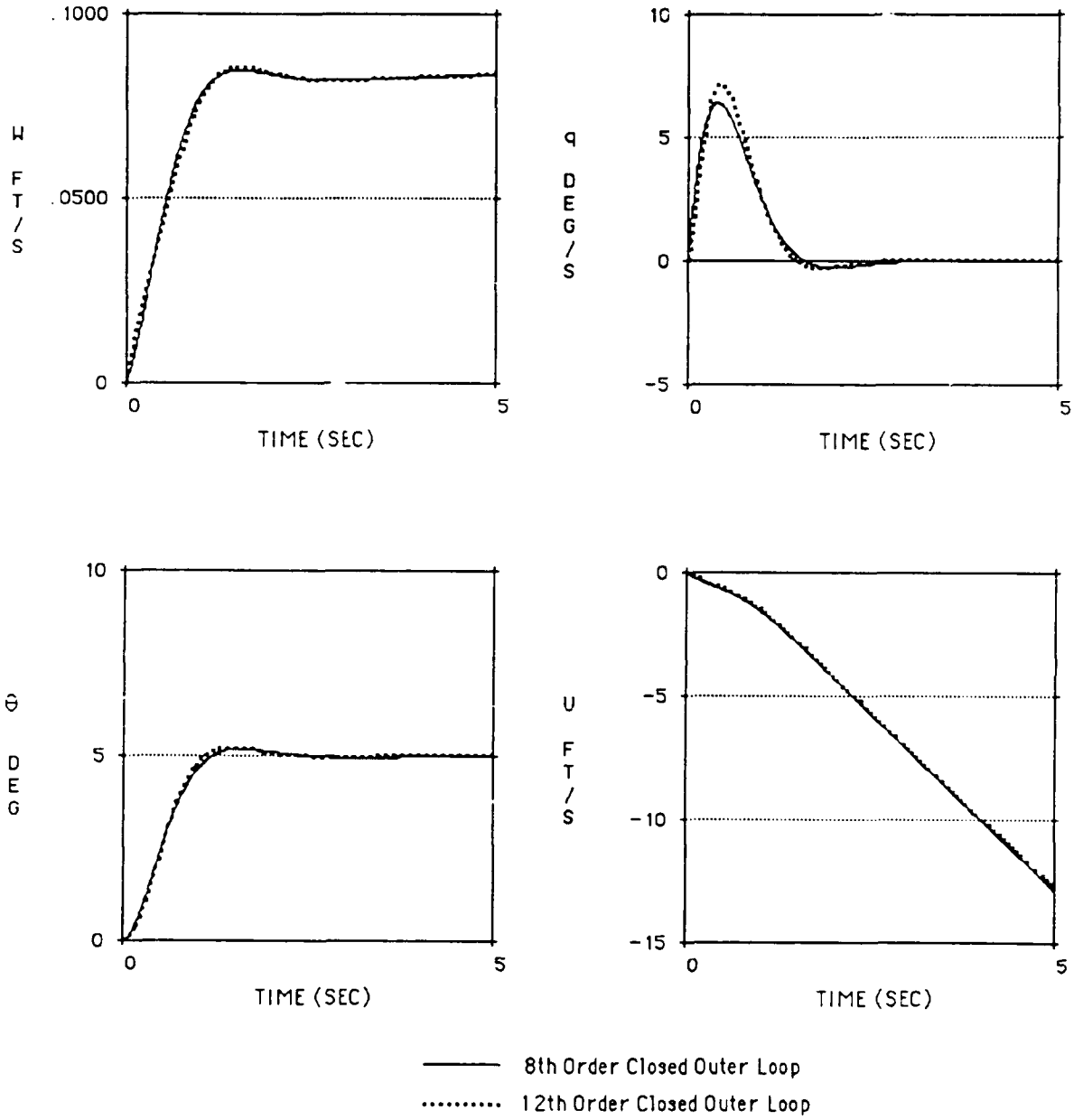

Fig. 6.29 12th Order and 8th Order Closed Loop Responses to a 5 Degrees Step Pitch Attitude Command.

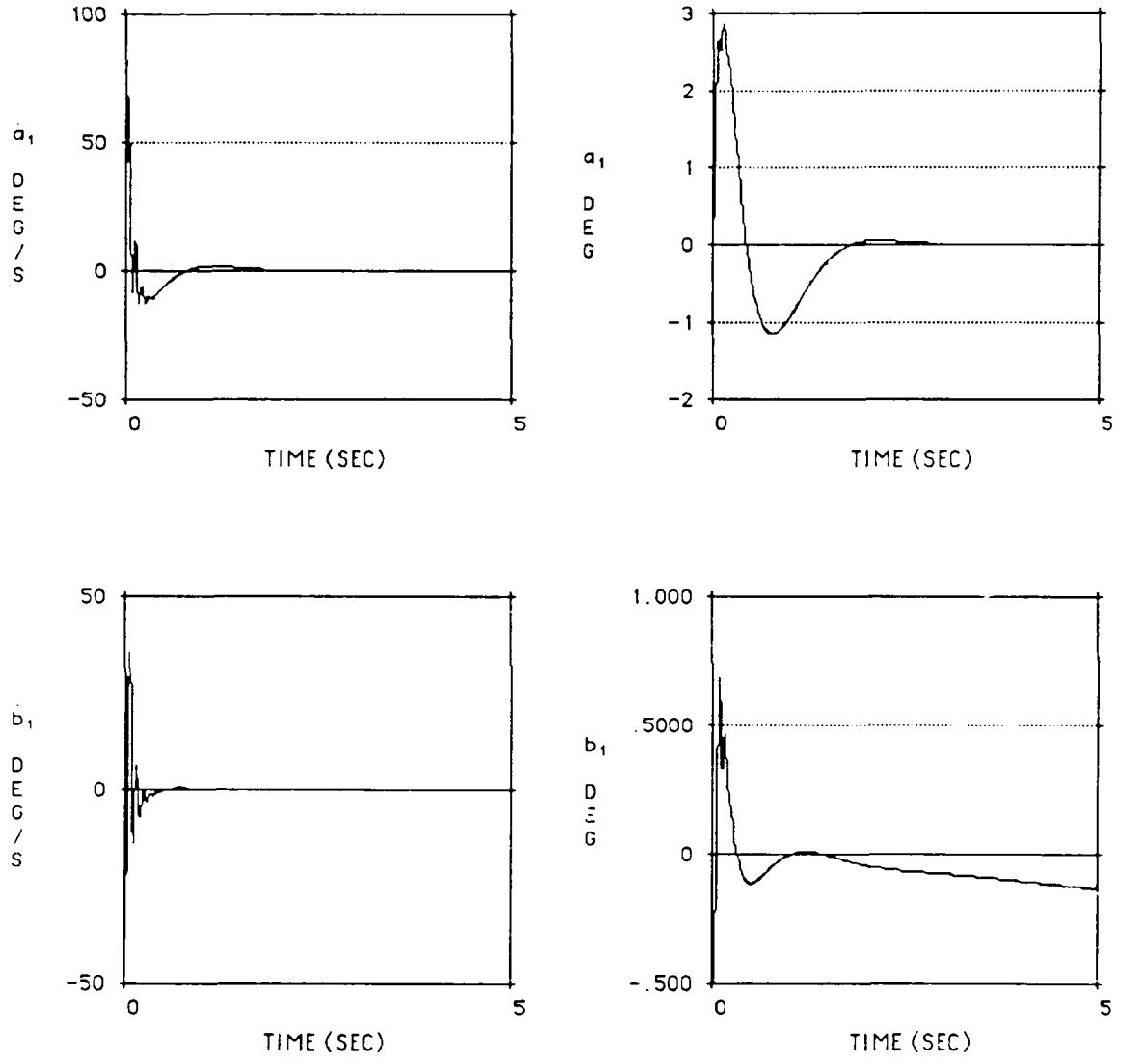

Fig. 6.30 12th Order and 8th Order Closed Loop Responses to a 5 Degrees Step Pitch Attitude Command.

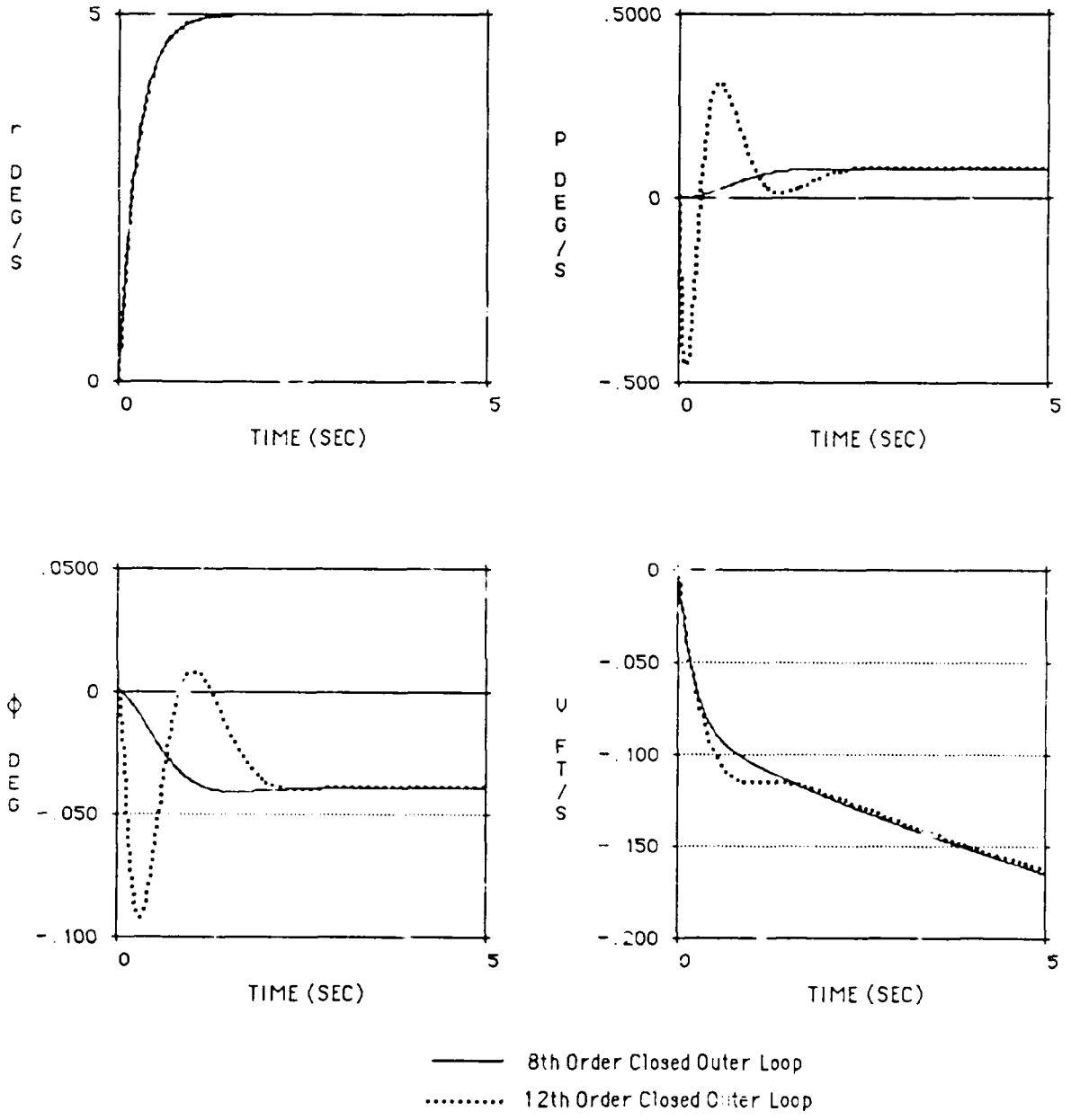

Fig. 6.31 12th Order and 8th Order Closed Loop Responses to a 5 deg./s Step Yaw Rate Command.

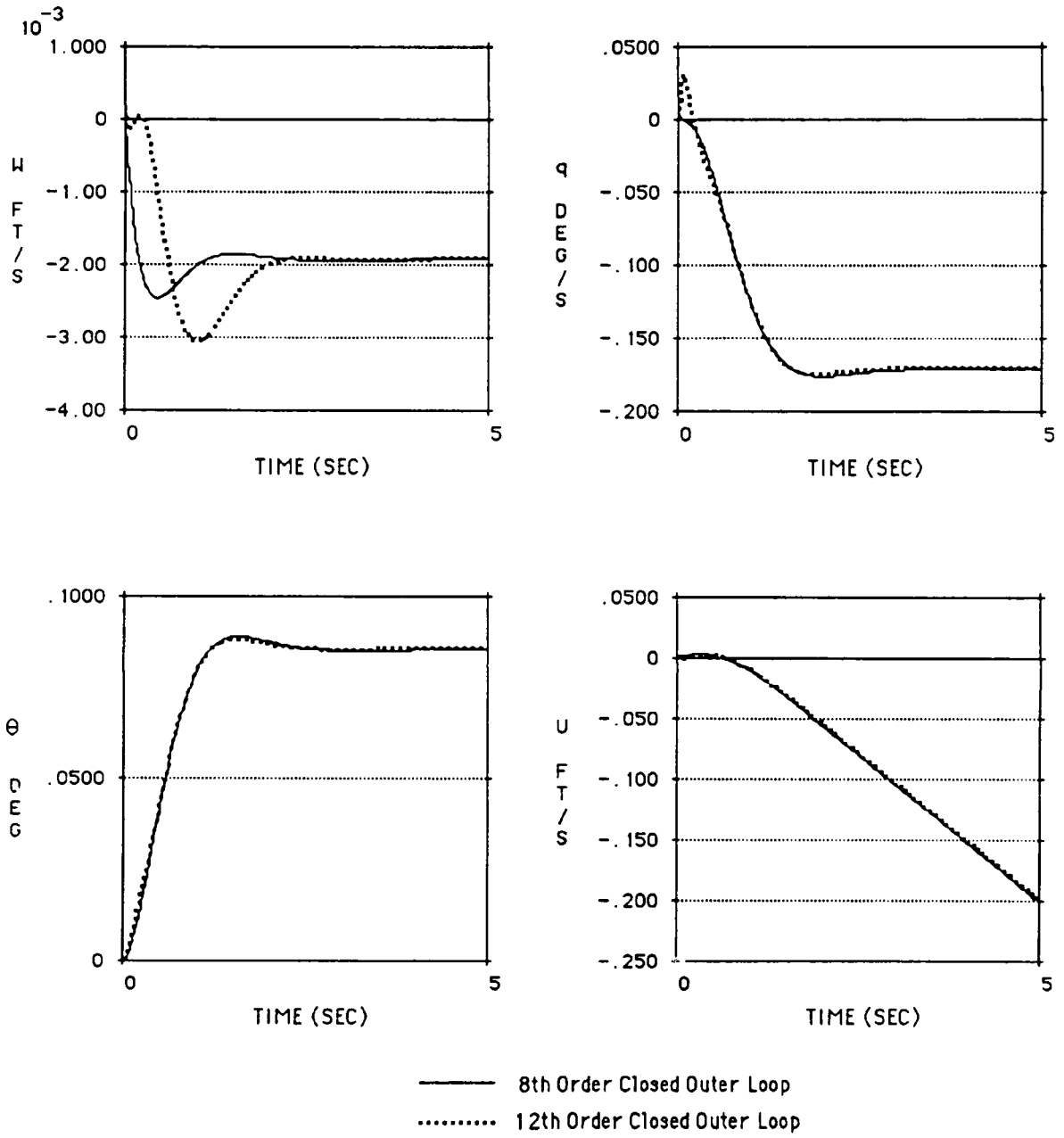

Fig. 6.32 12th Order and 8th Order Closed Loop Responses to a 5 deg./s Step Yaw Rate Command.

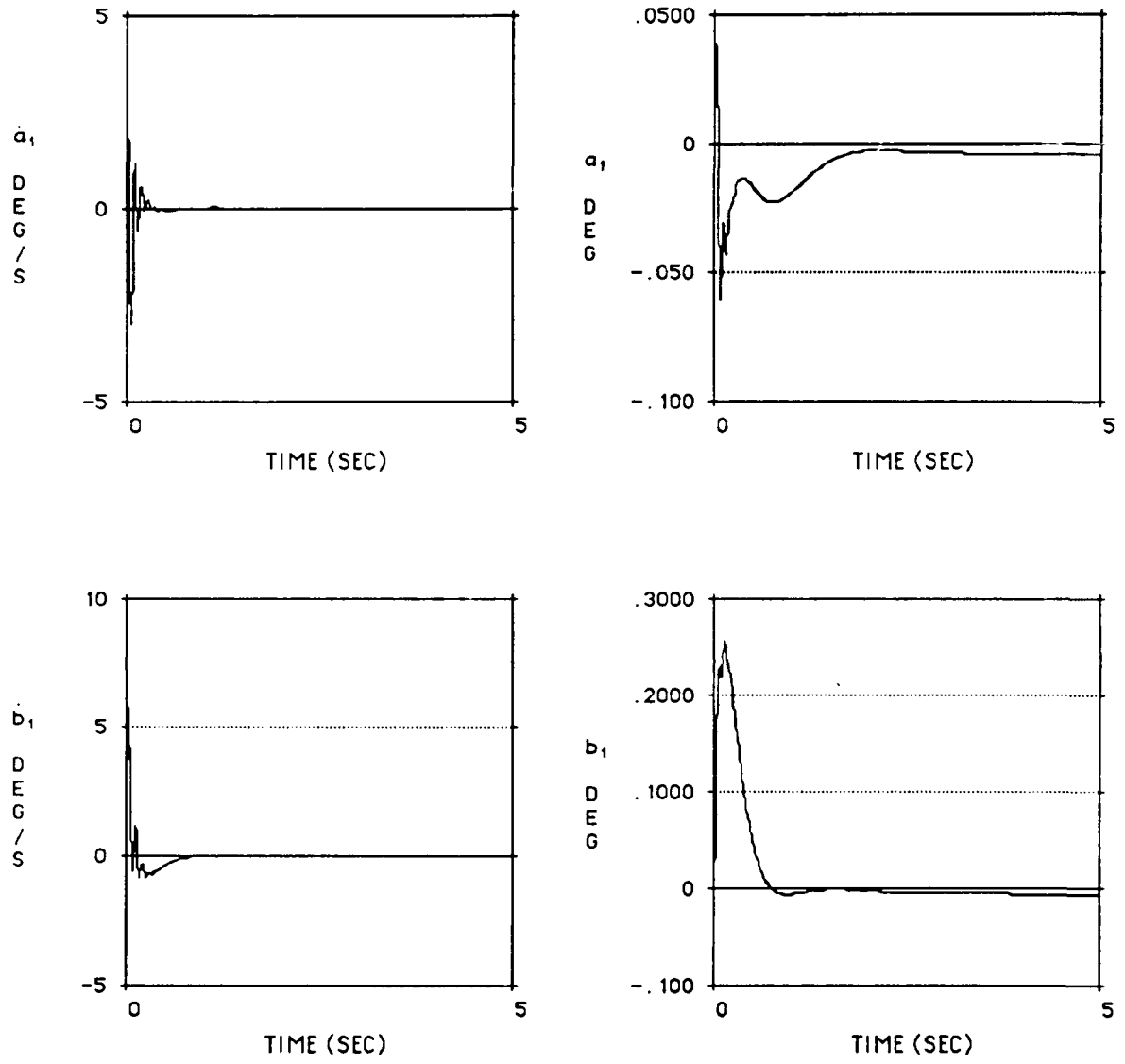

Fig. 6.33 12th Order and 8th Order Closed Loop Responses to a 5 deg./s Step Yaw Rate Command.

Figures 6.28 and 6.29 show the pitch attitude response resulting from the pilot longitudinal command of 5 degrees. The decoupling in all axes are essentially the same as the 8th order model. Similar overshoots in roll attitude, roll rate and yaw rate are seen in the plots. There is small coupling between the pitch attitude command and the lateral tilting angle as illustrated in Figure 6.30. Yaw rate response to a pilot command of 5 deg./s is shown in Figures 6.31 and 6.32. The small lag in the vertical velocity response is expected due to higher order dynamics of the 12th order model. Good decoupling in the longitudinal and lateral flapping modes is shown in Figure 6.33.

References

1. Stein, Gunter, and Barrett, Michael, "Developments in Control Theory," *Scientific Honeyweller*, pp. 88-100, Winter 1989.

2. Wall, Joseph E. Jr., and Hartmann, Gary, "Multivariable Control Design for Performance and Robustness," Professional Study Series preceding the AIAA Guidance and Control Conference, Seattle, Washington, Aug. 18-19, 1984.

3. Lehtomaki, N. A., Sandell, N. R., and Athans, M.,"Robustness Results in Linear Quadratic Based Multivariable Controller Design," *IEEE Trans. on Auto. Control*, Vol 26, Feb 1981, pp 75-92.

4. Lehtomaki, N. A., Castanon, D., Levy, B., Stein, G., Sandell, Jr., N. A., and Athans, M., "Robustness Test Utilizing the Structure of Modelling Error," Proceedings of the 20th IEEE Conference on Decision & Control, San Diego, CA, Dec. 16, 1981, pp. 1173- 1190.

5. Tischler, Mark B., Fletcher, Jay W., Morris, Patrick M., and George, T. Tucker, "Application of Flight Control System Methods to an Advanced Combat Rotorcraft," Proceedings of Royal Aeronautical Society International Conference on Helicopter Handling Qualities and Control, London, Nov. 1988.

6. Dailey, R. Lane, "Lecture Notes for the Workshop on H_∞ and μ Methods for Robust Control," 1990 American Control Conference, San Diego, CA, May 21-22, 1990.

7. Doyle, John C., "Analysis of Feedback Systems with Structured Uncertainties," Proceedings of the Institution of Electrical Engineers, Vol. 129, Part D, No. 6, pp. 242-250, Nov. 1982.

8. Doyle, John C., Wall, J. E., and Stein, G., "Performance and Robustness Analysis for Structured Uncertainty," Proceeding of the 21st IEEE Conference on Decision and Control, Orlando, Florida, Vol. 2, pp. 629-636, Dec. 1982.

9. Doyle, John C., et al. *ONR / Honeywell Workshop: Advances in Multivariable Control*, Minneapolis, October 1984.

10. Doyle, John C., "Structured Uncertainty in Control System Design," Proceeding of the 24th IEEE Conference on Decision and Control, Ft. Lauderdale, Florida, Dec. 1985.

11. Stein, Gunter, Hartmann, Gary, and Enns, Dale, "Analysis of Robust Stability and Performance for Multivariable Control Systems," American Control Conference Tutorial Workshop, Seattle, Washington, June 1986.

12. Packard, Andrew, and Doyle, John C., "Robust Control of Multivariable and Large Scale Systems," USAF/AFSC Final Report for the Period Oct. 1985 to March 1988.

13. Key, David L., and Hoh, Roger H, "New Handling Qualities Requirements and How They can be Met," American Helicopter Society 43rd Annual National Forum Proceedings, St. Louis, MO, May 1987, pp. 975-990.

14. Hoh, Roger H., Mitchell, David G., Ashkenas, Irving L., Aponso, Bimal L., Ferguson, Samuel W., Rosenthal, Theodore J., and Key, David L., "Proposed Airworthiness Design Standard: Handling Qualities Requirements for Military Rotorcraft," Systems Technology, Inc. Technical Report No. 1194-2, Contract No. NAS2-11304, Dec.20, 1985.

15. Hess, Ronald A., "Theory for Aircraft Handling Qualities Based Upon a Structural Pilot Model," *Journal of Guidance, Control, and Dynamics*, Vol. 12, No. 6, Nov.-Dec. 1989, pp. 792-797.

16. Hess, Ronald A., and Sunyoto, Iwan, "Toward a Unifying Theory for Aircraft Handling Qualities," *Journal of Guidance, Control, and Dynamics*, Vol. 8, No. 4, July-Aug. 1985, pp. 440-446.

17. Hess, Ronald A., "Structural Model of the Adaptive Human Pilot," *Journal of Guidance, Control, and Dynamics*, Vol. 3, No. 5, Sept.-Oct. 1980, pp. 416-423.

18. Aponso, Bimal L., Mitchell, David G., and Hoh, Roger H., "Simulation Investigation of the Effects of Helicopter Hovering Dynamics on Pilot Performance," ,Vol. 13, No. 1, Jan.-Feb. 1990, pp. 8-15.

19. McRuer, D. T., and Krendel, H. S., "Mathematical Models of Human Pilot Behavior," AGARD-AG-188, Jan. 1974.

20. Kazerooni, H., and Meidt, J. Douglas, "On the Stability of Robotics Systems Worn by Humans," Symposium on Robotics Presented at the Winter Annual Meeting of the American Society of Mechanical Engineers, San Francisco, Dec. 1989.

21. Bidian, Peter A., "Robust Analysis for a Helicopter Controller Using a Stochastic Approach," Plan B Master's Project, Dept. of Aerospace Engr. and Mechanics, Univ. of Minnesota, Minneapolis, MN, June 1990.

APPENDIX A

DIMENSIONAL 12TH & 8TH ORDER A AND B MATRICES

Dimensional 12th Order Helicopter A Matrix

A_{12} =

Columns 1 thru 8

-.0232	.0055	-.0059	-.0521	.7174	.0211	.0000	-32.1662
-.0569	-.0557	-.0061	-.8480	-.0519	.7144	32.1473	-.0169
-.0772	-.0748	-.3803	-.0413	-.3013	2.0310	1.1024	.4938
-.0219	-.0339	-.0039	-.5980	-.0431	.4003	.0000	.0000
.0039	-.0012	-.0036	.0077	-.1631	.0029	.0000	.0000
.0293	.0161	-.0007	.1352	.0423	-.4930	.0000	.0000
.0000	.0000	.0000	1.0000	.0005	-.0154	.0000	.0000
.0000	.0000	.0000	.0000	.9994	.0343	.0000	.0000
1.1291	-.3616	.0036	-70.2077	-34.8969	.3893	.0000	.0000
.0000	.0000	.0000	.0000	.0000	.0000	.0000	.0000
-.3414	-1.0981	.0058	-34.5620	70.2831	.4193	.0000	.0000
.0000	.0000	.0000	.0000	.0000	.0000	.0000	.0000

Columns 9 thru 12

.5483	-5.0970	-.0860	9.7470
-.0881	9.7240	-.5523	5.0490
-.0078	-.9641	.0288	-1.0320
-.0687	7.9190	-.4014	32.8146
-.0703	5.8210	.0111	-1.2540
.0377	-5.0972	.0573	-3.4304
.0000	.0000	.0000	.0000
.0000	.0000	.0000	.0000
-27.5297	-511.8210	-67.8411	-941.9460
1.0000	.0000	.0000	.0000
67.9287	935.7810	-27.2686	-540.1146
.0000	.0000	1.0000	.0000

Dimensional 12th Order Helicopter B Matrix

B_{12} =

-4.9320	-8.8350	25.4900	.0004
-3.9280	25.5100	8.7880	18.7500
-334.6000	.6213	-.2959	.0133
-5.3705	18.5905	6.4560	10.0067
-.6877	1.1350	-3.2690	-.1231
12.8487	-2.5707	-1.0964	-11.9561
.0000	.0000	.0000	.0000
.0000	.0000	.0000	.0000
-1.7003	855.9650	-395.4310	.1293
.0000	.0000	.0000	.0000
4.1285	380.5095	849.5440	-9.9949
.0000	.0000	.0000	.0000

Dimensional 12th Order Helicopter C Matrix

C_{12} =

0.	0.	1.	0.	0.	0.	0.	0.	0.	0.	0.	0.
0.	0.	0.	1.	0.	0.	0.	0.	0.	0.	0.	0.
0.	0.	0.	0.	1.	0.	0.	0.	0.	0.	0.	0.
0.	0.	0.	0.	0.	1.	0.	0.	0.	0.	0.	0.

Dimensional 8th Order Design Model A Matrix

A_8 =

-.0199	-.0058	-.0058	-.7304	1.1197	.0268	.0000	-32.1662
-.0452	-.0526	-.0061	-1.2567	-.7517	.7154	32.1473	-.0169
-.0788	-.0747	-.3803	.0375	-.2334	2.0306	1.1024	.4938
.0094	-.0536	-.0037	-2.9979	-.5308	.4155	.0000	.0000
.0076	.0040	-.0036	.0710	-.5943	.0013	.0000	.0000
.0226	.0151	-.0007	.4058	.4069	-.4940	.0000	.0000
.0000	.0000	.0000	1.0000	.0005	-.0154	.0000	.0000
.0000	.0000	.0000	.0000	.9994	.0343	.0000	.0000

Dimensional 8th Order Design Model B Matrix

B_8 =

-4.9064	-.9103	30.4980	-.0834
-3.9661	30.7245	.5566	18.8079
-334.5965	-.3527	.4905	.0099
-5.3885	47.5204	1.3582	9.9301
-.7124	.5789	-8.4358	-.0700
12.8683	-5.9781	3.1746	-11.983i
.0000	.0000	.0000	.0000
.0000	.0000	.0000	.0000

Dimensional 8th Order Design Model C Matrix

C_8 =

0.	0.	1.	0.	0.	0.	0.	0.
0.	0.	0.	1.	0.	0.	0.	0.
0.	0.	0.	0.	1.	0.	0.	0.
0.	0.	0.	0.	0.	1.	0.	0.

APPENDIX B

FULL STATE CLOSED INNER LOOP TRANSFER FUNCTION MATRIX

Full State Closed Inner Loop Transfer Function Matrix for the 8th Order Design Model

	Column 1	Column 2
$\frac{w}{w_c}$	$\frac{3.992}{(-4)}$	$\frac{w}{p_c}$ $\frac{0.077}{(-4)(-.00526)(-.0001)}$
$\frac{p}{w_c}$	$\frac{3.29E\text{-}5(-.1)(-.0000171)}{(-4)(-.00015)(-.002)}$	$\frac{p}{p_c}$ $\frac{4}{(-4)}$
$\frac{q}{w_c}$	$\frac{1.174E\text{-}4(-.00784)(.00497)}{(-4)(-.002)(-.00526)}$	$\frac{q}{p_c}$ $\frac{5.554E\text{-}4(-5.176E\text{-}6)}{(-4)(-.00526)(.0001)}$
$\frac{r}{w_c}$	$\frac{-7.956E\text{-}5(.007;.11)}{(-4)(-.002)(-.00015)}$	$\frac{r}{p_c}$ $\frac{9.896E\text{-}4(-.00143)}{(-4)(-.00526)(-.0001)}$

	Column 3	Column 4
$\frac{w}{q_c}$	$\frac{.2745(-.0357)}{(-4)(-.00015)(-.002)}$	$\frac{w}{r_c}$ $\frac{-.0186(1.122)(-.0214)}{(-4)(-.00015)(-.002)}$
$\frac{p}{q_c}$	$\frac{5.554E\text{-}4(-.00001542)}{(-4)(-.002)(-.00015)}$	$\frac{p}{r_c}$ $\frac{9.896E\text{-}4(3.5456)(-9.504E\text{-}6)}{(-4)(-.00015)(-.002)}$
$\frac{q}{q_c}$	$\frac{3.9778(.0077)}{(-4)(-.002)}$	$\frac{q}{r_c}$ $\frac{-4.91E\text{-}4(-.0042)(4.265E\text{-}5)}{(-.00015)(-.002)(-.00526)}$
$\frac{r}{q_c}$	$\frac{-4.909E\text{-}4(.44;.07)}{(-4)(-.002)(-.00015)}$	$\frac{r}{r_c}$ $\frac{3.9978(.000226)}{(-4)(-.00015)}$

Note : (λ) for real eigenvalues ; (ω_n ; ζ) for complex eigenvalues.